SYSTEMATIC STUDIES OF SIDE CHAINS ON OPTOELECTRONIC PROPERTIES OF 3,4-DIOXYTHIOPHENE-BASED POLYMERS

A Dissertation
Presented to
The Academic Faculty

by

Melony Achieng Ochieng

In Partial Fulfillment
of the Requirements for the Degree
Doctor of Philosophy in the
School of Chemistry and Biochemistry

Georgia Institute of Technology
May 2019

SYSTEMATIC STUDIES OF SIDE CHAINS ON OPTOELECTRONIC PROPERTIES OF 3,4-DIOXYTHIOPHENE-BASED POLYMERS

Approved by:

Dr. John R. Reynolds, Advisor
School of Chemistry and Biochemistry
School of Materials Science and Engineering
Georgia Institute of Technology

Dr. Angus P. Wilkinson
School of Chemistry and Biochemistry
Georgia Institute of Technology

Dr. Vladimir Tsukruk
School of Materials Science and Engineering
Georgia Institute of Technology

Dr. E. Kent Barefield
School of Chemistry and Biochemistry
Georgia Institute of Technology

Dr. Mostafa El-Sayed
School of Chemistry and Biochemistry
Georgia Institute of Technology

Date Approved: [March xx, 2019]

“Begin at the beginning and go on till you come to the end; then stop”

-Lewis Carroll

“Go confidently in the direction of your dreams! Live the life you've imagined.”

-Henry David Thoreau

To my family and friends

ACKNOWLEDGMENTS

I am truly thankful for the people and places that taught me that I am capable, brave, significant, and loved. I learned a lot from them. From my mother, paka yuayo tek, sibuor kital, I learned to never view myself as better than anybody else or anybody else as better than me; to discipline myself to work hard, work smart, and work long hours. After all, a little sleep, a little slumber, a little folding of the hands to rest, and poverty will come to you like a robber and need like a bandit. I am blessed with such a mother who keeps my pride in check and gives clear and frequent impressions about living, though I continue to fall short through my own faults. From my father, a man who always saw me as a Ph.D. holder despite my IQ level, I learned that it is worth waiting to marry a bread maker because you will be a breadwinner – to give a man who says, "You look like a woman I could take home to my mother and for whom a bull would be slaughtered in the presence of my ancestors, and they would be pleased, and my friends and enemies alike would wail in jealousy and regret," a chance. From my grandmother Risper, I learned that you should strive to leave a legacy so that one's grandchildren's children may find refuge in one's hard work, to have more than enough so that whenever I wished to help any person in their need I could do it, and to never desire more than the span of my arms. From my grandmother Susan, I learned that both the person who went to work and the one who stayed in bed will be tired at the end of the day. From my grandfathers, I learned that one should take care of necessities first before you throw caution to the wind. From my sisters, Jovia and Risper, and my brother, Ednan, people who love me so much that they gave me first-born rights, I learned to keep vigilance over myself and set standards for the Ochieng gang. I am truly

indebted to my siblings who continue to please me with respect and affection as I continue to make progress and adjust what it means to be the eldest. From Kevin Omolo, I learned to never respond when angry, make promises when happy, or decide when sad. I am thankful for his affection, support, level-headedness, and simplicity in the way of living.

From Dr. John R. Reynolds, I learned to keep the Carothers equation in mind when running reactions: "You will not be successful in polymer chemistry with 99.9% you need at least a 99.99% conversion rate." He also taught me to heap shame upon clutter in the lab, office space, and by extension, my dwelling place; to diversify my investments; and to keep a timetable – Do not wake up not knowing what you are going to do; plan days, weeks, months, and even years in advance. I am thankful that Dr. Reynolds accepted me into his lab and provided me with the space to fail over and over again. From Dr. Darlene Taylor, I learned to attend at least one conference a year where they pray before the banquet, dance to "Purple Rain", and calls you Sista. From my coaches, whether you come first or last, stay in your lane. From my former lab-mates, I learned that *not* following a man who gives you a two-week notice that he is moving to another university is sane. From my current lab mates, I learned to keep my head up and play kickball. From North Carolina Central University, the blackest experience that I needed, I learned that it is okay to think of oneself as a one-of-a-kind talent at least once in a lifetime. From the Georgia Institute of Technology, I learned how it feels to trip over your self-esteem and land on your pride every few days. From my friends, I learned to be my own superhero and to save a place for each other at the top while lifting each other out of the valley.

I am grateful to my committee members, Dr. Angus Wilkinson, Dr. E. Kent Barefield, Dr. Moustafa El-Sayeed, and Dr. Vladimir Tsukruk for their scientific inputs

and encouragement to keep going. I thank my brothers and sisters who stayed on their knees and prayed for blessing to follow me all the days of my life, for Nyasaye to keep poverty from visiting my doorsteps, and never enter a fight where I end up with broken tooth or torn clothes when a fight has nothing to do with me. I am thankful for the National Science Foundation and all the other grants that enabled this chapter of my life. To Nyasaye, I am indebted for having good grandparents, good parents, good siblings, good teachers, good friends, and good associates -nearly everything good.

Table of Contents

LIST OF TABLES

LIST OF FIGURES

LIST OF SYMBOLS AND ABBREVIATIONS

a*	greenness or redness
AcDOT	Acyclic DOT; 3,4(2-ethylhexyloxy)thiophene
ACN	Acetonitrile
b*	blueness or yellowness
BTD	benzothiadiazole
CMY	Cyan-magenta-yellow
CV	Cyclic voltammetry
CE	coloration efficiency
CIE	International Commission on Illumination (Commission Internationale de l'Eclairage
DPV	Differential pulse voltammetry (voltammogram
DCM	dichloromethane
DHAP	Direct (Hetero)Arylation Polymerization
DOT	3,4-dioxythiophene
D-A	Donor-acceptor
DMAc	*N*,*N*-dimethylacetamide
DSC	Differential scanning calorimetry
ECP	Electrochromic polymer
E_g	Band gap
ECD	Electrochromic Device
E_{ox}	Oxidation potential
EDOT	3,4-ethylenedioxythiophene
FTO	Fluorine-doped oxide

Fc/Fc^+	Ferrocene/ferrcenium
GOPS	3- glycidoxypropyl trimethoxysilane
GPC	Gel permeation chromatography
HOMO	Highest Occupied Molecular Orbital
ITO	Indium Tin Oxide
LiBTI	lithium bis(trifluoromethanesulfonimide)
L*	lightness
LUMO	Lowest Unoccupied Molecular Orbital
M_n	Number-average molecular weight
M_w	Molecular weight average
MCCP	Minimally color changing polymer
NIR	Near-infra-red
NMR	Nuclear magnetic resonance spectroscopy
NBS	*N*-bromosuccinimide
OPV	Organic photovoltaic
OLED	Organic light emitting diode
OECT	organic electrochemical transistors
OFET	Organic field-effect transistor
PC	Propylene carbonate
PEDOT	Poly(3,4-ethylenedioxythiophene)
PEDOT:PSS	poly(3,4-ethylenedioxythiophene) polystyrene sulfonate
Ph	Phenylene
Pt	Platinum
p-TSA	*p*-toluenesulfonic acid
PivOH	Pivalic acid

PS	Polystyrene
RGB	Red-green-blue
$TBAPF_6$	Tetrabutylammonium hexafluorophosphate
TCE	Transparent conducting electrode
TGA	Thermogravimetric analysis
THF	Tetrahydrofuran
WE	Working electrode
XDOT	dioxythiophene
X_n	Number-average degree of polymerization
λ_{max}	Wavelength of Maximum Absorption
Đ	Dispersity

SUMMARY

In the past three decades, solution-processable cathodically coloring π-conjugated polymers, specifically those based on dioxythiophene (XDOT), have received significant attention as an active layer in electrochromic devices (ECDs). This is due to their facile chemical modification, allowing wide color range/band gap; low oxidation potentials, enabling devices that operate at low voltages and reduced potential for limiting side reactions; high optical contrast between their vibrantly colored charge neutral states and their transmissive oxidized states; and solution processability, which facilitates the fabrication of devices using solution-based printing and patterning techniques easily adaptable to large surface substrates.

In general, the conjugated backbone determines the optoelectronic properties of the resulting polymer. Consequently, most research efforts have focused on tailoring optoelectronic properties through chemical modifications of the conjugated backbone, accounting for continuous improvements in device performance and establishing structure-property relationships. While these studies have led to significant advances in polymer design, solubilizing side chains are regularly used to improve the molecular weight and processability of the polymers. Recently, a few studies have shown that side chains can affect the optoelectronic properties of XDOTs. However, these results are complicated when accounting for the diversity in side chains of electrochromic polymers. Thus, systematic investigations into the effects of side chains on the optoelectronic properties of electrochromic polymers are needed. In this dissertation, a series of XDOT polymers with varying side chains are synthesized and the changes in optoelectronic properties are

correlated to side chain functionality. Specifically, this dissertation highlights how side chains affect solubility, optical gap/color, ionization potential, electrochromic contrast, switching speeds, and switching stability when alkyl or oligoether side chains are attached to an XDOT backbone.

The first chapter begins with a brief overview of XDOTs, the various components of ECDs, and the parameters used to evaluate the performance of XDOTs. This is followed by a brief discussion of the strategies used in backbone engineering to tune optoelectronic properties. The main body of Chapter 1 highlight previous studies of different solubilizing groups and how those results established the foundation for the hypotheses in this dissertation. In Chapter 2, the two polymerization methods, oxidative polymerization and direct (hetero) arylation polymerization (DHAP), used in this dissertation are taught. This chapter also focuses on the different techniques used to evaluate the properties of the polymers synthesized. Specifically, key measurement techniques such as cyclic voltammetry (CV) and differential pulse voltammetry (DPV), chronoabsorptometry, spectroelectrochemistry, and temperature-dependent UV-vis spectroscopy are discussed. Once the history and techniques are established in Chapter 1 and Chapter 2, the structural design and synthesis of five XDOT-based polymers with linear and branched side chains are reported. Using a range of analysis methods, it was determined that changing from linear to branched side chains affects ionization potential, optical bandgap, perceived color, electrochromic contrast, switching speed, and switching stability. The polymers with branched alkyl side chains had higher onsets of oxidation, optical bandgaps, and demonstrated sudden coloration change when compared to polymers with linear alkyl side chains. Chapter 4 presents two polymers where the branching position on the alkyl side

chains are changed. The effects of the side chains on the oxidation/reduction potentials are discussed in addition to the effects on the optical properties. Chapter 5 introduces oligoether side chains as a model system to synthesize water-compatible XDOTs to circumvent environmental and safety issues from organic-soluble polymers. In this chapter, it was determined that XDOT polymers with oligoether side chains had faster switching speeds and lower onset of oxidations when compared to their organic soluble counterparts. Finally, in Chapter 6, the concluding chapter, new design guidelines for future materials and the challenges in establishing structure-property relationships in XDOTs are presented.

CHAPTER 1. INTRODUCTION

Electrochromism is the reversible optical change that occurs in certain materials when an electrochemical potential is applied. In the field of electrochromism, solution-processable electrochromic conjugated polymers (ECPs) have garnered a lot of attention over inorganic materials and organic small molecules, due their ease of processability from organic and aqueous solvents,[1-16] synthetic tunability of color,[17-18] high optical contrast ratios,[16, 19-25] low switching voltage, and long electrochemical switching cycles.[26-27] ECPs are currently being investigated as active layers in a wide variety of electrochromic devices (ECDs), including large-area displays,[28] data storage,[29] camouflage technologies,[22, 30-31] and plastic "smart" windows[32]. The continued establishment/understanding of the relevant structure-property relationships for ECPs has improved the performance of the mentioned electrochromic devices. While most research efforts have focused on the conjugated backbone, little research has sought to understand the influence of side chains on the optical and electrochemical properties of solution-processable ECPs. This chapter provides a comprehensive background for ECPs, the parameters used to evaluate their performance, the results of backbone engineering, and the development of side chain engineering.

1.1 The Fundamental of Conjugated Polymers

The underlying physical phenomena which govern the electrical and optical changes in π-conjugated materials can be explained by band theory. Conjugated polymers consist of alternating carbon-carbon double bonds and carbon-carbon single bonds, which have three different hybridization configurations: sp, sp^2, and sp^3. In the sp^2 configuration, the $2p_x$ and $2p_y$ orbital combine to form the σ bonds while the $2p_z$ orbitals remain

perpendicular to the plane. The remaining $2p_z$ orbitals overlap with neighboring $2p_z$ orbitals, leading to a splitting into π bonding and anti-bonding molecular orbitals. Electrons fill molecular orbitals according to minimum total potential energy and Pauli exclusion principles. In ethylene, which has eight valence electrons, the 1s σ and σ* orbital and the sp^2 σ orbital will be filled first. The remaining two electrons from the *p*-orbitals will fill the π-bonding, the highest occupied molecular orbital (HOMO), while the next highest orbital π*, which is referred as the lowest unoccupied molecular orbital (LUMO), will remain empty. The energy difference between the HOMO and LUMO is known as the band gap. When three or more *p*-orbital (alternating σ-π) are parallel and interacting, as in 1,3-butadiene, the electron density can be shared or *delocalized* across all p-orbitals.

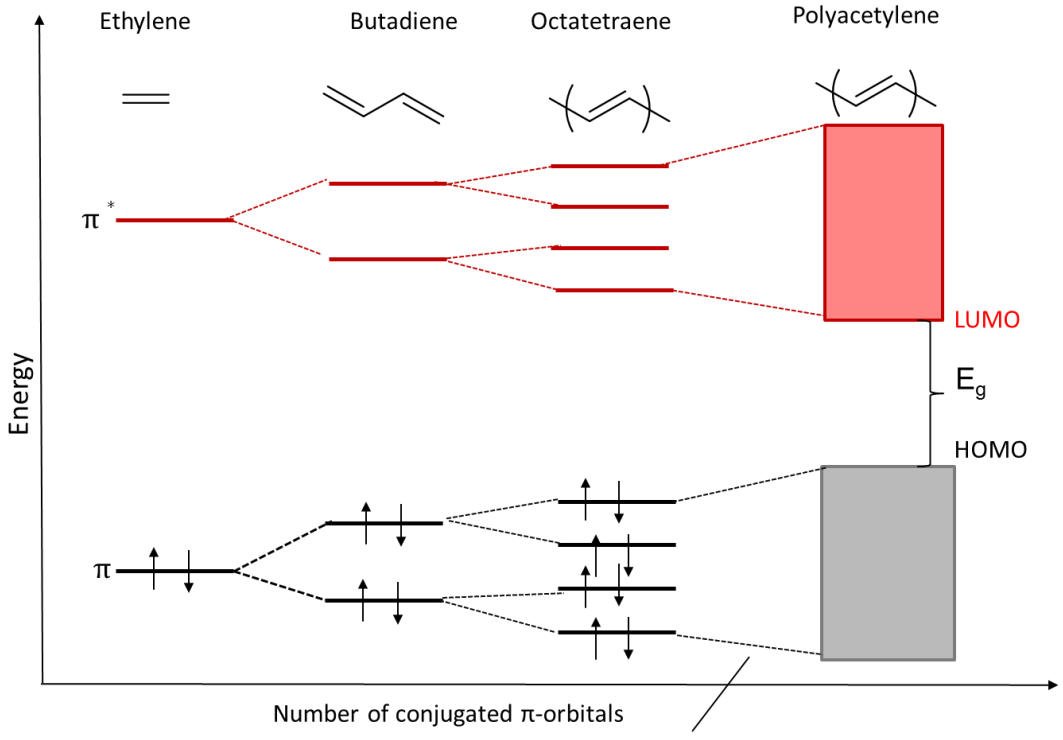

Figure 1.1. a schematic displaying the effects of decreasing bandgap between the HOMO and LUMO as conjugation increases from a) ethylene, b) butadiene, c) octatetraene, and d) polyacetylene. Adapted with permission from Salzer et al.[33] Copyright 1998 American Chemical Society.

As the number of delocalized electrons increases, i.e. the conjugation length increases, the number of bonding and anti-bonding levels increase, while the energy gap decreases, as seen in the progression from butadiene to octatetraene then to polyacetylene. In principle the band gap should converge to zero, leading to a metallic type material. However, the instability of a quasi one-dimensional structure of sp^2 hybridized carbon-carbon bonds leads to a distortion of the chains in order to provide stabilization through a lower energy arrangement.[33] The physical effect of this stabilization is seen through bond-length alternation (BLA) between single and double bonds.[34] This phenomenon, known as a Peierls-distortion, which is similar to Jahn-Teller distortion, lowers the HOMO and raises the LUMO thus preventing conjugated materials from achieving zero-energy band gap. In addition to BLA, planarity, electron-withdrawing/electron-donating substitution, aromaticity, and interchain interactions play a role in determining the band gap of conjugated polymers.[34]

From an electrochromic perspective, the two most important aspects of a conjugated polymer are the ability to tune the band gap and dope the material. Doping through the generation of positive (p-doping) or negative (n-doping) charge carriers, introduces new electronic states (polaron or bipolaron) in the bandgap. In p-doping, an electron is extracted from the HOMO level of the conjugated backbone and generates a radical cation, also called a polaron. The removal of an electron causes a localized geometric defect in the polymer backbone. In the past 30 years, the removal of an electron from the HOMO has been conceptualized as the formation of two mid-state energy levels inside the band gap. This traditional view neglects to account for both Madelung (coulombic) and Hubbard interactions. Recently, the Koch group revised the model to

account for the Coulomb repulsion.[35] In the revised model, the removal of an electron shifts both the HOMO and LUMO levels while forming new energy states.[35-36] In both the traditional model and the revised model, the removal of an electron from the HOMO can be observed through the formation of new optical transitions in the absorbance spectra. If a second electron is removed from the already-oxidized section of the polymer, either a second independent polaron is created or it can dimerize to form a bipolaron.[18] This results in more conformation changes in the conjugated backbone, usually by enhancing the tendency for co-planarity of the units.

1.2 Polythiophenes

Polythiophenes (PTs) are of particular interest as electrochromic polymers due to their excellent optoelectronic properties and processability.[37] The first preparation of polythiophene was reported independently in 1980 by the Dudek and Yamamoto groups.[38-39] The electrochemically prepared films of the polythiophene switched from a dark blue (λ_{max} = 730 nm) in the oxidized state to red (λ_{max} = 470 nm) in the neutral state. Even though the polymer films displayed attractive colors, they were not soluble. To improve the solubility of PTs, different side chains were explored in the late 1980s. This led to numerous novel polythiophenes with various alkyl, alkoxy, and aryl side chains, resulting in polymers with enhanced solubility and optoelectronic properties. Out of the different polythiophene derivatives, symmetrically substituted poly(3,4-dialkylthiophenes) and poly(3,4-dialkoxythiophenes) are reported to be similar in color and tend to have higher optical gaps than their monosubstituted analogs, because of the increase in steric hindrance.[40-41] The main difference between the dialkoxy- and the dialkyl-substituted thiophenes is the two oxygen substituents on the β-positions of the thiophene rings. The

oxygen atoms increase the electron density in the thiophene rings, allowing the polymer to have lower oxidation potentials and stable radical cations and dications.[42-43] The electron donating ability of the oxygens on the 3- and 4-position also enhances the reactivity of the α-positions. This results in polymers with fewer α-β and β-β coupling defects during oxidative coupling.[41] Specific to this discussion, α-β and β-β coupling events result in polymers with irregular backbones and poor electronic properties.

1.3 Electrochromic Device (ECD) Architecture

ECDs can be broadly divided into two main groups, herein referred to as "all-in-one" or single layer and "layered" configurations.[44-45] The term "all-in-one" is used to describe the symmetric device architecture where an electrochromic (EC) material and a redox mediator are dissolved in an electrolyte and the resulting single EC mixture is sandwiched between two substrates.[45-46] An ideal substrate should simultaneously possess high optical transparency and electrical conductivity, good chemical durability, low thermal expansion coefficient, and mechanical durability.[45] Currently, most ECDs are built on rigid substrates such as a transparent conducting electrodes (TCE) of glass. The most extensively used TCEs are indium tin oxide (ITO) and fluorine-doped tin oxide (FTO) due to their low resistivity and high transparency. The advantages of the all-in-one layer device includes the ability to optimize the manufacturing process by reducing the number of coating steps, prevent leakage of the electrolytes, reduce the waste of materials, and increase device stability.[47]

The layered configuration can be classified into three different classes, which are essentially the same, but with different approaches to the ion transport and ion storage

layers. Type-I layered devices have electrochromic molecules and a redox agent dispersed in a polymer matrix, which is sandwiched between two ITO-coated glass substrates. Type-II layered devices contain electrochromic molecules with chelating groups, such as viologens with phosphonate groups, bound to a mesoporous metal oxide film backed by a TCE. Finally, Type-III devices are based on a thin-film battery-type configuration.[44] The typical layered-type-III ECD architecture, from top to bottom as shown in Figure 1.1a, consists of a transparent conducting substrate, a conjugated polymeric material, an electrolyte layer, an ion-storage layer, and another transparent conducting substrate. During construction, the electrochromic material of interest, in this example an ECP, is deposited onto the transparent conducting substrate to become the working electrode. A different electroactive or electrochromic polymer is deposited onto the other transparent conducting substrate, which is the counter electrode. The second polymer, sometimes referred to as an "ion-storage layer," must assume a charged state opposite that of the working electrochromic layer, as shown in Figure 1.1b. The two electrodes are sandwiched together with an electrolyte layer, filling the space between them, thus constituting a battery-like structure.[48-49] The electrolytes can either be organic, aqueous, ionic liquid, or gel based. The conventional organic electrolyte is a liquid solution such as tetrabutylammonium hexafluorophosphate ($TBAPF_6$), lithium bis(trifluoromethanesulfonimide) (LiBTI), lithium perchlorate ($LiClO_4$) in propylene carbonate (PC) or acetonitrile or potassium chloride (KCl), sodium chloride (NaCl) or LiBTI in water in the aqueous electrolytes. Usually, these liquid electrolytes have high ionic conductivities and leakage problems. An example of a type III electrochromic device is shown in Figure 1.2. When a sufficient voltage is applied to the working electrode, electrochromic polymer (1) is doped, while

polymer (2) is de-doped. This new bias drives the ions from the ion storage layer into the electrochromic polymer to balance the new charges created, while electrons are inserted into polymer (2). This allows the device to switch from a colored state to a clear state. This optical change can be readily reversed when the opposite voltage is applied.

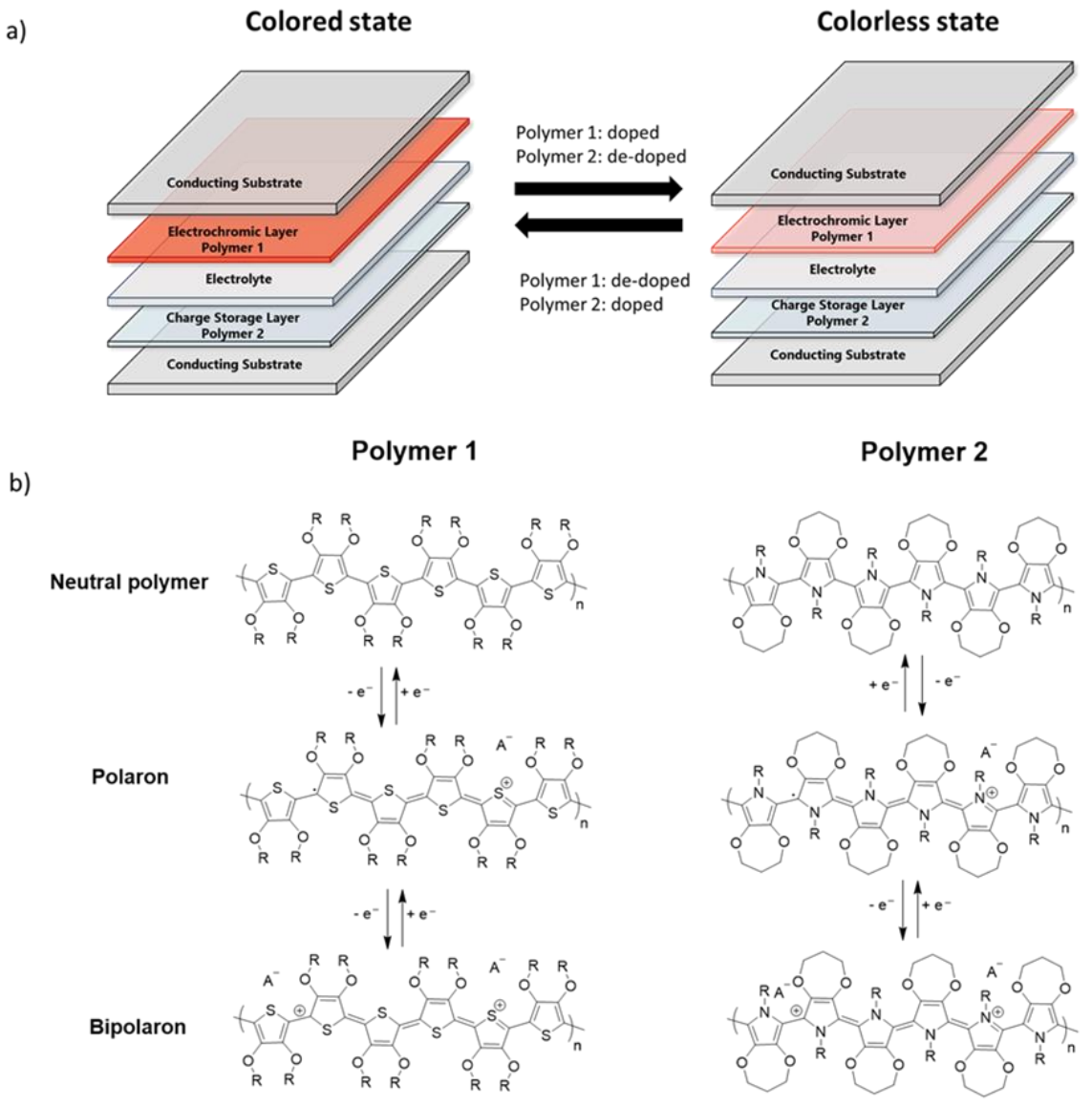

Figure 1.2. a) Schematic representation of ECD architecture at two extreme operating voltages. Schematic adapted with permission from reference.[36] Copyright 2017 American Chemical Society. b) mechanistic explanation of the electrochemical doping/dedoping process of two different polymers.

Depending on the application, ECDs can be categorized as either transmissive or reflective and the device design rules that govern the construction of either one is different. In the construction of transmissive (i.e. window type) ECDs, the color change of the two polymer coatings is important, since light must be transmitted through both thin films before reaching the viewer's eye. For that reason, a colorless-to-colorless conjugated polymers based on dioxypyrrole[50], known as minimal color changing polymer (MCCP), shown in Figure 2b, or a complementary material, are required to be the ion storage layer.[50-52] For the same reason, the conducting substrates must also be transmissive to the wavelength range of interest (often 400-700 nm, which encompasses the visible region). In terms of application, transmissive ECDs are usually used in smart windows[50], optical shutters, and window-type displays[53].

For reflective ECDs, a diffusive light reflecting gel electrolyte can be used so that when electrochromic switching occurs, only the color change of the front electrochromic layer is observed, and the color change behind the reflecting gel electrolyte is not observed. If a reflective gel is not used, then a reflective layer can be coated behind the bottom conducting electrode creating a mirrored surface. Reflective ECDs based on viologens are now ubiquitous, albeit barely noticeable to the uninitiated observer, in the automobile business. Electrochromic antiglare mirrors are typically controlled with a photosensor, requiring no input from the driver for operation. For both transmissive and reflective ECDs, the degree of the coloration can be controlled by the amount of charge passed through the cell and the amount of polymer deposited on the electrode.

1.4 Evaluating Electrochromic Performance

The techniques used for analysis and characterization of electrochromic polymers are in general valid for devices as well. The major difference is that ECP films are usually electrochemically characterized in a three-electrode setup where the potential is applied relative to a known reference potential while most devices do not have a reference electrode. For the ECPs synthesized in this dissertation, the polymers will be evaluated for their color, oxidation potential, electrochromic contrast (i.e. optical contrast), coloration efficiency (CE), optical memory, switching speed, and switching stability in a three-electrode setup.[17, 49, 54]

1.4.1 Color

One of the most important metrics of an ECP is color. However, color is subjective to interpretation since the perception of color varies among individuals. Thus, it is important to characterize color quantitatively for valid comparisons. The two main systems used to quantify color are the *xyY* and CIE *L*a*b** color spaces. In the *xyY* color space, the *Y* values are the luminance while *xy* represents the hue and saturation values calculated from the *X,Y,* and *Z* tristimulus values. The *xyY* color space is horse-shoe shaped, with achromatic colors residing at the center and spectral colors increasing towards the edges of the arc. The main drawback of *xyY* color space is that it lacks uniformity in geometric distance between color points. The CIE *L*a*b**, established by the International Commission on Illumination (Commission Internationale De L'Eclairage, or CIE), allows for 3-dimensional uniformity in color points. The *L** represents the lightness or luminance of a color, where 0 is black and 100 corresponds to white. The *a** and *b** axes represent

the relative saturation of four quaternary colors: red (+a*), green (-a*), blue (-b*), and yellow (+b*) so that a vibrant color with a high degree of saturation will have large a* and/or b* values. Colorimetry of ECPs is usually done by spectroelectrochemistry, where the color can be tracked as a function of oxidation state

1.4.2 Coloration Efficiency

Coloration efficiency (CE) is another tool used to evaluate ECPs. CE is defined as the ratio between optical modulation (ΔA) and the consumed charge density necessary to induce a full switch (Q) at a specific wavelength. As shown by Equation 1, it is derived from the Beer−Lambert law,[17, 54]

$$CE = \frac{\Delta A}{Q} = \frac{\log(\frac{T_{ox}}{T_{red}})}{Q} \quad (1)$$

where Q is reported in C cm^{-2}, CE is reported in cm^2 C^{-1}, and T_{ox} and T_{red} refer to the neutral and oxidized state transmittance values, respectively. Given equation (1), a parameter that affects CE values substantially is the level of transmissivity attained in each extreme state of the electrochrome. The ideal colored-to-transmissive electrochromic material would exhibit a large optical change with minimal charge consumption.[55] The analysis of CE is important, yet the methods utilized to calculate it varies between research groups, making comparisons between systems difficult. One approach to characterize the extent of optical change undergone by an electrochrome at a given wavelength, consists of estimating a composite coloration efficiency (CCE) measured at a representative percentage (e.g., 95%) of the total optical change.[17, 56]

1.4.3 Electrochromic contrast

Electrochromic contrast, or optical contrast. is probably the most important factor in evaluating colored to transmissive electrochromic materials. It is commonly reported as the difference in percent transmittance change (ΔT, %) at a given wavelength, usually reported at the peak absorption maximum (λ_{max}) where the electrochrome exhibits its highest contrast.[17] Transmittance values are generally recorded upon application of square-wave potential steps to the electroactive film placed in the beam of a spectrophotometer. While the measurement for electrochromic contrast is simple, the property is dependent on different factors such as the amount of chromophore deposited on the electrode, incomplete bleaching when oxidized, and wavelength at which the measurement is taken. Contrast is limited by the time interval of the square wave pulse, *i.e.* faster switching times often result in lower contrast.[19] In an ideal situation, the electrochromic contrast for transmissive ECDs is 100%, that is, the material is opaque in the colored state and fully transparent in the bleached state under alternating potentials. Until now, the XDOT with a highest electrochromic contrast is the electrochemically polymerized dibenzyl-subsituted ProDOT derivative with an optical contrast of 89% at λ_{max} with a switching time as fast as 0.4 s (thickness of the film was not given).[21]

1.4.4 Oxidation Potential

The oxidation process corresponds to the removal of the electron from the HOMO energy level while the reduction corresponds to the addition of electron to the LUMO energy level. In polythiophenes, studies have shown that derivatizing the 3- and 4-position on the thiophene ring with an alkylenedioxy bridge lowers the oxidation potential due to

the two electron donating oxygen atoms. Lowering the oxidation potential can be understood in terms of the energy levels, where raising the HOMO energy lowers the voltage necessary to extract an electron from the π-system. Determination of oxidation potentials is usually performed using a three-electrode cell set-up using CV or DPV. For CV and DPV, the working electrode is usually gold or glassy carbon (for optical studies a transparent electrode such as ITO is used), while a Pt counter electrode balances the current passed at the working electrode during the CV or DPV experiment.

1.4.5 Optical Memory (Open-circuit Memory)

The optical memory is defined as the ability of an EC material to maintain its colored/bleached state under open circuit conditions. In effect, high optical memory allows the material to maintain a redox state without a continuous power supply, as the electrochemical doping/dedoping process is stable and not spontaneously reversed.[29, 49] This is an important parameter for energy-efficient electrochromic devices. The optical memory of conjugated polymers last as long as weeks, while the colored state of viologens quickly bleaches upon termination of current due to the diffusion of soluble electrochromes away from the electrodes.[17, 54] Optical memory is often not reported as a material property and has not been studied to an extent that allows for strong structure-property relationships to be established.

1.4.6 Switching Speed

Switching speed can be defined as the time needed for an electrochromic material to switch from its fully colored state to its fully bleached state, or *vice versa*. Switching speeds depend on several parameters, such as film thickness, electrolyte conductivity,

substrate resistance, and cell geometry. Similar to CE measurements, the quantification of switching rate suffers from the variety of methods commonly used, making further data comparisons between different groups often difficult. Some groups define the switching speed as the time needed for the EC system to reach 95 % of its full modulation between the transmissive and colored states.[56] The value of 95% is chosen as the human eye is relatively insensitive to the final 5% of a color change. Other groups report switching speed at 60%[57],66%[58],70%[59], to 80%[60] of its full modulation. Reporting switching time values of incomplete switching is inaccurate and confusing since transmittance vs. time response is not linear. Switching times reported at lower contrast will inherently be faster and overestimate the film/device performance. In an effort to establish structure-property relationships between different values, Padilla and co-workers proposed a new method to determine switching time for films and devices.[61] It involves applying a series of symmetrical potential steps while varying the pulse length and ensuring that at least the longest pulse length allows the material to achieve full contrast. This allows results from various groups, and on different materials or devices, to be directly compared using two parameters: a full switch contrast and a time constant.

1.4.7 Redox Stability (Long-Term Stability)

Depending on the application, redox stability or lifespan is an important requirement for ECDs. For an ECP material, redox stability represents the number of cycles that can be performed before any significant degradation occurs. Factors that affect redox stability are mostly related to the components utilized in the fabrication of the device. This includes the electrolytes, TCE, ion storage layer etc. Other factors include the applied potential and photo-degradation.[27, 62-63] In XDOT-based ECPs, redox stability of 10^5 cycles

with over 85+% retention of contrast is not uncommon for low-gap polymers, but not for high-gap polymers. High-gap materials, especially yellow-to-clear dioxythiophenes that use phenylene units, tend to require high oxidation potential to switch due to their high degree of aromaticity relative to thiophenes.[13, 64-66] The high oxidation potentials are hypothesized to contribute to the poor redox stability of high gap XDOTs. Another reason specific to many yellow XDOTs involves the open positions on the phenylene units, which are poised for reactivity of the radical cation when the polymer is oxidized, leaving an opportunity for nucleophilic attack and radical-radical coupling.[67-69] This results in a break in conjugation, photo-bleaching/oxidation, or film delamination.[70-71] The long-term switching stability of ECPs is usually evaluated on an ITO glass slide or button electrode. When the stability is done on a button electrode, any changes in the charge density *Q*, and therefore the coloration, is monitored. When the stability is done on ITO glass slides, the electrochromic contrast is monitored. Since *Q* is an indirect measurement for coloration, it is advised that long-term stability should be done on ITO glass because it allows for the monitoring of any color changes over many switches. Also, ITO is often the electrode of choice for building transmissive ECDs devices.

1.5 Design Principles in Conjugated Polymers

Considering the many applications of ECPs, the identification of relevant structure-property relationships, both through backbone and side chain engineering, has become a cornerstone of materials design.

1.5.1 Backbone Engineering

In terms of backbone engineering, there are three synthetic handles that chemists have used to change the conjugated backbone. This involves (i) changing the conjugation length along the conjugation backbone through covalent bonding (e.g. fluorenes and polycyclic aromatic systems) or through noncovalent interactions (e.g. hydrogen bonds and other electrostatic interactions).[34, 72] (ii) decreasing the aromaticity of the monomer units and increasing the quinoidal character of the conjugated backbone. For example, the torsional angle of a biphenyl is about 45 °[73] from the electron diffraction studies while the bithiophene torsional angle is at 30 °[74], making the bithiophene more planar. The thiophene-thiophene C-C bond is also shorter than the phenyl-phenyl C-C bond, making the quinoidal form of the bithiophene more favorable than biphenyl, i.e. the phenyl ring is more aromatic. (iii) alternating between electron-rich donor units with electron-poor acceptor units. The hybridization of the energy levels associated with the covalently connected donor and acceptor units results in an unusually small HOMO-LUMO separation. The donor untis are able to raise the HOMO while the acceptor unit lowers the LUMO. In sum, this results in narrowed bandgaps for donor-acceptor copolymers.

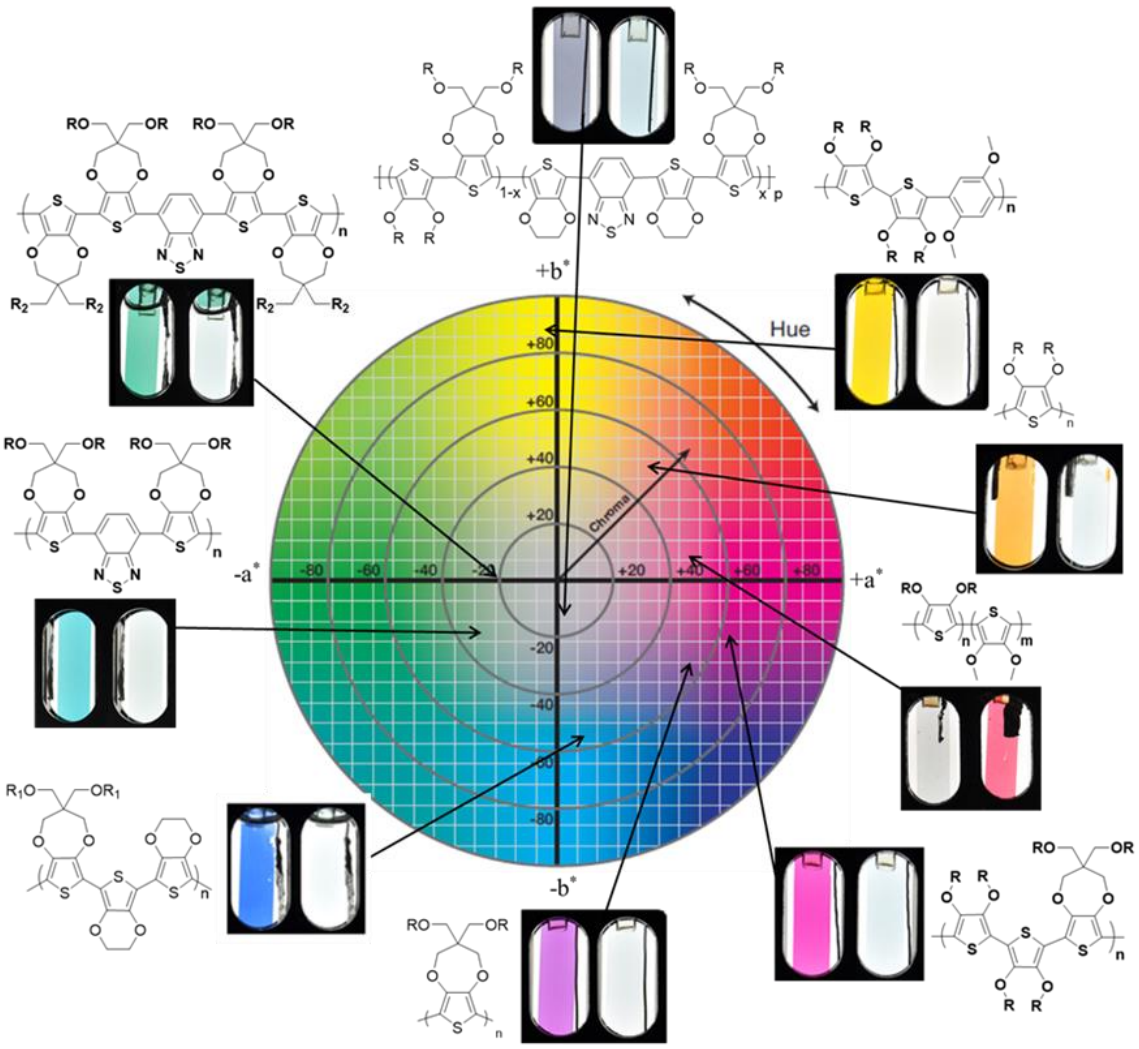

Figure 1.3. Structures of black, green[10, 24, 75], cyan[24, 76], blue[77], purple[4], magenta[78], red, orange, and yellow[23] ECPs with the corresponding photos in the neutral and fully oxidized state. Absorptions in the middle of the visible spectrum give magenta-to-transmissive ECPs while increasing steric strain gives red, oranges, and yellows. Variation of Donor-Acceptor interactions yields low band gap materials, resulting in blue, cyan, green, and black ECPs. Photos reprinted with persmission from the references except for black ECP which was taken by Dr. Kin lo and red ECP which was taken by Dr. Graham Collier.

To demonstrate the concepts that relate steric and electronic effects to observed color, each color of cathodically coloring XDOT-based polymers are discussed using the color wheel as a guide in Figure 1.3.

Green and Cyan: To obtain green/cyan-to-transmissive, the XDOT must have a dual-band absorption, one in the blue (short wavelength) and one in the red region (long wavelength), which must deplete simultaneously when the polymer is oxidized. The first report of a green XDOT came in 2002, when Dubois synthesized a green-to-gray switching electrochrome using bi-EDOT as the donor unit and pyrido[3,4-b]pyrazine as the acceptor unit.[79] Two years later, the Wudl group used the acceptor-donor approach to synthesize a soluble green polymer through oxidative electropolymerization and chemical polymerization of dioctyl-substituted 2,3-di(thien-3-yl)-5,7-di(thien-2-yl)thieno[3,4-b]pyrazine (DDTP). The resulting polymer had a low Δ%T at λ_{max} (12-23%) due to the significant residual yellow-brown hue in the oxidized state, leaving room for improvements.[6] In 2012, Beaujuge *et al* synthesized a series of green-to-transmissive ECP's consisting of blocks of 3,4-bis(octyloxy)thiophene (BAcDOT) or ProDOT as the donor units and 2,1,3-benzothiadiazole (BTD) as the acceptor unit.[75] The resulting polymers had various shades of green with absorption centered around 439-458 nm in the short wavelength and 642-667 nm in the long wavelength. The polymers had electrochromic contrasts ranging from 38-42%.

Obtaining a cyan-to-transmissive ECP, after understanding the green-to-transmissive ECP, is straightforward. The main difference between ECP-green and ECP-cyan is the band gap, ECP-cyan has a higher band gap. To increase the band gap the Reynolds group lowered the ratio of ProDOT units to BTD. The decrease in the overall electron-richness increases the band gap and blue shifted the high energy absorption by 50 nm while simultaneously red-shifting the low energy band by 15 nm.[24, 75] Depending on the strength of the donor (e.g. acyclic dioxythiophene (AcDOT), 3,4-

propylenedioxythiophene (ProDOT), and 3,4-ethylenedioxythiophene (EDOT)) or the acceptor (BTD or benzoselenadiazole BSD), the energy gap can be fine-tuned, resulting in various hues and saturations of greens and cyans with Δ%T at first λ_{max} up to 53% and low oxidation potentials. [10, 80-83]

Blue: Moving counterclockwise on the color wheel, the next color is blue. The first blue polymer, poly(3,4-ethylenedioxythiophene) (PEDOT), was discovered by Bayer AG research laboratories. Neutral PEDOT exhibits an optical band gap in the range of 1.5 -1.7 eV with a λ_{max} at 610 nm. The polymer switches between a deep blue neutral state to a transmissive sky-blue state when oxidized. However, the polymer is not processable.[84] Following the success of the first blue ECPs, different research groups over the past decades attempted to synthesize processable blue-to-transmissive polymers using a donor-acceptor approach by tuning the torsional strain between rings with different solubilizing groups.[11, 85] The first soluble blue-to-transmissive polymer was reported by the Reynolds group, an alternating ProDOT-BTD synthesized by an inverted Suzuki coupling method in 2007. In 2015[78] and 2016[77], an all donor polymers containing EDOT and ProDOT($CH_2OEtHx)_2$) were synthesized by tuning the amount of ProDOT-($CH_2OEtHx)_2$ incorporated in the copolymer. This resulted in fully soluble, blue-to-transmissive ECPs with a slightly blue-shifted absorbance when compared to PEDOT.

Purple and Magenta: The next colors from blue, on the color wheel, are purple and magenta, two colors that absorb in the middle of visible spectrum and therefore transmit red and blue light. The first cathodically-coloring purple ECP, the tetradecyl substituted derivative of poly(3,4-ethylenedioxythiophene) (PEDOT) synthesized by oxidative polymerization, was reported 1996.[2] Unlike the unsubstituted PEDOT, which is

blue, the alkyl side chains on PEDOT reduced backbone planarity resulting in a polymer with an optical gap of 1.78 eV and electrochromic contrast of 54% measured at λ_{max}. Since then, polymers with various alkyl side chain lengths substituted at the 3-position of PEDOT have been synthesized.[4, 86-87] The side chains greatly enhanced solution-processability without significantly changing the electrochromic properties of the polymers. Outside of PEDOT, ProDOT derivatives have also been used to synthesize purple-to-transmissive ECPs.[4, 87] The most widely recognized structure is PProDOT-($CH_2OEtHx)_2$), which has a high contrast ratio (80%) and switching rate (95% of a full switch in 0.6 s) when compared to all other solubilizing groups studied thus far.[4] While different derivatives of purple polymers have been synthesized, few magenta-to-transmissive ECPs has been reported. The most popular strategy used to design magenta-to-transmissive electrochromic polymers is to copolymerize an acyclic dioxythiophene (BAcDOT) with ProDOT. BAcDOT induces more steric interactions, reducing the conjugation length, resulting in a polymer with a band gap of 1.93 eV.[78]

Yellow: Coming to the top of the color wheel, we end up at the color yellow (by skipping orange and red-ECPs which are discussed in the side chain engineering section of this dissertation). The first yellow-to-transmissive ECP (ProDOT-Ph) was synthesized in 2011 by the Reynolds group and involved phenylene repeat units. The polymer, unfortunately, had a high oxidation potential and low redox switching stability.[66] To lower the oxidation potential and increase redox stability, a variety of ProDOT-arylene conjugated polymers were synthesized.[64] The study showed that increasing the electron richness of the arylene unit lead to a decrease in oxidation potential while maintaining a high optical gap due to steric interactions between the ProDOT and the ortho C-H on the

arylene.[78] Using the lessons learned from previous studies, a copolymer of AcDOT units and 2,5-methoxy-1,4-phenylene, was synthesized in 2016.[23] The electron-rich methoxy units in place of the smaller hydrogen atoms of the phenylene rings raised the HOMO level resulting in a polymer with a lower oxidation potential. Using the methoxy groups not only resulted in a polymer with a lower oxidation potential but also increased the redox stability by blocking the open sites in the phenyl ring from nucleophilic attack and radical coupling.

Black: The syntheses of black-to-transmissive ECPs have proven to be difficult because the ECP needs to absorb the entire spectrum evenly, and then become transmissive when oxidized. The first black-to-transmissive ECPs were synthesized via the donor-acceptor approach in 2008.[88] The polymer was formed from a random copolymerization of ProDOT as the donors and BTD as the acceptor in 1:4 molar ratio, giving a material that absorbs broadly over the entire spectrum with a maximum electrochromic contrast of 52% at 592 nm.[88] Due to the synthetic complexity of the polymer, which involved the synthesis and chromatographic separation of donor-acceptor-donor (DAD) trimers, in 2016 the Stille polymerization was used to synthesize the same polymers.[89] The Stille polymerization method not only simplified the synthetic process, but the resulting polymer films showed higher optical contrasts, faster switching times, and long-term redox switching stability due to the higher degree of randomness possible with Stille polymerization. Other researchers have synthesized black-to-transmissive polymers using the donor-acceptor (D-A) strategy, however the polymers have poorer electrochromic properties.[90-92]

1.5.2 Side Chain Engineering

Introduction of side chains on the conjugated backbone has expanded the field of conjugated polymers by allowing new structures to be synthesized through solution-based polymerization.[93-96] These polymers have well-defined molecular weights,[97] and are characterized through standardized methods such as NMR and GPC and processed via common solvents. However, solubility is just one of the many properties that can be manipulated through side chains. In fact, side chains such as alkyl, fluoroalkyl, oligoether, and ionic side chains not only improve solubility but also influence the optoelectronic properties of the ECPs and the diffusion of counterions in and out of the films. Since the role of side chains in organic electrochromics is quite complex and highly dependent on the conjugated backbones, this section will highlight the effects of alkyl, fluoroalkyl, oligoether, and ionic side chains on polythiophenes.

1.5.2.1 Alkyl side chains

The most common side chain used to solubilize conjugated polymers are linear and branched alkyl side chains. They confer solubility by interrupting π-π interactions between main chains and by permitting more entropic freedom of the polymer in solution. Increasing the length of linear alkyl side chains results in greater solubility, as more rotational degrees of freedom are added to the structure and secondary interactions between main chains are decreased. This is associated with an increase in the free volume and changes to the absorbance of the polymer. Compared to linear side chains of the same mass, branched side chains confer greater solubility due to the increase in torsional disorder and repulsive steric interactions between side chains. This torsional disorder not only affects

the solubility, but it also changes the optoelectronic properties through steric interactions causing the backbone to distort.

The two colors that have been synthesized through side chain engineering are orange and red. The first orange-to-transmissive and red-to-transmissive polymers were synthesized in 2010.[98] The homopolymer, 3,4-bis(2-ethylhexyloxy)-thiophene, P(BAcDOT), and a copolymer of 3,4-bis(2-ethylhexyloxy)-thiophene and 3,4-dimethoxythiophene P(BAcDOT-DMT), were synthesized by oxidative polymerization.[98] The orange-to-transmissive polymer had an optical gap of 2.04 eV and an absorption maximum at 483 nm. On the other hand, the random incorporation of DMT units into the growing backbone reduced the steric interactions, lowered the band gap slightly to 2.00 eV and shifted the λ_{max} significantly to 525 nm to yield a red-colored polymer. Both polymers were found to be effective ECPs, with an electrochromic contrast of 48% (Δ%T at λ_{max}) for the orange polymer and 60% (Δ%T at λ_{max}) for red polymer. The main challenge with the P(AcDOT) was the long switching time (>5 seconds for a film coated to 0.98 absorbance) and short redox stability while the P(BAcDOT-DMT) had a pink hue.[98] Since then, various groups have attempted to synthesize other red-to-transmissive polymers, but these polymers retained hues of magenta and pink color.[16, 99-102] To synthesize a true red-to-transmissive polymer, in 2018 the Reynolds group copolymerized dialkylthiophene (DAT) with 3,4-propylenedioxythiophene (ProDOT) (DAT-ProDOT) using direct hetero(arylation) polymerization (DHAP). [24, 103] The DAT monomer provides inter-ring strain with alkyl chains directly appended to the backbone, thereby helping the copolymers obtain wide optical gaps while blocking possible reactive sites for the radical cations. Meanwhile, the ProDOT unit increased the electron richness of the polymer to maintain a

low oxidation potential. The resulting polymer (DAT-ProDOT) film had λ_{max} of 491 nm, thus giving rise to a vibrant orange color with an oxidation potential of 74 mV vs Fc/Fc^{+}. Upon electrochemical conditioning or break-in, this polymer exhibits an increase in absorbance and red-shifting to a λ_{max} of 500 nm leading to a red-colored polymer. The break-in observed in the polymer is caused by reorganization of the polymer chains as the polymer is oxidized and is forced to planarize and swell with solvated ions. After repeated cycling, the polymer obtains the lowest energy conformation in its charge neutral state for the redox cycling that may result in a shift in the absorbance. To increase steric interactions, the DAT unit was copolymerized with 3,4-(1,3-dimethylpropylene)dioxythiophene (DMP). The resulting polymer DAT-DMP, had a λ_{max} at 466 nm, yielding a vibrant orange colored polymer and an oxidation potential at 160 mV *vs.* Fc/Fc^{+}. Both polymers showed minimal contrast loss after 10,000 redox cycles.

In 2011, the Sotzing group did a different study to understand how steric interactions influence optoelectronic properties. They synthesized four ProDOT-based polymers with varying side chains (*t*-butyl, *n*-hexyl group, isopropyl, and methyl) using 1,3-substitution on systems as opposed to the common 2,2-substituent, as shown in Figure 1.5a.[104] The side chains disrupted the backbone planarity, resulting in polymers with neutral-state colors that varied from yellow to dark purple, Figure 1.5b.[104] The polymer with the *t*-butyl side chain resulted in an ECP with a yellow neutral state, which transitioned to a green color upon oxidation. A dark blue-purple neutral state was observed for the polymer with the methyl group, which switched to a transmissive light blue upon oxidation. The ionization potentials for the polymers were not reported, but the Sotzing group indicated that the ionization potentials remained essentially the same for each derivative.

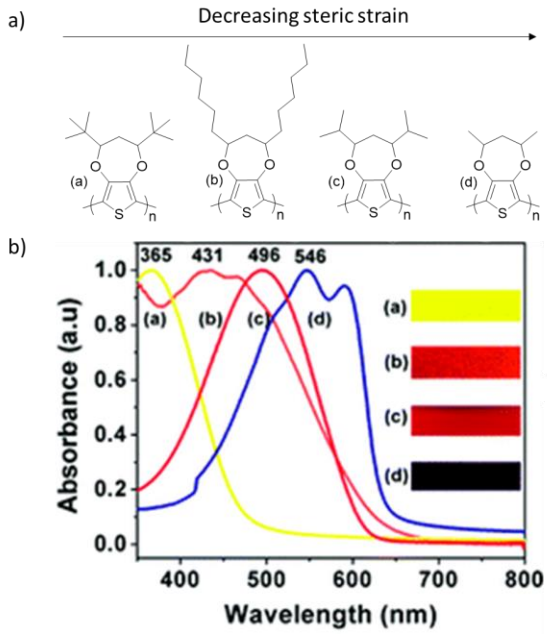

Figure 1.4. Structures of polymers b) Tuning steric interactions through side chains results in polymers that range from yellow to dark purple (Figure is modified with permission from Reference[104]. Copyright © 2011, American Chemical Society).

1.5.2.2 Fluoroalkyl Side Chains

In the field of electrochromic polymers, incorporation of electron withdrawing atoms onto the conjugated backbone has been shown to affect HOMO and LUMO energy levels of the conjugated backbone. Fluorine atoms in particular can also affect the planarity of the conjugated polymers due to their small atomic radius. Fluoroalkyl side chains have also been investigated due to their unusual properties which arise as a consequence of the hydrophobicity, rigidity, thermal stability, chemical and oxidative resistance, and self-organization.[5, 105-106] Fluoroalkyl or semifuoroalkyl groups can be easily introduced onto the EDOT and 3,4-ethlenedioxypyrrole (EDOP). For synthetic reasons, most of the structures reported to date feature an "insulating" spacer (alkyl, O, $SiMe_2$) between the fluorinated fragment (usually a perfluoroalkyl group) and the heteroaromatic core, which greatly attenuates or even reverses the electronic effects of fluorocarbon substitution.

In 2003, the Reynolds group reported the synthesis of pentadecafluoro-octanoic acid 2,3-dihydro-thieno(3,4-b)(1,4)dioxin-2-ylmethylester (PEDOT-F) along with poly(3,4-ethylenedioxythiophene) (PEDOT), 3,3-diethyl-3,4-dihydro-2H-thieno-[3,4-b][1,4]dioxepine (PProDOT-Et_2), 2,2-dimethyl-3,4-propylenedioxythiophene (PProDOT-Me_2), and 3,4-Propylenedioxythiophene (ProDOT).[107] The oxidation potential of PEDOT-F compared to PEDOT was negligible since the perfluoroalkyl chains were not close enough to the conjugated backbone to affect its electronic properties. However, the optical contrast was significantly different, PEDOT-F having a higher optical contrast (Δ%T = 66%) when compared to PEDOT (Δ%T = 54%). PEDOT-F displays the highest coloration efficiency (586 cm^2/C) when compared to its analogous PEDOT (183 cm^2/C), shown in Figure 1.6. The enhanced composite coloration efficiency of PEDOT-F was hypothesized to be due to a combination of the electronic effects imparted by the fluorine substitution as well as the increased steric bulk. The high coloration efficiency observed in PEDOT-F suggests that a device where the active layer is made with PEDOT-F, as opposed to PEDOT, would require a lower voltage to operate. While the underlying reasons behind such improvements are unclear, the authors suggested that improvements may be due to a more porous morphology of the films which would allow faster diffusion of counter-ions during oxidation and reduction. In addition, the higher CE may be due to the low oxidation level required to attain high optical contrast in PEDOT-F.

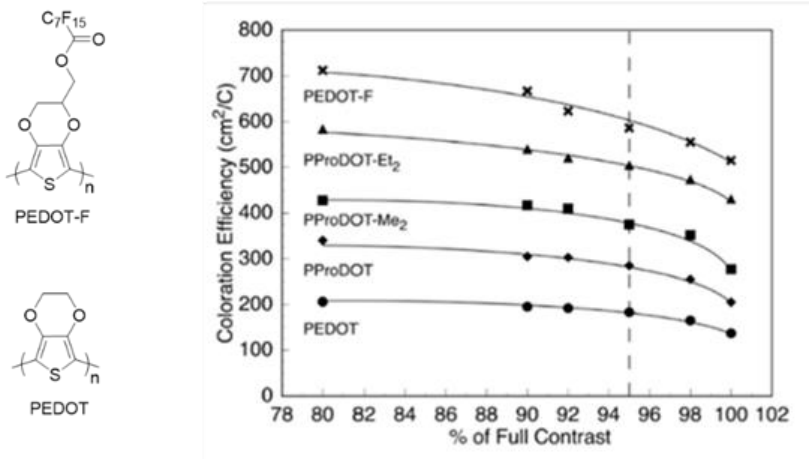

Figure 1.5. Comparison of coloration efficiency of different polymers. Reprinted with permission from reference[107]. Copyright © 2003 WILEY-VCH Verlag GmbH & Co. KGaA, Weinheim.

In 2015, the Xu group prepared a series of thiophene and benzothiadiazole-based copolymers through Stille coupling polymerization with two mono- and di-fluorinated benzothiadiazole analogous: PDAT-DTBT-F (1F) and PDAT-DTBT-2F (2F).[108] The introduction of fluorine atoms onto the conjugated polymer backbone influenced the optical, electrochemical and morphological properties, which in turn, influence the electrochromic performance of the fabricated devices. In comparison to PDAT-DTBT, both PDAT-DTBT-F (1F) and PDAT-DTBT-2F devices had an enhanced reduction process to sub-second speed, high coloration efficiencies, and were stable at ambient conditions. They hypothesized that the enhanced stability of the fluorinated polymers was due to their deeper HOMO levels, which inhibited oxidative degradation, and the hydrophobicity of the fluorocarbons which repel neighboring nucleophiles present in electrochromic devices (e.g. water). The microstructures of the polymer films were analyzed using XRD measurements. They observed an increase in peak intensities in PDAT-DTBT-F and PDAT-DTBT-2F when compared to PDAT-DTBT. The results

suggest that the fluorinated polymers are more ordered, hence the higher charge transport observed during electrochemical switching.

1.5.2.3 Oligoether Side Chains

The majority of the ECPs are only soluble in common organic solvents such as toluene, chloroform, and chlorobenzene. However, such chlorinated and aromatic solvents are hazardous to the environment and human health. To mitigate the negative ramifications of such solvents, oligoether side chains have been used to promote material compatibility in water and other polar organic solvents.[15, 109-110] In addition, these side chains have been reported to facilitate ion transport in conjugated polymers, allowing ions to penetrate into the bulk during electrochemical redox reactions in both aqueous and organic electrolytes.[1] While the incorporation of oligoether side chains have been shown to enhance solubility in polar solvents, the influence of oligoether side chains on electrochromic properties of conjugated polymers is less investigated and poorly understood.

Since the 1990s, Roncali and co-workers have studied various electrochromic polythiophenes with oligoether side chains.[111-112] In their earlier studies, they synthesized conjugated polymers where the oligoether groups were physically decoupled from the conjugated backbone by a $-(CH_2CH_2)-$ spacer.[113] The side chain did not have any significant effect on the optoelectronic properties of the resulting polymers. In 2002, Roncali and co-workers reported the synthesis of oligoether substituted PEDOT derivatives that bonded directly to the backbone.[114] The polymers were electropolymerized from a monomer composed of two EDOT units connected by oligoether side chains. Depending on the length of the oligoether linker and doubly charged electrolyte cations such as Sr^{2+},

Ca^{2+} or Ba^{2+} produced considerable positive shifts in the anodic peak potentials, up to 400 mV, for the resulting polymers. More importantly, extreme electrolyte-dependent absorbance profiles were observed. For instance, transferring a film of the polymer from an acetonitrile electrolyte to water resulted in a 100-nm red shift in the absorption maximum after electrochemical oxidation. They hypothesized that the effect was due to enhanced sensitivity towards molecular oxygen in the electrolyte.[115] A comparative analysis of the cyclability of these polymers showed that the polymer comprising two oligoether-linked EDOT moieties were more stable under long-term redox cycling than the alkyl EDOT analogue.[115]

In 2017, Xu's group reported the sysnthesis of five polythiophenes with oligoether or alkyl side chains.[116] They observed that all five polymers were able to undergo full reversible electrochromic switching from neutral to oxidized states. Polythiophenes functionalized with oligoether side chains resulted in a blue shift (by ~ 20 nm) in absorption from the parent polymer, poly(3,4-ethylenedioxy bithiophene)s (PEDT), while the corresponding alkyl-substituted groups showed a red-shifted absorbance spectra (by ~ 80 nm). The optical switching times, measured at the time to complete 95% of its full contrast, were between 2.5 to 1.6 seconds with contrast ratios between 24% to 41%. The oligoether functionalized PEDT had a faster switching time compared to the alky-functionalized PEDT. They attributed the faster switching time to the oligoether side chains, which provides a high ionic exchange between polymers and PC/$LiCLO_4$ electrolyte. In addition to the faster switching speed, the oligoether-functionalized polymers showed a higher CE than the alkyl-functionalized polymers. Once again, they attributed the higher CE values to the higher ionic conductivity of the polymers in aqueous electrolyte. This study showed

how oligoether side chains interactions with electrolytes can enhance ionic conductivity, leading to faster switching speeds and higher coloration efficiencies of the resulting polymers.

In 2018, the Reynolds group used the same strategy of combining oligoether side chain and alkyl side chains to synthesize 3,4-alkylenedioxythiophene (XDOT)-based polymer, ProDOT(OE)-DMP via direct(hetero) arylation polymerization (DHAP).[117] The resulting polymer had an Mn of 22.5 kDa and dispersity of 2.0 with a solubility exceeding 30 mg mL^{-1} in $CHCl_3$. They confirmed that the ProDOT(OE)-DMP could electrochemically switch between a vibrant purple color in the neutral state to a highly transmissive color in the oxidized state in both the organic electrolyte and aqueous electrolytes, as shown in Figure 1.7a and 1.7b. The polymer had a slightly lower E_{ox} onset in the aqueous system (E_{ox} onset = -0.29 vs. Ag/AgCl) compared to the organic solvent (E_{ox} onset = -0.20 vs. Ag/AgCl). In the fully oxidized state, there was little tailing from any charge carrier absorption bands into the visible region, affording a highly transmissive oxidized state and electrochromic contrast at λ_{max} exceeding 70% in both electrolytes. They evaluated the switching rates using drop-casted films on glassy carbon electrodes and monitored the charge to switch over 1,000 cyclic voltammograms, as shown in Figure 1.7c. During extended cycling, the current–voltage response underwent a gradual change characterized by a merging of the two oxidation peaks into a single broad peak and a slight lowering of the E_{ox}. However, the cumulative charge passed by the polymer film remained constant over 1,000 redox cycles in water, demonstrating exceptional electrochemical stability. The ProDOT(OE)-DMP films maintained 95% of their maximum contrast for switching times as low as 2 s (0.5 Hz) in 0.5 M $TBAPF_6$/PC and <1 s in O.5 M $NaCl/H_2O$.

The faster switching times measured in aqueous electrolyte were attributed to the higher ionic conductivity of the electrolyte.

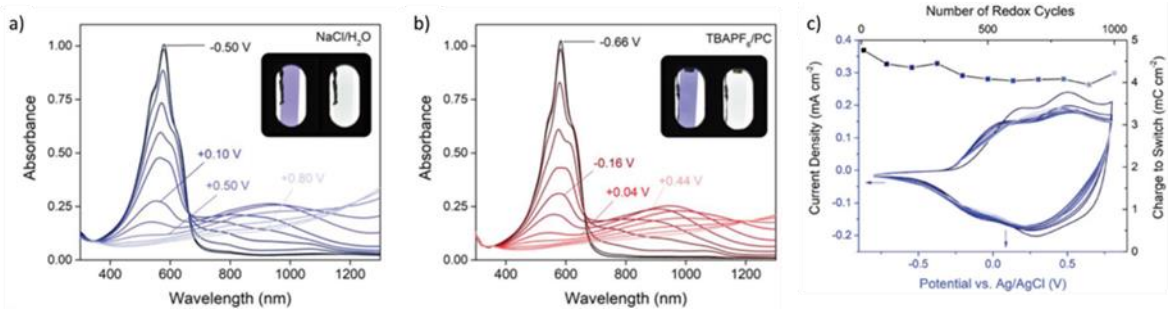

Figure 1.6. Spectroelectrochemistry of ProDOT(OE)-DMP in a) 0.5 m NaCl/H_2O from −0.5 to +0.8 V vs Ag/AgCl, and B) in 0.5 m $TBAPF_6$/PC from −0.66 to +0.44 V vs Fc/Fc^+. Photographs show films in neutral and oxidized states in the respective electrolyte. c) Superimposed cyclic voltammograms of ProDOT(OE)-DMP in 0.5 m NaCl/H_2O from cycle 1 (black) to 1000 (light blue). The cumulative charge passed is shown as a function of number of redox cycles. Reprinted with permission from reference[117]. Copyright © 2018 WILEY-VCH Verlag GmbH & Co. KGaA, Weinheim

1.5.2.4 Ionic Side Chains

Conjugated polyelectrolytes (CPEs) are ECPs with ionic side chains. Commonly used ionic side chains include sulfonate (SO_3^-), carboxylate (CO_2^-), phosphonate (PO_3^{2-}) and quaternary ammonium (NR_3^+). The interest in ionic side chains is mainly due to their hydrophilicity, which provides a number of positive attributes, such as environmentally conscious processing methods, applications to biological systems due to their "soft" character, and control of ionic properties and interactions that are not possible with typical organic-solvent compatible compositions.[7] In addition, most CPEs are amphiphilic due to the ionic side chains and the significant hydrocarbon backbone which allows these polymers to self-assemble into aggregates in solution.[7] Furthermore, these polymers are not susceptible to moisture-driven degradation mechanisms typical of an organic soluble conjugated polymer, which may improve their stability under atmospheric conditions.

Lastly, it has been reported that ionic side chains can improve the performance of ECPs by effectively enhancing ionic mobility and conductance in aqueous electrolytes. One major drawback of CPEs is that the films of these polymers can *redissolve in aqueous electrolytes*.

To overcome the problem of CPEs redissolving in aqueous electrolytes, the Reynolds group synthesized a polymer based on 3,4- propylenedioxythiophene with a cleavable side chain in 2012.[118-119] A ProDOT monomer bearing multiple alkyl ester-based side chains was copolymerized with BTD using Stille polymerization.[12] The resulting polymer was soluble in common organic solvents which allowed the polymer to be characterized using conventional methods, such as GPC and NMR. The polymer was subsequently saponified, resulting in the formation of the corresponding water-soluble carboxylate salt that can be processed into thin films using aqueous solvents. Protonation with dilute acid converts the water-soluble CPE into its acid form to render the polymer films insoluble in both organic and aqueous media and are thus solvent resistant (SR). Once the polymer becomes solvent resistant it cannot redissolve in the electrolytes, but it is still able to switch in both the organic and aqueous electrolytes solutions. They investigated how the organic soluble form (ECP-Blue-A), the aqueous form (WS-ECP-Blue-A), and the solvent resistant form (ECP-Blue-R) form of the polymers affected its optoelectronic properties. In terms of color, all three forms resulted in blue-to-transmissive polymers with the typical dual-band absorption. Looking closely at the absorbance spectra, the water-soluble form and the solvent resistant forms had 30 nm red shifts in the long wavelength absorption compared to the organic soluble form. The electrochromic contrast of the polymers are 48% for the organic form and 40% for the water-soluble form monitored at

655 nm for a 10 s switch. The electrochromic contrast for the solvent resistance form was monitored at 555 nm for a 10 s switch, increased to 54%. In terms of switching speed, the water-soluble form switches faster than the organic-soluble form of the polymer.

In 2017, the Reynolds group synthesized an all donor conjugated polymer poly(ProDOT-alt-EDOT) *via* direct hetero arylation polymerization using the same ester-based side chains, Figure 1.8a.[26] The resulting polymer had a molecular weight of 25 kDa with a dispersity of 2.8. When they compared the onset of oxidation of the organic form and the solvent resistance form, the solvent resistant form had a lower onset of oxidation (-0.76 V vs Fc/Fc^+) compared to the organic form (+0.21 V *vs.* Fc/Fc^+), Figure 1.8b. They hypothesized that the solvent resistant form had a lower onset of oxidation due to the decrease in the steric bulk once the ethyl hexyl side chains are cleaved. Further studies on the solvent resistant form of the polymers films showed a linear scan rate dependence of the peak currents, to show that the polymer's electrochemistry was not diffusion limited. This resulted in a rapid electrochromic switching (~0.2 s) from a vibrant blue neutral state to a highly transmissive oxidized state. The versatility of this polymer was further demonstrated in a series of organic and aqueous electrolyte systems, including biologically compatible electrolytes (NaCl/water, Ringer's solution, and human serum) and even sports drinks, demonstrating the robustness of this polymer to different ionic conditions.

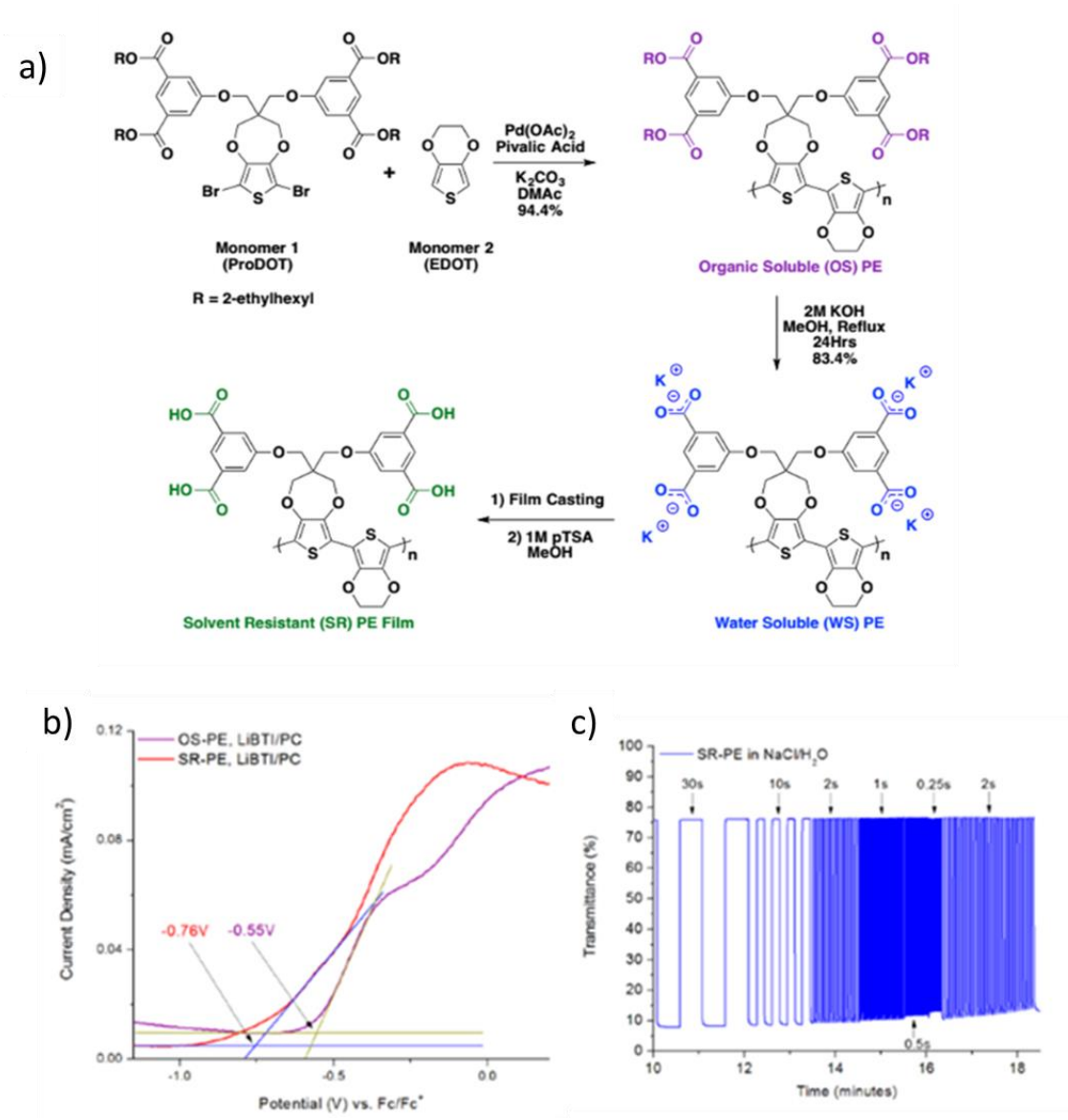

Figure 1.7. Synthesis of the poly(ProDOT-alt-EDOT) to make organic soluble polymer followed by the conversion to the water-soluble CPE form and by acid treatment to make it solvent resistant polymer. b) CV recorded in 50 mV increments from −0.80 to 0.70 V (vs. Ag/AgCl). c) Chronoabsorptometry of the SR-PE in biologically-relevant electrolytes at a scan rate of 50 mV/s. Reprinted with permission from reference[26]. Copyright © 2017, American Chemical Society.

1.6 Overview of Dissertation

This dissertation encompasses the design, synthesis, and characterization of solution-processable cathodically coloring π-conjugated polymers, specifically those based on dioxythiophene (XDOT), with varying side chains with the goal of understanding how alkyl and oligoether side chains affect optoelectronic properties. Specifically, this dissertation highlights how side chains affect solubility, optical gap/color, ionization potential, electrochromic contrast, switching speeds, and switching stability when alkyl or oligoether side chains are attached to an XDOT backbone. In Chapter 1, I gave a brief overview of XDOTs, the various components of ECDs, and the parameters used to evaluate the performance of XDOTs. This was followed by a brief discussion of the strategies used in backbone engineering to tune optoelectronic properties and highlights of previous studies on the effects of different side chains on optoelectronic properties. In Chapter 2, the two polymerization methods, oxidative polymerization and direct (hetero) arylation polymerization (DHAP), used in this dissertation will be taught. Chapter two will also focus on the different techniques used to evaluate the properties of the polymers synthesized. Specifically, key measurement techniques such as cyclic voltammetry (CV) and differential pulse voltammetry (DPV), chronoabsorptometry, spectroelectrochemistry, and temperature-dependent UV-vis spectroscopy will be discussed. Chapter 3 will describe the structural design and synthesis of five XDOT-based polymers with linear and branched side chains. Using a range of analysis methods, it was determined that changing from linear to branched side chains affects ionization potential, optical bandgap, perceived color, electrochromic contrast, switching speed, and switching stability. The polymers with branched side chains had higher onsets of oxidation and optical bandgaps. During

spectroelectrochemistry, the polymers with branched alkyl side chians demonstrate sudden coloration change when compared to polymer with linear alkyl side chains.

Chapter 4 presents a series of six polymers where the branching position, length, and bulkiness on alkyl side chain were varied. It was determined that by changing the branching point from the second carbon to the to the first carbon away from the backbone significantly changed the effective conjugation length, red-shifting the λ_{max} by 100 nm. This resulted in a polymer with a smaller optical bandgap, changing the color from orange to purple. Increasing side chain bulkiness by increasing the side chain length from propyl to octyl or increasing the ratio of branched side chain from 1:1 to 1:2 resulting in new shades of magenta and orange polymers. Chapter 5 introduces oligoether side chains as a model system to synthesize water-compatible XDOTs to circumvent environmental and safety issues from organic-soluble polymers. In this chapter, it was determined that XDOT polymers with oligoether side chains had comparable electrochromic properties as their organic counterparts. Finally, in Chapter 6, the concluding chapter, general conclusions, limitations, and recommendations arising from this dissertation are presented.

CHAPTER 2. EXPERIMENTAL METHODS AND CHARACTERIZATION TECHNIQUES

The feasibility of conjugated polymers as active materials in ECDs hinges on the ability to mass produce the materials while satisfying the demands concerning cost and environmental issues. For the most part, conjugated polymers are prepared via Miyaura-Suzuki and Migita-Stille cross-coupling techniques. Both polymerization methods require two distinct monomers. Stille coupling reactions require monomers with organotin groups, while Suzuki requires monomers with boronic acid groups. Functionalizing the monomers before polymerization increases the number of steps and makes scalability difficult. Another disadvantage of Stille and Suzuki polymerizations is the production of stoichiometric amounts of organotin and boronic acid reagents. The organotins are well known neurotoxins[120] while boronic acids have been shown to be genotoxic[121]. To reduce the number of steps and eliminate toxic by-products, direct (hetero) arylation polymerization (DHAP) was used in this dissertation to synthesize most of the homopolymers and copolymers. The rest of the polymers were synthesized by oxidative polymerization as they could not be synthesized by DHAP. In this chapter, the mechanism of chemical oxidative polymerization and DHAP are discussed. This is followed by monomer and polymer synthesis for Chapters 3-5, as well as purifications of the synthesized polymers. The bulk of the chapter focuses on basic characterization, such as chemical structure and composition, as well as spectroscopic, electrochemical, and thermal analysis of polymers.

2.1 Chemical Oxidative Polymerization

The first method developed to synthesize conjugated polymers was oxidative polymerization, which can be accomplished through either chemical or electrochemical process. Chemical oxidative polymerization is advantageous because it does not require expensive reagents and involves shorter reaction times to produce high molecular weight polymers. The generally accepted mechanism of chemical oxidative polymerization, using acyclic thiophene as the monomer and $FeCl_3$ as the chemical oxidant, is shown in Figure 2.1. According to the mechanism, a thiophene monomer undergoes a one-electron oxidation to form a resonance-stabilized radical cation. In the second step, the radical cation monomer couples with another radical cation to form a dicationic dimer via dissociation of HCl as a by-product in the reaction mixture. As coupling progresses, radical cation monomers, dimers, and oligomers will couple to form polymer chains. The process continues as long as the oxidant is present in excess or the polymer precipitates out of the solution. The polymer formed is partially in the oxidized state with $FeCl_4^-$ complexed to the backbone to charge balance the cations.[122] Reduction of the polymer is accomplished by the addition of a strong base such as hydrazine. The process of chemical reduction can be followed by visible change in the color of the solution. In chemical oxidative polymerization, stochiometric quantities of the oxidant are needed because initiation and propagation are dependent on the availability of the oxidant. In practice, excess amount of the oxidant is used to produce longer chains in short amount of time.[123-126] The excess metal ions such as Fe^{3+} are removed by repeated purification steps.

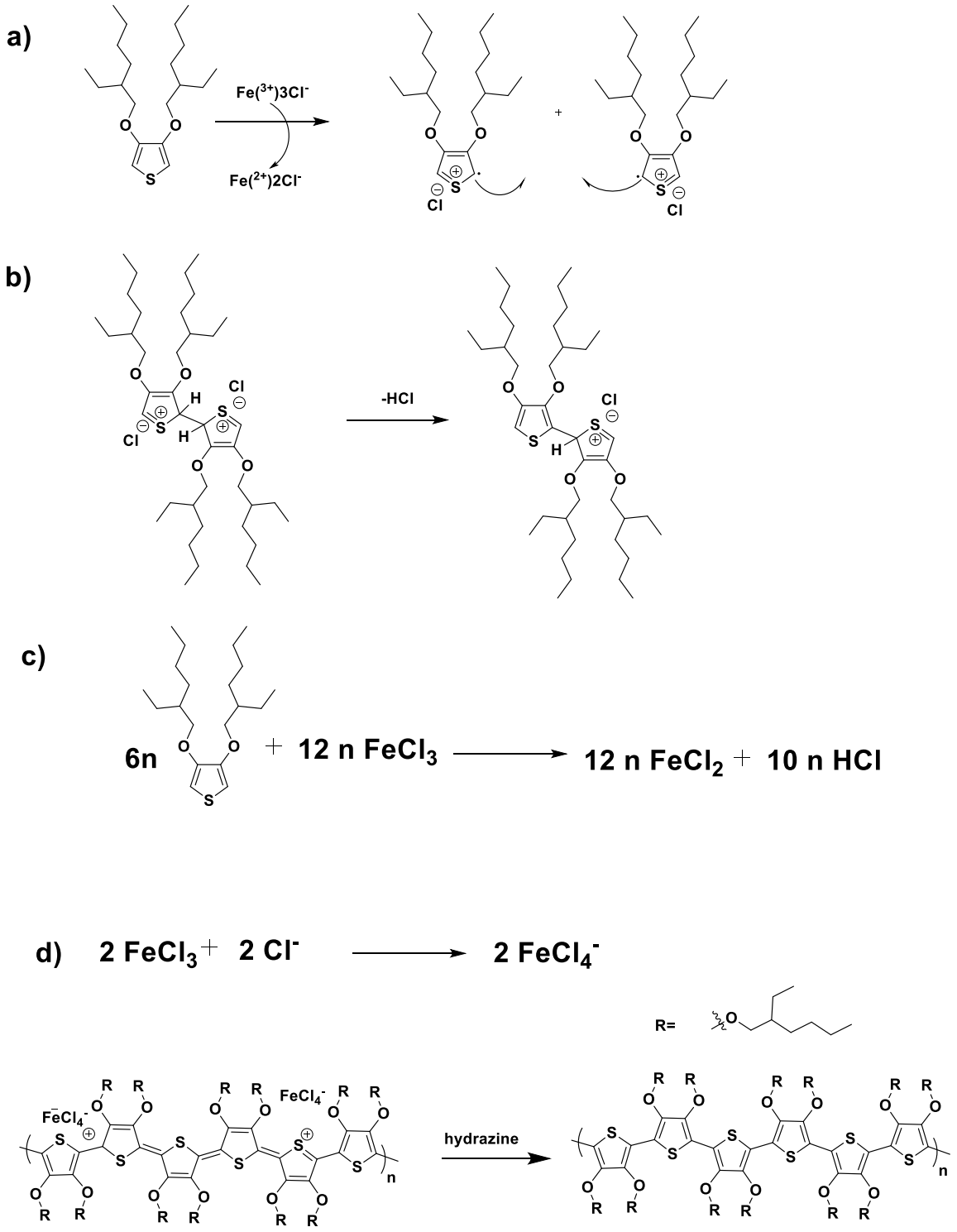

Figure 2.1. General mechanism for oxidative polymerization of P(BAcDOT).[123] a) oxidation of the monomer b) formation of thiophene dimer and elimination of HCl c) continued polymerization of thiophene d) reduction of the oxidized polymer.

There are two main problems associated with chemical oxidative polymerization. The first problem is that the polymer initially formed is in the oxidized state, resulting in increased rigidity in the polymer backbone. This increased rigidity causes the growing polymer chains to precipitate out of the reaction mixture. Over the years, the solubility of the polymers has been improved by the use of long linear or branched side chains. Another problem with chemical oxidative polymerization is the abundance of side reactions. For heterocycles, coupling at the 2-and 5- position (α-α coupling) is favored because it is the most electron-rich. However, coupling is also possible at the 3- and 4-positions (α-β and β-β couplings) resulting in an irregular polymer backbone. To avoid coupling at the β-positions, the 3- and 4-positions of the heterocycles can be blocked to allow only α-α coupling.

In this dissertation, specific polymers were prepared by oxidative polymerization of the relevant dialkoxythiophene monomers with excess $FeCl_3$ in ethyl acetate at room temperature. A five-fold excess of oxidant was used to maximize yield and molecular weight. Even though oxidative polymerization is simple, it is still important to choose a solvent that dissolves both the oxidant, monomer, and polymer. To exemplify this point, let's consider P(BAcDOT) with M_n 44 kDa and P(LAcDOT-DMP) with M_n 5 kDa. Both polymers were synthesized under the same conditions, however the molecular weights vary drastically. It is suspected that the low molecular weight of P(LAcDOT-DMP) relative to P(BAcDOT) is due to the decreased conformational entropy of the linear AcDOT and DMP monomers unit relative to branched AcDOT monomer unit. This results in poor solubility of the P(LAcDOT-DMP) polymer chains in the reaction medium thus reducing molecular weight.

2.2 Direct (Hetero) Arylation Polymerization (DHAP)

In the last five years, a lot of reports have detailed the use of DHAP to synthesize conjugated polymers.[94, 127-135] Unlike Suzuki and Stille polymerization, the DHAP method eliminates the need to functionalize the monomers with expensive organoboron or organotin groups. Instead, the monomer with the most "active hydrogen" is able to couple with a halogenated monomer to form the C-C bond.[94, 127-128, 131] Currently, there are two different classes of conditions used in DHAP reaction that have consistently resulted in high molecular weight and almost defect-free polymers. The first was inspired by the pioneering work of Fagnou et al.[136] This method typically uses amide solvents such as *N*,*N*-dimethylacetamide (DMAc), potassium carbonate (K_2CO_3) as a base, and pivalic acid as the carboxylate ligand/proton shuttle. The second conditions are based on the work of Ozawa *et al*.[137] in which phosphine ligands and organic solvents such as toluene or superheated THF are utilized. The conducting polymers synthesized by the Ozawa conditions may or may not utilize a carboxylic acid. In both conditions, Pd(II) or Pd(0) is often used as the catalyst. In this dissertation, the Fagnou conditions were used to synthesize the polymers.[129-130]

Since DHAP is relatively new, the mechanism is not fully understood, and they are several mechanisms that have been proposed. The "concerted metalation deprotonation" pathway suggested by Lafrance and Fagnou is generally more accepted.[136, 138] For this dissertation, a proposed cycle based on the work by Lafrance and Fagnou is shown in Figure 2.2, for the synthesis of P(BAcDOT-DMP). The cycle begins with the oxidative addition of a Pd(0) species to the dibromide BAcDOT to form an intermediate while raising the oxidation state of the metal center to Pd(II). This complex is stabilized by the conjugate base of the pivalic acid (pivalate) in solution. Next, the pivalate displaces the bromide ion to form a transition state

where DMP is inserted into the catalyst and coordinates with pivalate. A proton from DMP is then transferred to the pivalate to facilitate the concerted C-H activation. At this point, both monomers are coordinated to the Pd center and the carboxylate salt is regenerated by the excess potassium carbonate present. The final step is the reductive elimination to yield the desired C-C bond and regeneration of the Pd(0) source. This cycle continues until the polymer precipitates out of solution or stops due to stochiometric imbalance of the functional groups (C-H and C-Br) or impurities. As this is a relatively new polymerization method, readers are encouraged to explore C-H activation for synthesizing conjugated materials further in the open literature and anticipate new literature.[132, 134-135, 139]

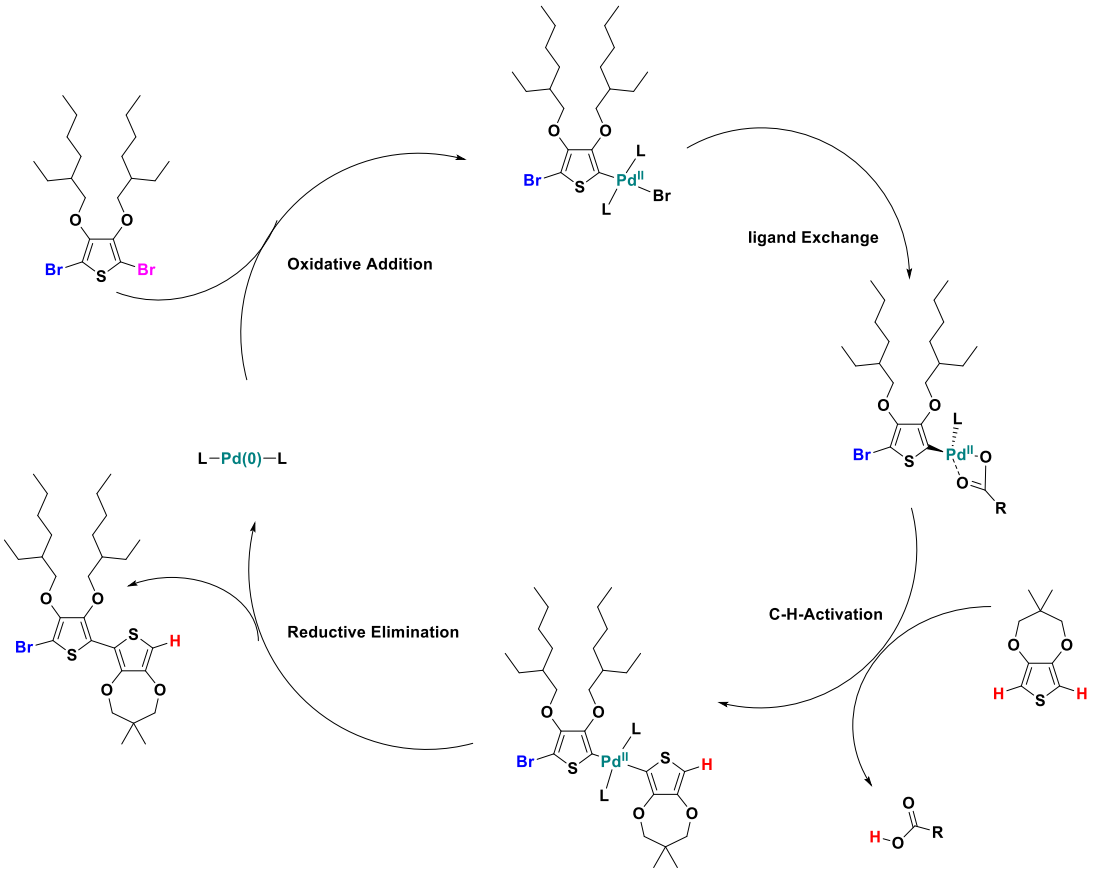

Figure 2.2. A proposed catalytic cycle for DHAP toward a substituted P(BAcDOT-DMP) with the various steps of the cycle outlined. This figure is based on the literature precedent.[129]

While DHAP has many advantages over other traditional cross coupling reactions, its success rate is still dependent on the optimization of reaction parameters such as monomer choice. A lot of monomers have multiple C-H bonds with close dissociation energies. In DHAP those C-H bonds can be activated to react with a C-halogen bond resulting in cross linking or branching. Homocoupling may also occur since two Pd(II) complex intermediates bearing equal (hetero) aryl groups can undergo a disproportionation reaction.[93, 95-96, 140-142] The branching, crosslinking, and homocoupling can be reduced significantly through the use of monomers where the 3- and 4-positions of the heterocycles are blocked. The XDOT heterocycles are particularly appropriate for DHAP because the oxygen groups in the 3- and 4- position renders the lack of C-H selectively a non-issue.

2.3 Polymer Purification

Once the polymerization is completed/terminated, the resulting solution typically consists of unreacted monomers, oligomers of varying structures, low and high molecular weight polymers, and impurities. To obtain the highest molecular weight polymer, the polymers synthesized by DHAP are precipitated into methanol and then filtered directly into the Soxhlet thimble for Soxhlet extraction using methanol, acetone, hexanes, toluene, toluene, and chloroform (in order). The extractions were conducted until color was no longer observed in the solution by placing a white tissue paper against the glass. The polymers synthesized by chemical oxidative polymerization are first suction filtered then dissolved into chloroform before they are reduced by hydrazine. Once the polymers are reduced they follow the same procedure as those synthesized by DHAP. The materials that are usually collected in the methanol fraction are catalyst, salts, and monomers. The acetone and hexane fraction usually collect the oligomers and the low molecular weight

polymers. However, some polymers with branched side chains, such as P(BAcDOT), have high solubility, so the highest molecular weight were extracted in the hexanes fraction. For most polymers, the toluene and chloroform fraction usually contained the highest molecular weights, while the insoluble products were left in the soxhlet thimble. To remove metal content, the fraction of the polymer kept are dissolved in chloroform, stirred with 18-crown-6 (a potassium scavenger) and diethylammonium diethyldithiocarbamate salt (a palladium scavenger) for at least two hours at 50 °C. The Pd scavenger has a great affinity to bind to metal ions like potassium and palladium respectively and the resulting complexes are soluble in most organic solvents, including methanol and chloroform.[143] Solubility of the complex form in the methanol is important since the high molecular weight polymer precipitates. Once the polymer is stirred in methanol for several hours, the precipitates are filtered then dried under vacuum to remove residual solvents prior to characterization. It is important to note that the Pd scavenger is not effective at removing palladium species that are chemically bound to polymers.[144] If the GPC results show high Đ (above 4) then the Soxhlet extraction can be done again with additional solvents like DCM or THF added before final dissolution of the product. This usually occur with polymers with low solubility where the polymer forms

2.4 Structural Characterization

^{1}H and ^{13}C NMR spectra of monomers were collected using a 300 MHz spectrometer to confirm structure and purity before polymerization. The chemical shifts for chloroform-*d* as the internal standard were referenced to the residual solvent peak, ^{1}H: $\delta = 7.26$ ppm, ^{13}C: $\delta = 77.23$ ppm. For new monomers, high-resolution mass spectroscopy was performed at The Georgia Institute of Technology Bioanalytical Mass Spectrometry

Facility by Mr. David Bostwick and Dr. Cameron Sullards using an LTQ Orbitrap XL™ ETD Hybrid Ion Trap-Orbitrap Mass Spectrometer and Applied Biosystems Voyager-DE™ STR Workstation.

Once the polymers were synthesized and worked up, the structure and purity were determined by ^{1}H NMR using the Bruker Corporation DRX 700 MHz spectrometer. The number average molecular weight (M_n), weight average molecular weight (M_w) and dispersity (Đ) of the polymers were determined by gel permeation chromatography (GPC) in $CHCl_3$ at 40 °C or in THF at 35°C calibrated *vs*. polystyrene (PS) standards. The GPC using $CHCl_3$ as the eluent was performed using a Waters Associates GPCV2000 liquid chromatography system at UCSB's materials research laboratory by Dr. Rachel Behrens or the TOSOH Ecosec HLC-8320 model at the Georgia Institute of Technology by Dr. Bing Xu or Dr. Graham Collier. The GPC using THF as the eluent were performed by Dr. James Ponder using a combination of Waters HPLC pump 1515, UV-Vis Detector 2487, and a Refractive Index Detector 2414 system. For both the $CHCl_3$ and THF GPC, a polymer solution was prepared and filtered through a Mini-UniPrep PTFE vial with a 0.45 μm filter. Elemental compositions were analyzed for the carbon, hydrogen, nitrogen, and sulfur contents at Atlantic Microlab, Inc. While the polymers have oxygen atoms in the repeat unit, it is not reported because oxygen is introduced in the combustion chamber.

2.4.1 Materials and Reagents

All reagents and starting materials were purchased from commercial sources and used without further purification unless otherwise stated in each chapter. Reactions were done under an argon atmosphere using Schlenk line techniques unless otherwise stated.

Silica (60 Å porosity, 40-64 μm particle size) used for column chromatography was purchased from commercial sources.

2.5 Polymer solution and Film formation

For the polymers discussed in this dissertation, polymer solutions with concentrations ranging from 0.5 to 5 mg/mL in toluene or chloroform were used to make films. Depending on the solubility of the polymer, additional heating and stirring was required. Immediately prior to casting, polymer solutions were filtered using a 0.45 pore size PTFE syringe filter, to remove insoluble material and large polymer aggregates. For electrochemical measurements, a thin film of the polymer was deposited onto a platinum disk electrode (area = 0.02 cm^2) or a glassy carbon (area = 0.07 cm^2) button electrode via drop-casting using a 5.0 μL micropipette for precise measurements. The solutions were left to air-dry in a ventilated spray booth. For the rest of the experiments, the films were spray-coated using a handheld commercial airbrush sprayer (Iwata-Eclipse HP-BC, 15 psi) onto ITO glass slides (7 × 50 × 0.7 mm, sheet resistance, R_s 8–12 Ω/sq, Delta Technologies, Ltd). Before the films were sprayed onto the ITO glass slides, they were cleaned by sonication in toluene, acetone, and then isopropanol. The measurements were done using a three-electrode set up with a platinum flag as a counter electrode and a Ag/Ag^+ reference electrode (filled with 10 mM $AgNO_3$, 0.5 M tetra *n*-butylammonium hexafluophosphate ($TBAPF_6$) (98 % from Acros) recrystallized from ethanol, purchased from Sigma-Aldrich), in acetonitrile (ACN)). The working electrode was the button electrode or the ITO/glass coated with the polymer film. The electrolyte solution was 0.5 M $TBAPF_6$ in propylene carbonate (PC). The calibration of the scans was done by measuring the oxidation half

potential of the ferrocene/ferrocenium (Fc/Fc^+) couple dissolved in the electrolyte solution versus the Ag/Ag^+ reference.

2.6 Electrochemistry (DPV and CV)

Cyclic voltammograms (CV) and differential pulse voltammograms (DPV) were used to study the electrochemical properties of the synthesized polymers. Electrochemical measurements were performed using a three-electrode cell using the conditions described above. The stable potential window for the polymers was determined by cycling through a range of potentials at a scan rate of 50 mV s^{-1}. Once the potential window was identified, a new film was deposited on the button electrode and electrochemically cycled. From the CV, the cathodic peak (E_{pc}) and peak current (i_{pc}) during the forward scan and anodic peak (E_{pa}) and peak current (i_{pa}) during the reverse scan can be determined. Once the CV measurements were completed, the same film was used to determine the onset of oxidation using DPV. DPV is used to determine the onset of oxidation because the capacitive or charging current is minimized. Thus, DPV curves become more symmetric with a higher signal to noise ratio, resulting in better defined onsets of faradaic oxidation and reduction. DPV and CV measurements were carried out using an EG&G Princeton Applied Research model 273A potentiostat/galvanostat under CorrWare control.

2.7 Spectroelectrochemistry and photography

Spectroelectrochemistry determines the optical transitions of an ECP at incremental potentials across a switching window using an Agilent Cary 5000 UV-vis / NIR spectrophotometer. Spectroelectrochemistry measurements were performed using a similar three-electrode cell as that used in DPV and CV. Instead of the button electrode, the

working electrode consisted of a thin film of polymer spray-cast onto ITO/glass slides. The absorbance spectra were collected in the range between 1800-300nm. This range allows for both the polaron and bipolaron bands to be studied when the polymer is in its oxidized states. After the polymer film is sprayed onto the electrode; a pristine photo was taken. After electrochemical break-in, potentiostatic conditions are applied and photos of the neutral and transmissive oxidized states of the polymer are taken. The films were broken-in by cycling for 10-25 times between the determined potential window until a constant current response was achieved. Photography was performed in a light booth designed to exclude outside light with a D50 (5000K) lamp located in the back of the booth providing illumination, using a Nikon D90 SLR camera with a Nikon 18-105 mm VR lens.

2.8 Colorimetry

Colorimetry is a technique used to quantify color relative to an observer's field of view. There are two types of color specification systems. The Munsell color system is based on the color appearance while the 1976 International Commission on Illumination (CIE) L*a*b* is based on additive color mixing. While the Munsell color system is easier to understand because it utilizes color chips to form the basis of its system, it suffers from low precision when comparing systems. Thus this dissertation will use the L*a*b* color space to quantify color. [145] Briefly, the L^* coordinate represents the white−black balance, with more positive values being lighter and more negative values being darker. The a^* represents the green-red balance, with positive a^* values being red and negative values being green, as shown in Figure 2.3. b^* is the yellow−blue balance of a given color, with positive values being yellow and negative values being blue. In addition to $L^*a^*b^*$, CIE has developed color-matching functions that represent average color vision in humans. These

functions are called a standard observed. Using the $L^*a^*b^*$coordinates of a material, the difference in color between two objects can be quantitatively compared. In this dissertation, colorimetry measurements were obtained using Star-Tek colorimetry software using a D50 illuminant, 2 deg observer, and the $L^*a^*b^*$color space, which converts spectra into the color values in a variety of spaces with different illuminants instantly, as shown in Figure 2.3.

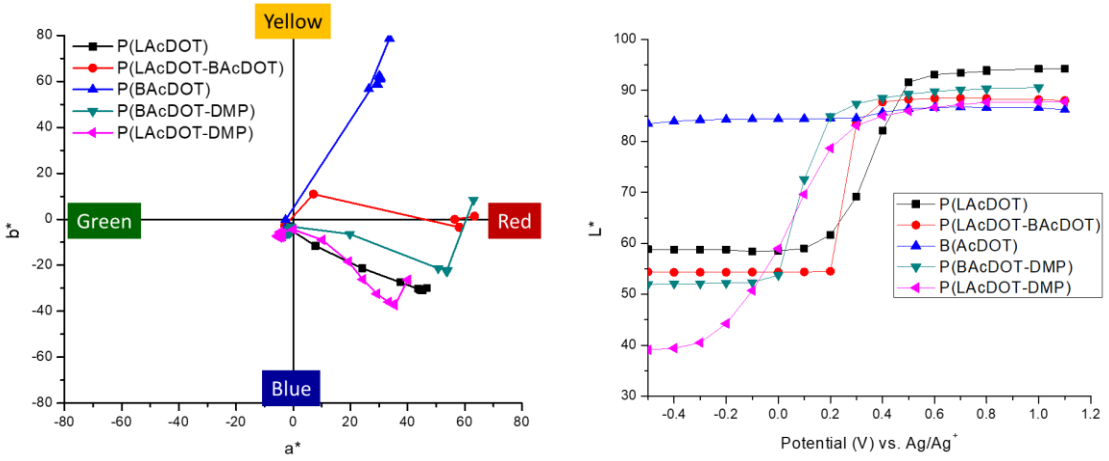

Figure 2.3. a) a^*b^* plot showing the color change as a function of electrochemical potential for the copolymer series, including the pristine films, the charge neutral states oxidized states, and the films in 0.1 V increments and (b) the change in L^* as a function of potential on ITO glass in 0.5 M $TBAPF_6$/PC vs. Ag/Ag^+.

2.9 Chronoabsorptometry

Chronoabsorptometry is a technique used to analyze the change in light absorption of an ECP at a variety of switching speeds. Most commonly, this is assessed at one specific wavelength, usually the wavelength corresponding to the peak absorption maximum (λ_{max}), as that tends to afford the highest contrast value. While the spectrophotometer allows light of a single wavelength to reach the detector, the potential is switched repeatedly between the two potentials to access the neutral and most oxidized transmissive states. The voltage is held at these two voltages for varying lengths of time, starting with 60 s switches at the

longest switching time and ending at 1s pulses as the shortest as shown in in Figure 2.4a. After the shortest switching time, the film is then switched at 30 s to demonstrate reversibility of the film and its ability to endure a variety of speeds. The Δ%T is taken by subtracting the percent transmittance in the neutral for from the percent transmittance in the most oxidized form as shown in Figure 2.4b while the switching speed is reported as the time it takes to reach 95% of full contrast switch.

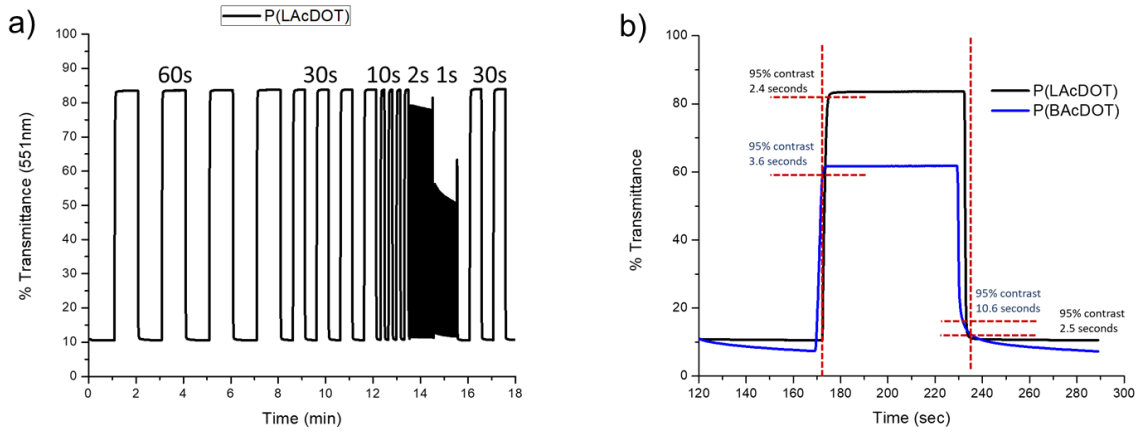

Figure 2.4. a) Chronoabsorptometry for a film of P(LAcDOT) and b) Percent transmittance and time to reach 95% of the full optical contrast for P(LAcDOT) and P(BAcDOT).

2.10 Temperature-dependent UV-vis

Temperature-dependent UV-Vis measurements of ECP in solution were used to investigate the structural order of the materials. Even though the polymer dissolves more easily in chloroform than toluene, toluene was chosen because it has a higher boiling point (111 °C for toluene *vs.* 61 °C for chloroform), which allows the study of solutions over a much wider temperature range. The temperature-dependent UV-Vis absorption measurements were performed using an Agilent Cary 5000 UV-vis / NIR spectrophotometer. The temperature was controlled using a Quantum Northwest external temperature controller, which drives

a Peltier heat pump attached to both the sample and reference holders. Thermocouples in the sample holder are used to provide feedback to regulate the sample temperature. To help control the temperature, a circulating bath of water was attached to the sample holder. The dilute solutions (~10 μg/mL) were placed in quartz cuvettes, other conventional materials (e.g. glass) would block the passage of UV light, for measurements. The polymer solutions were heated to 105 °C to make sure the polymers were fully dissolved. The solutions were then cooled from 105 °C to room temperature in increments of 10 °C. The solutions were allowed to equilibrate at each temperature before each absorption spectrum was recorded. The order-disorder transition of some polymer, such as P(LAcDOT) shown in Figure 2.5a as opposed to P(BAcDOT) shown in Figure 2.5b, is proposed to occur in three steps when the temperature is decreased: (a) planarization of the disordered phase, (b) aggregate formation, (c) planarization of the aggregated phase.[146]

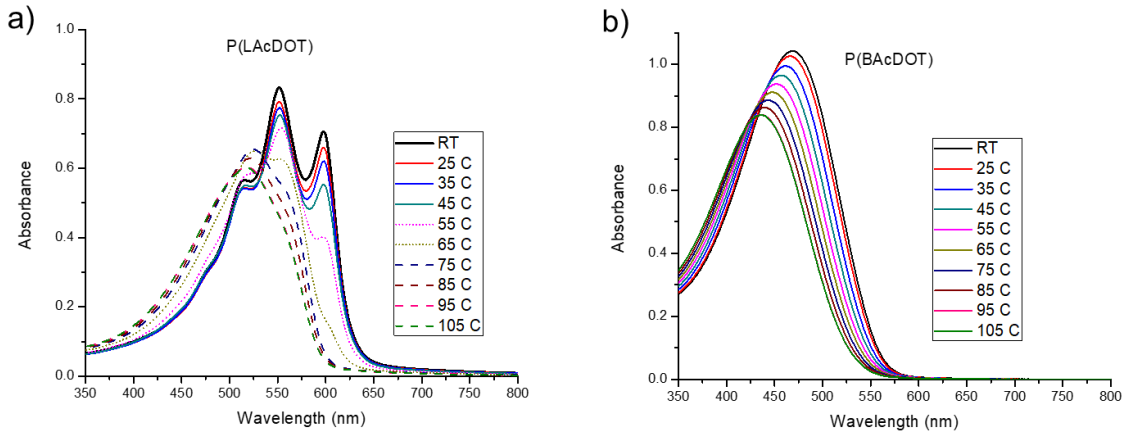

Figure 2.5. a) Temperature-dependent UV-Vis absorption spectra showing spectral changes of P(LAcDOT) and b) P(BAcDOT) as the polymer solution is heated from room temperature to 105 °C.

2.11 Thermal characterization (TGA and DSC)

Thermogravimetric analysis (TGA) is used to characterize a polymer's thermal stability for research, development, and quality control. TGA measures the amount and rate of change in the mass of a sample as a function of temperature and time in a controlled atmosphere. The measurements are used primarily to determine the thermal and/or oxidative stabilities of materials as well as their compositional properties. The technique can analyze materials that exhibit either mass loss or gain due to decomposition or impurities such as residual solvents or starting materials. In this dissertation, the thermal decomposition temperature was determined as the temperature in which the polymer lost 5% of its total weight. TGA measurements were carried out on a PerkinElmer Pyrus 1 using 5-10 mg of sample in a Pt pan, heated at a rate of 10 °C/min from 50 °C to 600 °C under a nitrogen chamber (20 mL/min). The polymers synthesized in this dissertation have high thermal stability, with high decomposition temperatures (defined as the temperature at which ~ 5 % of the sample weight is lost), Td > 2750 °C as shown in Figure 2.6a.

Once the decomposition temperature for each polymer was established by TGA, differential scanning calorimetry (DSC) was performed using a TA Instruments Q200 to study thermal and phase transitions. For amorphous and semi-crystalline polymeric materials, a morphological change occurs first at the glass transition temperature (T_g), where the polymer changes from brittle glassy state to an elastic material to due to greater segmental chain motions at an elevated temperature. The value of Tg is dependent on various factors such as the molecular weight, presence of moisture, and impurities.Materials can also possess a melting temperature (T_m), which occurs at a higher temperature than T_g. T_m is the temperature at which the crystallites in the polymer melt due

to heating. The difference between T_m and T_g is that T_m is a first order transition involving both changes in heat capacity and latent heat. At some temperature above the T_g, the polymer chains would have enough energy to form ordered arrangements and undergo crystallization (T_c). The T_g and T_m usually occur during the heating of the polymers as endothermic events. The reverse process (cooling) is exothermic and is associated with the Tc and reformation of the glass. It is worth noting that not all polymers undergo all three transitions. In fact, amorphous polymers to not have a T_m and T_g.

DSC measurements were conducted by loading 5-10 mg of sample into an aluminum pan and sealing it hermetically with an aluminum lid to determine thermal transitions between -50 °C and below the decomposition temperature as determined by TGA. The samples were scanned for three cycles at a rate of 10 °C/min, the first cycles were used to erase the thermal history of the sample to remove inconsistencies between samples, while the last two cycles were used to determine the reproducibility and stability of any thermal transitions. The DSC cycles reported in this dissertation will include the cycle number that is studied. Figure 2.6b, highlights a set a family of polymers studied in Chapter three. One of the polymers synthesized shows a glass transition temperature (Tg) and melting (Tm) and crystallization (Tc) transition temperatures.

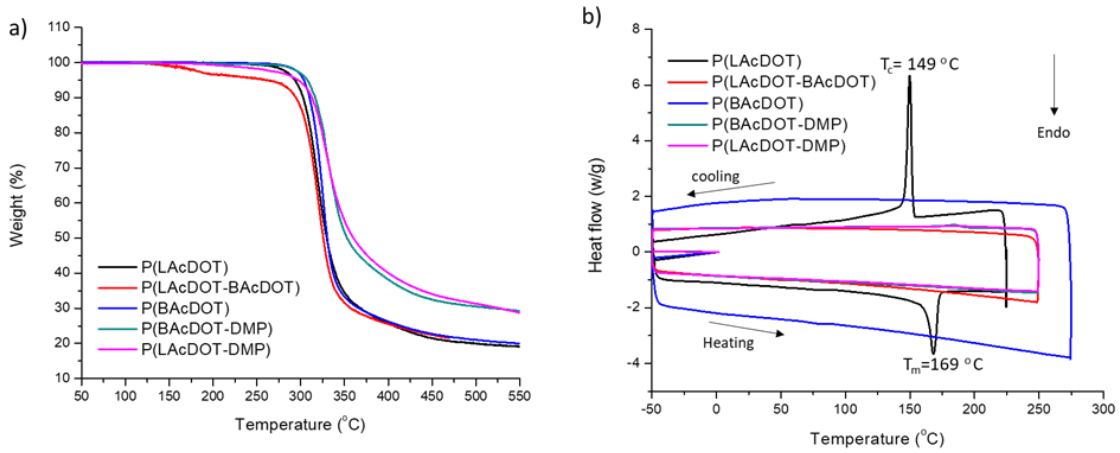

Figure 2.6. a) TGA studies performed at a rate of 10 °C/min and b) the third cycle DSC thermogram for five polymers reported in this dissertation in Chapter 3 performed at 10 °C/min.

CHAPTER 3. EFFECTS OF LINEAR AND BRANCHED SIDE CHAINS ON THE REDOX AND OPTOELECTRONIC PROPERTIES OF 3,4-DIALKOXYTHIOPHENE POLYMERS AND COPOLYMERS

3.1 Introduction

Conjugated polymers have developed rapidly due to their promising applications in low-cost, lightweight, and flexible electronics, such as organic field-effect transistors (OFETs)[147-148], light-emitting diodes (OLEDs)[149-150], organic photovoltaics (OPVs)[151-152], and electrochromic devices (ECDs). Thorough structure-property relationships for these materials have been established, and as a result, the performance of conjugated polymers has steadily improved and commercial applications are seemingly imminent. This is especially true in the field of organic photovoltaics, where power conversion efficiencies exceeding 10% has been achieved, in part due to an improved understanding of how polymer backbones and side chains can be engineered for better device performance.[153] In parallel, solution-processable dioxythiophene (XDOT) based polymers have been extensively researched for ECDs[44] due to their wide color range (optical band gap), low oxidation potentials, and high optical contrast between their vibrantly colored charge neutral states and their transmissive oxidized states.[4, 17] Through backbone engineering, a series of polymer representing the complete color palette with fast switching times, low switching voltage, and long switching cycles have been achieved.[17, 23, 64, 66, 78, 154-156] However, beyond processing considerations, the effects of side chains on the properties of electrochromic polymers have been minimally investigated. [26, 157]

An early attempt to understand the influence of side chains on the optoelectronic properties of XDOT polymers was performed in 1998.[20] This study focused on alkyl-substituted and unsubstituted poly(3,4-alklenedioxythiophene)s, where the size of the alkylenedioxy ring or the side chains were varied.[20] It was shown that increasing the ring size, or the size of the side chains, influenced the electrochromic contrast and the electrochromic switching time. However, it was difficult to differentiate which effects could be attributed to the size of the bridging ring, and which were purely the result of side chain differences. In 2004, four new ProDOT-based polymers, synthesized by Grignard metathesis, were reported.[4] In this study, the size of the alkylenedioxy ring was consistent across all polymers, while the side chains were either linear or branched. The polymer films were able to switch reversibly from a dark indigo to a transmissive sky-blue state upon oxidation with sub-second kinetics and electrochromic contrast ranging from 40-70%. The study revealed that polymers, in this system, with branched side chains had faster switching times when compared to the polymers with linear side chains. In 2011, a similar study was conducted by the Sotzing group.[104] They synthesized and reported four polymers with the same propylenedioxy ring but varied side chain structures.[104] The polymers with *tert*-butyl, hexyl, isopropyl, or methyl groups as the side chains distorted the backbone planarity to varying degrees, resulting in polymers films with colors ranging from yellow to purple.[104] However, these polymers were insoluble in common solvents.

The first study to focus on side chains effects in acyclic dioxythiophene (AcDOT) was reported in 2010.[98] The homopolymer 3,4-bis(2-ethylhexyloxy)-thiophene P(BAcDOT) and a random copolymer of 3,4-bis(2-ethylhexyloxy)-thiophene and 3,4-dimethoxythiophene (DMT) P(BAcDOT-DMT) were synthesized by oxidative

polymerization.[98] The branched alkoxy side chains on the P(BAcDOT) were reported to distort the backbone planarity, resulting in an orange polymer with an optical band gap of 2.04 eV and an absorption maximum (λ_{max}) at 483 nm in the colored (neutral) state. On the other hand, the random incorporation of DMT units into the backbone reduced the steric interactions, lowering the band gap slightly to 2.00 eV and shifting the λ_{max} significantly to 525 nm, resulting in a red polymer. When the switching speeds of the two polymers were compared, the red polymer had a switching speed of 2.3 seconds, while the orange polymer had a switching speed of 5.3 seconds. In this study, switching speeds correspond to the kinetics of an optical transition from the neutral (colored) state to a fully oxidized (colorless) state for films with an optical density of 0.98, measured at t_{95}. The electrochromic contrast, the difference in percent transmittance between two redox states, was 60% for the red polymer and 48% for the orange polymer. The slower switching time and lower electrochromic contrast for the orange polymer were surprising. In ProDOT based polymers, larger-inter chain separation, due to the side chain size or length, has been shown to enhance electrochromic contrast by minimizing charge carrier band tailing into the NIR and switching speed by promoting more effective counter ion diffusion through the film.[4, 21] With this logic, the orange polymer should have had a faster switching time and higher electrochromic contrast. In comparison to other XDOTs (ProDOT and EDOT), AcDOTs have received the least amount of research and have shown relatively poor electrochromic performance.

3.2 Design Principles

To understand how side chains affect optoelectronic properties in XDOTs, a series AcDOT homopolymers and copolymers with linear and/or branched side chains were

designed and synthesized. These materials were characterized and studied to extract structure-property relationships. Within this family of polymers, three of the materials were designed to have i) an AcDOT conjugated backbone, ii) the same number of carbon atoms (eight) in the alkoxy side chains, and iii) different ratios of linear and branched side chains. To gain further insight into the side chains steric interactions and associated optoelectronic consequences, the linear and branched AcDOT monomers were copolymerized with 3,3-dimethyl-3,4-dihydro-2H-thieno[3,4-b][1,4]dioxepine (DMP). DMP was chosen because polymers based on this repeat unit have shown adequate color contrast, long term redox cyclability, and a coplanar backbone.[23, 78]

As illustrated in Scheme 3.1, it was hypothesized that: (1) Branched side chains would induce torsional strain between aromatic rings due to the large van der Waals radii in the branching position.[78] (2) This strain leads to a decrease in the effective conjugation length, giving rise to higher energy (lower wavelength) absorption transitions. (3) In DMP copolymers of branched AcDOT systems, steric interaction would be reduced, resulting in an increased effective conjugated length and a bathochromic shift of the optical transition.

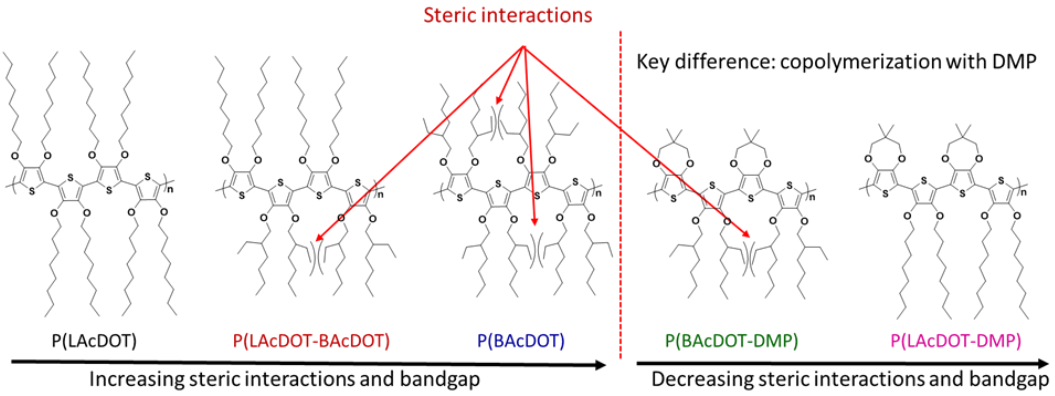

Scheme 3.1 Chemical structures of the XDOT polymers synthesized either direct hetero arylation polymerization or oxidative polymerization, with varying steric interactions between adjacent units.

3.3 Synthesis of Monomer and Polymers

The monomers were synthesized through a transetherification route. The method proceeds *via* nucleophilic aromatic substitution of the 3,4-dimethoxythiophene with the appropriate diol in the presences of a catalytic amount of *p*-toluenesulfonic acid (*p*-TSA), yielding the desired monomers shown in the experimental section below. The repeat unit structures of the polymers, shown in Scheme 3.1, were synthesized via direct (hetero)arylation polymerization (DHAP) or oxidative polymerization; detailed synthetic routes are outlined in the experimental section below.[98, 127-128, 130-133] The ^{1}H-NMR and elemental analyses correspond to the expected repeat unit structure, theoretical chemical composition, and high purity, as shown in Figure 3.9 in the experimental section. The molecular weights of the polymers were estimated by gel permeation chromatography (GPC) in tetrahydrofuran (THF) or chloroform ($CHCl_3$), Figure 3.10 in the experimental section. The results, summarized in Table 3.1, indicated that all the polymers are of sufficient molecular weight (M_n ranging from 5 kDa to 44 kDa) likely correlating with a degree of polymerization above 10, where optical properties are thought to become independent of molecular weight. As demonstrated by Meier et al., the absorption energy of π-conjugated polymers depend on molecular weight until the maximum effective conjugation length (ECL) is reached.[158] This "length" is based on the number average repeat unit and is typically achieved at ~10 rings for polythiophenes. The range in molecular weights of the polymers synthesized in this work is due to differences in the solubility, as dictated by the side chain and backbone structure. It is suspected that the lower molecular weight of P(LAcDOT-DMP) relative to the other polymers is due to the decreased conformational entropy of the LAcDOT and DMP monomer, resulting in a lower

overall solubility of the copolymer in the reaction medium and thus limiting the propagation of the polymer chain. The high molecular weight of P(BAcDOT), on the other hand, is attributed to the branched side chains which prevents the precipitation of low molecular weight compounds early in the polymerization. Another reason for the molecular weight range may involve polymerization methods. DHAP is sensitive to stoichiometric imbalance of constituent comonomers, while oxidative is not.

Table 3.1. Molecular weights of the polymers obtained via GPC.

Polymer	Mn (kDa) [a]	Mw (kDa) [a]	$Đ$ (M_w/M_n) [a]	X_n [c]
P(LAcDOT)	15	32	2.2	43
P(LAcDOT-BAcDOT)	16	42	2.6	23
P(BAcDOT)	44[b]	138[b]	3.0[b]	130
P(BAcDOT-DMP)	15	31	2.1	28
P(LAcDOT-DMP)	5	7	1.4	10

[a] The molecular weight information was determined by GPC in $CHCl_3$ at 40 °C calibrated *vs.* polystyrene standards. [b] Values obtained from GPC in THF at 35 °C calibrated *vs.* polystyrene standards. [c] Values calculated from corresponding GPC results and repeat unit mass.

3.4 Results

3.4.1 Electrochemical properties

To investigate the electrochemical properties of the polymer series, the polymers were dissolved in toluene at 1.0 mg/mL, except for P(LAcDOT) which was dissolved in toluene at 0.5 mg/mL. From these solutions, 4.0 μL (8 μL for P(LAcDOT)) of each solution was drop-cast on glassy carbon electrodes and then electrochemically cycled between −0.5 V and 0.8 V (*vs.* Ag/Ag^+) twenty-five times to condition the films to the influx of electrolyte (referred to as electrochemical annealing, or break-in).[159] After repeated electrochemical cycling, the polymers are thought to assume their lowest energy

conformation in their charge neutral states. Following the electrochemical break-in, the films were used to determine the onset of oxidation by differential pulse voltammetry (DPV); the results are presented in Table 3.2.

Table 3.2. Optical and electrochemical properties of the studied ECPs.

Polymer	E_{ox}[a] (V *vs.* Ag/Ag^+)	λ_{max}[b] (nm)	$E_{g,opt}$[b]
P(LAcDOT)	0.05	513, 551, 598	1.98
P(LAcDOT-BAcDOT)	0.25	535, 583	2.01
P(BAcDOT)	0.33	466	2.13
P(BAcDOT-DMP)	0.01	545, 593	1.97
P(LAcDOT-DMP)	-0.30	560, 611	1.89

[a]Values determined by DPV as the onset of the anodic peak. [b]For films cast onto ITO-coated glass. [b]Bandgap determined by the high-energy onset of light absorption from thin films.

From the results in Table 3.2, it is apparent that the onset of oxidation can be readily controlled by increasing the steric interaction through branched side chains. To understand the results, first focus on the P(LAcDOT), P(LAcDOT-BAcDOT), and P(BAcDOT), which are expected to show progressively more steric interactions by the incorporation of more branched side chains. In this series, the E_{ox} substantially increases from +0.05 V to +0.25 V, then to +0.33 V. The increase in oxidation potential is attributed to the steric hindrance from the branched side chains, which cause the thiophene rings to partly twist out of the plane, even in their conditioned state. This results in a greater ionization potential, thus requiring a higher voltage to oxidize the material.[23, 64, 78] The same trend is preserved when the BAcDOT and LAcDOT monomers are copolymerized with DMP. P(LAcDOT-DMP) has an oxidation potential at -0.30 V, while the oxidation onset for P(BAcDOT-DMP) is +0.01 V. P(BAcDOT-DMP) has a higher onset of oxidation due to the presence of branched side chains, which increase steric interactions and distort backbone

planarity.[139] Looking more closely to the XDOT polymers, it is apparent that the polymers with DMP have an overall lower onset of oxidations than the other XDOT polymers comprising exclusively AcDOT units. The difference in oxidation potential can be explained as an intricate yet subtle interplay of steric and electronic factors in the π-system. Broadly speaking, the DMP unit is more electronically rich and less sterically hindered when compared to the AcDOT unit due to the propylene bridge in the DMP, hence the overall lower onsets of oxidation in the DMP-based materials.[20, 42-43, 75]

3.4.2 Optical properties

To allow for direct comparison of the optical switching properties between several films, measurements of optical density rather than film thickness was used.[98, 160] Once the polymer was spray cast to a thickness corresponding to an approximate absorbance of ~1.0 a.u., the films were electrochemically conditioned for 25 CV cycles. After break-in, some of the absorbance profiles were red-shifted relative to the pristine states, as shown by the color change in Figure 3.2a. This break-in phenomenon is attributed to the incorporation of solvent molecules and ions into the films, causing morphological changes.[159] After break-in, the normalized spectra of each thin film, shown in Figure 3.2b, were analyzed and compared for more insight into the structural difference imparted by the specific side chain structure. The optical band gaps follow the expected trend based on steric interactions resulting from branched side chain content. From this trend, P(BAcDOT), an orange polymer with a λ_{max} at 466 nm is the most blue-shifted. This is followed by P(LAcDOT-BAcDOT), a magenta-colored polymer with 50% linear side chains and a λ_{max} at 535 nm, and P(LAcDOT), a purple-colored polymer with 100% linear side chains and a λ_{max} at 551 nm as shown in Figure 3.2b. Copolymerization of the AcDOT monomers with DMP

resulted in polymers that absorb lower energies (longer wavelength of light), resulting in dark-magenta and dark-purple colors respectively, as shown in Figure 3.1a and 3.1b.

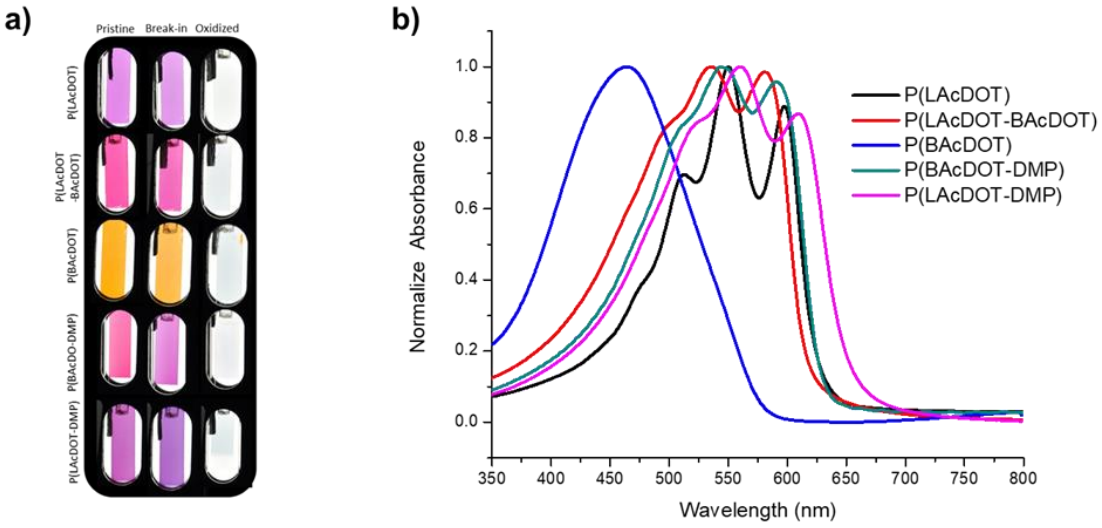

Figure 3.1. a) normalized absorption spectra comparing all five polymers on ITO-coated glass in 0.5 M $TBAPF_6$/PC electrolyte solution normalized to an optical density of 1.0. b) Photographs of the films in their pristine, post break-in (-0.5 V), and oxidized states (+0.8V), all on ITO-coated glass in a three-electrode cell setup.

3.4.3 Electrochromic contrast

All the polymers studied exhibit desirable electrochromic contrast, between 54% and 73%, as shown in Table 3.3, switching from a vibrant colored state to a highly transmissive state. This has been attributed to the electron-rich nature of XDOTs, where the oxygen groups in the β-positions impart stabilization to the oxidized form, red-shifting the overall absorption when it is fully oxidized.

Table 3.3. L*a*b* color coordinates for all polymers in the neutral and transmissive states and total change in contrast upon switching

Polymer	Δ%T[a] (at λ_{max})	neutral state L*, a*, b* color coordinates[b]	oxidized state L*, a*, b* color coordinates[b]	t_{95} [b] colored to bleach (s)	t_{95} [b] bleach to colored (s)
P(LAcDOT)	73	59, 47, -30	94, -1, -3	2.4	2.5
P(LAcDOT-BAcDOT)	66	55, 63, 1	88, -3, -6	2.4	4.3
P(BAcDOT)	54	86, 34, 78	86, -4, -6	3.6	10.6
P(BAcDOT-DMP)	72	52, 53, -22	90, -2, -4	1.8	2.1
P(LAcDOT-DMP)	61	44, 40, -26	88, -4, -6	1.8	1.8

[a]Difference between steady-state transmittance at λ_{max} measured at fully oxidized and fully neutral states. [s]Switching speed reported corresponds to the time required to reach 95% from fully colored to oxidized (clear), and fully oxidized (clear) to colored for films cast onto ITO-coated glass.

This is illustrated in Figure 3.3a where all the polymers are able to transition to NIR-absorbing states with minimal absorption in the visible spectrum. It is important to note that P(BAcDOT), the polymer with the most blue-shifted absorbance spectrum, has the most tailing into the visible region of the spectrum. This results in a perceptible pale blue color in the fully oxidized state. The tailing into the visible is decreased as more linear side chains are incorporated into P(LAcDOT-BAcDOT) and P(LAcDOT). It is hypothesized that the increase in tailing (hence reduction in electrochromic contrast) is due to the steric interaction from the branched side chains, which disrupt the sulfur and oxygen interaction by twisting the polymer backbone slightly out of plane in the oxidized state. Studies have shown that S-O interactions between neighboring XDOT repeat units can red-shift absorption by inducing planarization.[161] When the AcDOT monomers are copolymerized with DMP, the results do not follow the trend of the other three polymers. In the oxidized state, the bipolaron band from the most sterically hindered polymer

P(BAcDOT-DMP) has less tailing than P(LAcDOT-DMP). This inconsistency in the amount of tailing is due to the fact that P(BAcDOT-DMP) was sprayed to a higher optical density than P(LAcDOT-DMP). Since electrochromic contrast is a property that is dependent on the amount of chromophore present on the electrode, in this situation, increasing the optical density beyond 1.0 a.u. increases electrochromic contrast.[162-163]

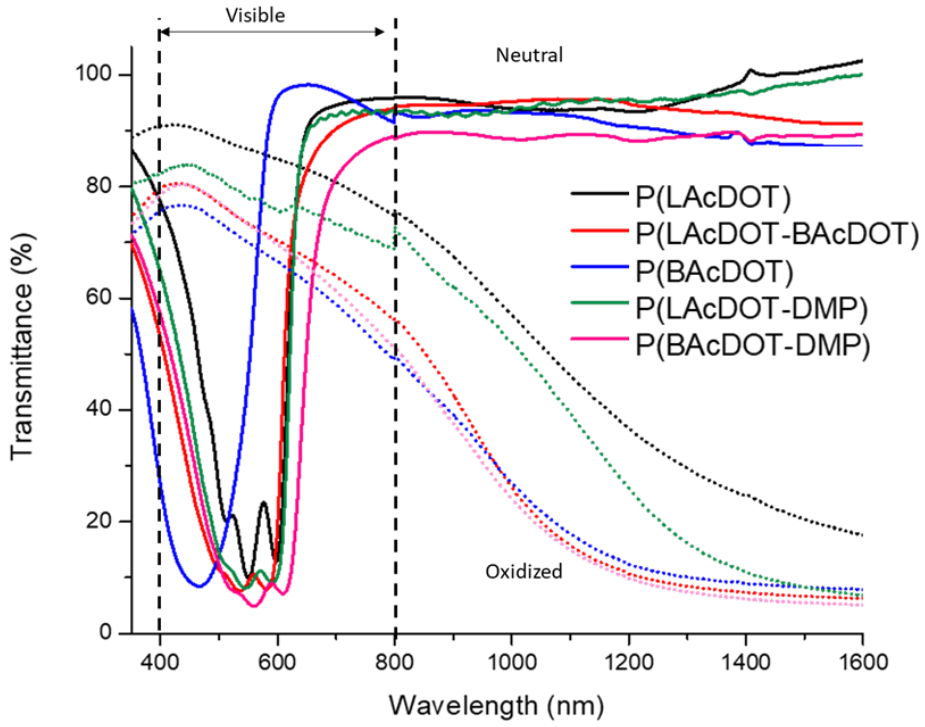

Figure 3.2. Transmittance spectra (without normalization) of the polymers in the charge neutral state and oxidized states.

The most common way to assess electrochromic contrast is to monitor the change in transmittance ($\Delta T(\%)$) at λ_{max} as a function of time by applying square-wave potential steps. For these polymers, the potential was switched from -0.5 V to +0.8 V with residence time of 60, 30, 10, 2, and 1 s. As shown in Figure 3.3b, all the polymers are able to switch with their highest contrast at 10 seconds or greater. At switching times less than 10 seconds,

the overall electrochromic contrast decreases due to diffusion limiting process or electron transfer kinetics.

3.4.4 Spectroelectrochemistry

Spectroelectrochemistry was carried out on all of the polymers in the same three-electrode set-up. During the spectroelectrochemical measurement, the desired potential was applied to the film and held at that potential until the absorbance measurements were taken. The applied potential was increased by 0.1 V increments, starting with -0.5 V to +1.1 V, the highest stable potential as determined by the CV. Looking at the spectroelectrochemical data as shown in Figure 3.4, all the polymers with branched side chains (Figure 3.3b, 3.3c, and 3.3d) have a large optical change in both the visible and NIR between a small potential step of 0.1 V. The sudden changes for P(LAcDOT-BAcDOT), P(BAcDOT), and P(BAcDOT-DMP) occur between +0.3 and +0.4 V, +0.4 and +0.5 V, and -0.3 and -0.4 V, respectively. This differs from the polymers with linear side chains, P(LAcDOT) and P(LAcDOT-DMP), where the oxidation proceeds more gradually as a function of potential, as seen in Figure 3.3a and 3.3d. The sudden optical changes in absorbance have been observed in other polymer systems.[8, 98, 139] This large change in optical absorption over a small voltage range may be due to a cooperative intramolecular domino effect similar to the "twistons" effect, which can be considered delocalized conformation defects.[78, 98, 164-165] In the neutral state, the polymer exists in a nonplanar (less conjugated) form. When a small positive potential is initially applied, the polymer chain resists planarization. However, as the applied potential is increased, localized planarization begins to occur, which has a cooperative domino effect on neighboring repeat units, resulting in a sudden change in color.[166-167]

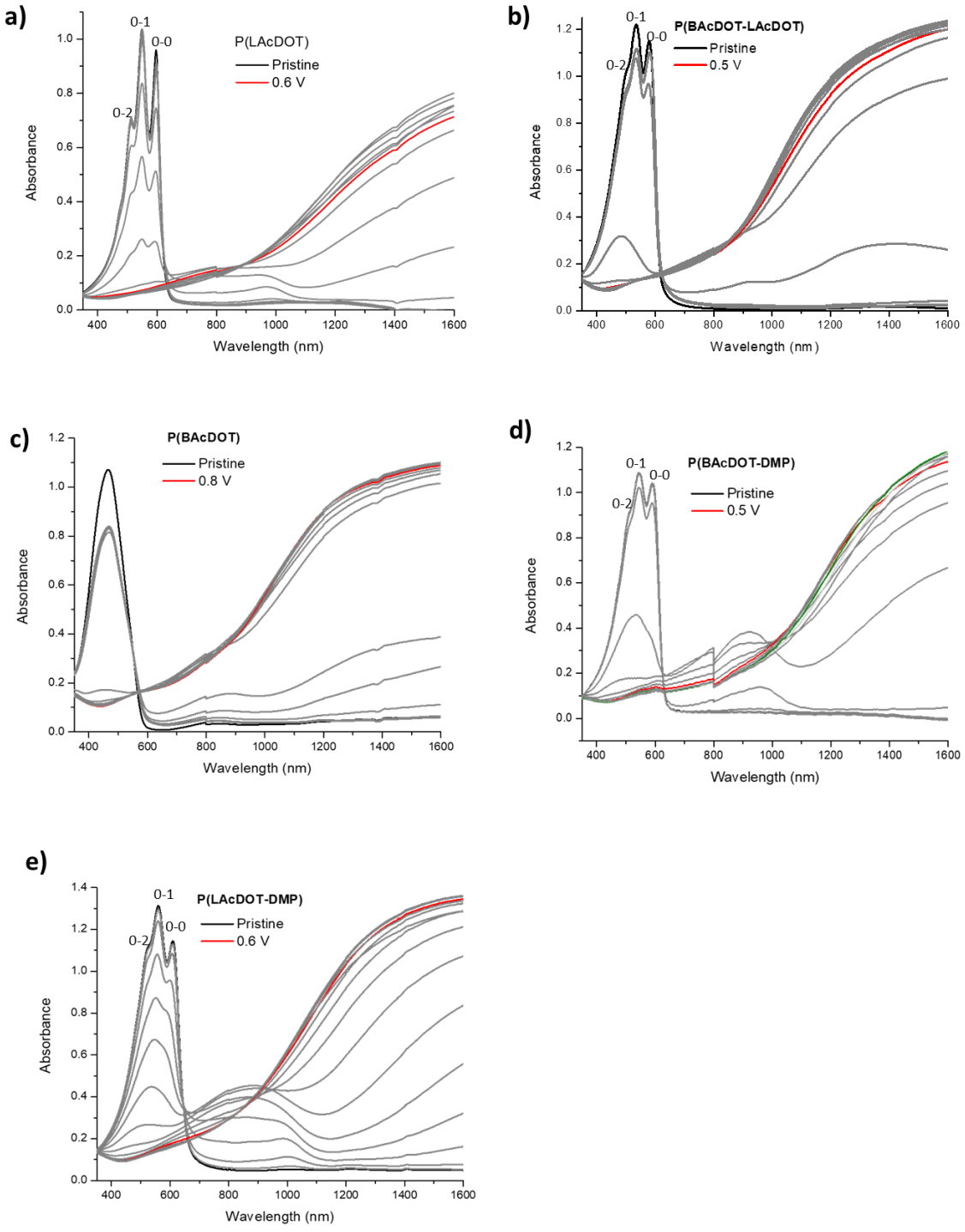

Figure 3.3. Spectroelectrochemistry of a) P(LAcDOT), b) P(LAcDOT-BAcDOT), c) P(BAcDOT), d) P(LAcDOT-DMP), e) P(BAcDOT-DMP). The applied potential was increased by 100 mV steps between the fully colored and bleached states in 0.5 M $TBAPF_6$/PC.

A careful comparison of the spectroelectrochemical data for the polymers reveals that steric interactions from the side chains influence the presence of vibronic fine structures in the solid state. P(LAcDOT) has three distinct vibronic peaks at 513 nm, 551 nm, and 598 nm while P(LAcDOT-BAcDOT) has two vibronic peaks at 535 nm and 583 nm. When the branched side chain percentage is increased to 100% in P(BAcDOT), the resulting absorbance spectra do not show any vibronic features. The same trend is seen in P(LAcDOT-DMP) and P(BAcDOT-DMP), where P(BAcDOT-DMP) shows a decrease in vibronic coupling as well as intensity in the peaks. This result supports the idea that the absence of vibronic fine structure indicates that the films are more disordered, and that steric interaction can be used to tune order/disorder in conjugated polymers. Furthermore, spectroelectrochemical data suggested preferential doping of H-aggregated species when the ratio of 0-0, and 0-1, transitions during oxidation is compared. [168-169] The only exception is P(BAcDOT) which appears amorphous and shows no fine structure throughout the doping process.

3.4.5 Colorimetry

One of the most important parameters used to characterize ECPs is color, however, color is subjective to interpretation since the perception of color varies between individuals. For valid comparisons, the CIE L*a*b system, established by the International Commission on Illumination (Commission Internationale De L'Eclairage, or CIE), was used to track the changes in color during the oxidation process. In the (a*,b*) plot, Figure 3.5a, polymers show high values of a* and b* in the as-sprayed state, which is indicative of colorful neutral state. Upon electrochemical conditioning, polymer chains reorganize, leading to color changes for all polymers. This effect is more drastic in P(BAcDOT-DMP),

where the as-sprayed polymer has +b* at 10 and +a* at 60, after electrochemical switching, the color coordinates change to -b* at 20 and +a* at 50 resulting in a color change from magenta to purple. This change is also is reflected by shifts in λ_{max} and $E_{g,opt}$. After electrochemical conditioning, the potential is increased by 0.1 V and the color at each potential is recorded. Increasing the potential leads to the (a*,b*) values approaching the origin, which indicates that the polymers are becoming progressively more transmissive. The lack of color is also observed in the change in L* values, the dark to light component, as a function of potential, shown in Figure 3.5b.

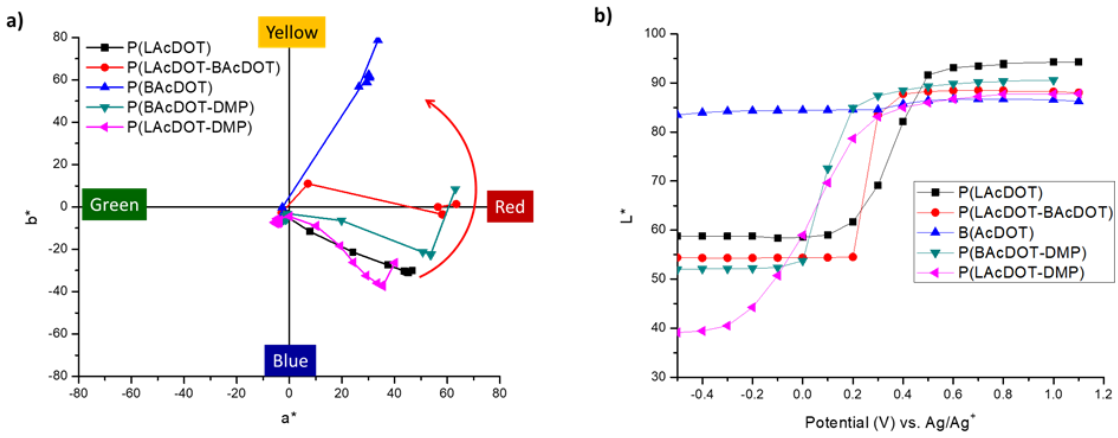

Figure 3.4. a) (a*,b*) diagram of the polymers, showing the color changes occurring during electrochemical oxidation. b) The L* value for each material shown as a function of the applied potential.

3.4.6 Chronoabsorptiometry

To determine how the side chains affect the switching kinetics in spray-cast films, the Δ%T was monitored during the application of a square wave potential as shown in Figure 3.6. The potential square waves were executed between −0.5 V (neutral state) and +0.8 V (fully oxidized state) with various potential residence times of 60s, 30 s,10 s, 2 s, 1 s, followed by another 30 s, as shown in Figure 3.5 a-e.

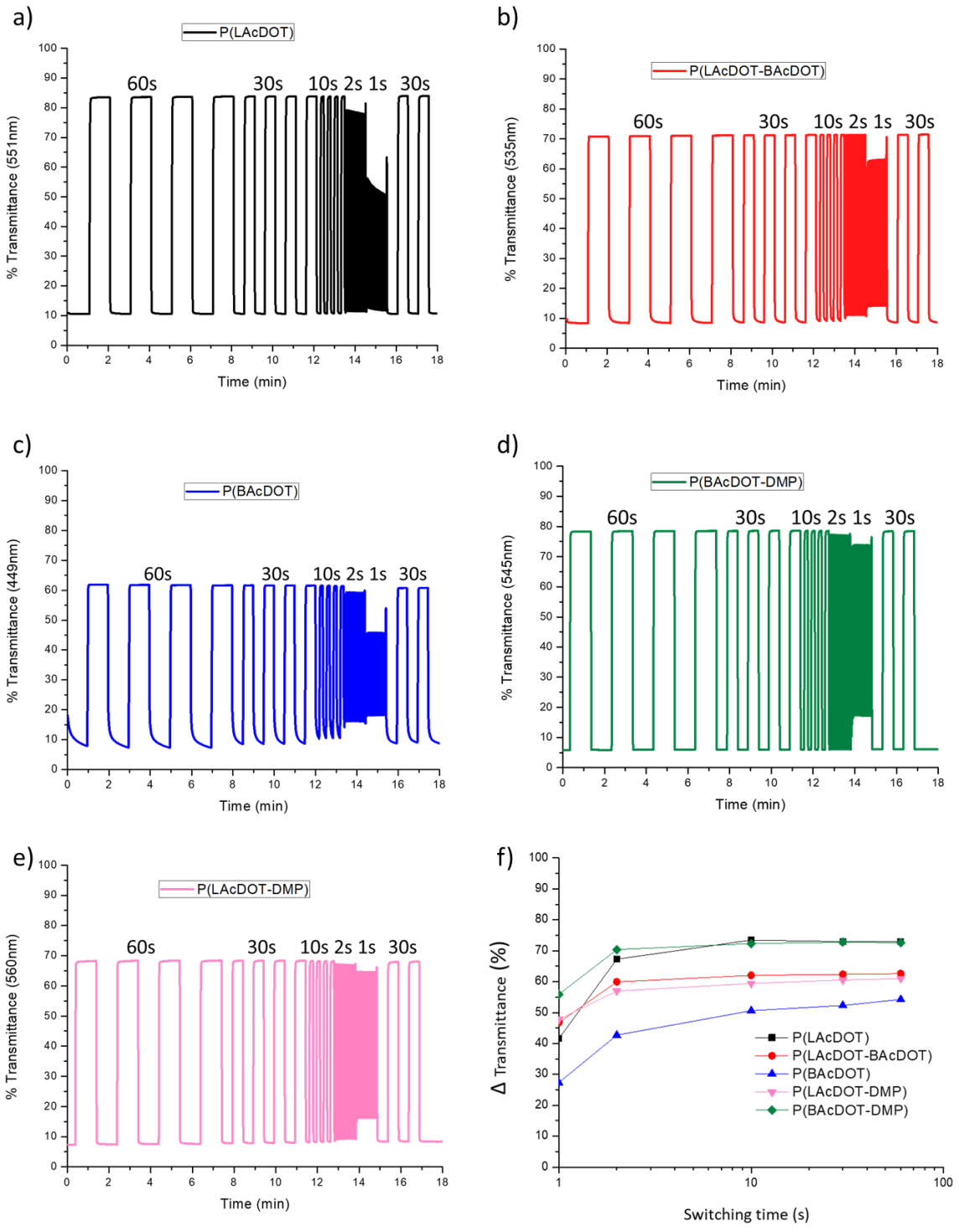

Figure 3.5. a) Chronoabsorptometry of all the polymers(a-e) in 0.5 M $TBAPF_6$/PC electrolyte solution measured at λ_{max}. All the polymers were switched between -0.5 V and +0.8 V for periods ranging from 60 seconds to 1 second. f) ΔT at λ_{max} of each polymer as a function of switching time from 60 seconds to 1 second.

The switching speeds for the polymers were reported as the time required for the polymer to reach 95% of full contrast upon bleaching and coloring during the 60 s switching period, as shown in Figure 3.5f for P(LAcDOT) and P(BAcDOT). As shown in Table 3.3, the polymers switched between 1.8 s to 3.6 s, going from color to bleach, and 1.8 s to 10.6 s from bleach to color. With the exception of P(LAcDOT-DMP), the polymers have faster bleaching than coloration. It is hypothesized that dedoping of the polymer is slower due to the injection of electrons to charge balance the polymer at the polymer electrode interface. Making it insulating and slowing dedoping of the rest of the film, hence slower coloration. Taking a closer look at the switching speeds, P(LAcDOT) has the fastest coloring time of 2.5 s. Increasing the steric interaction by incorporating 50% of the branched side chains increases the coloring time to 4.3 s. When the polymer has 100% branched side chain, the coloring time is even slower at 10.6 s. When the AcDOT monomers are copolymerized with DMP, the overall coloring time is faster when compared to the other three AcDOT polymers, but the material with the branched side chains still has a slower coloring time. While the structure-property relationships affecting switching speed is not fully understood, there are several consistent trends among the AcDOT and ProDOT family. Polymers containing branched AcDOTs display slow redox switching between the reduced and oxidized states, while polymers containing ProDOTs are faster.[23]

3.4.7 Switching stability of P(LAcDOT)

As stated earlier, previous studies involving AcDOTs have reported poor performance, especially regarding redox stability.[75, 78, 98, 139] It is unclear if the instability stems from the fact that the structure lacks a protective bridge, as in ProDOT and EDOT, or if it originates from the branched side chains. To answer this question, the long-term

switching stability of P(LAcDOT) was tested. A spray-cast film of P(LAcDOT) was prepared and placed in a three-electrode cell using the same setup as the spectroelectrochemical studies. The electrolyte solution (0.5 M $TBAPF_6$/PC) was degassed *via* argon bubbling for ten minutes in the cuvette before the working electrode, reference electrode, and counter electrode were added. The three-electrode set-up was placed in the UV-vis instrument without special sealants to prevent oxygen or moisture infiltration. The absorption spectra of P(LAcDOT) in the neutral state was taken at -0.5 V and then at its fully transmissive state 0.8V, as shown in Figure 3.6a as black lines. The film was then switched between 0.5 to 0.8 V in a chronoabsorptiometry experiment, as shown in figure 3.6b for 1,000 cycles with residence time of 10 s. Spectra of the neutral and oxidized state were recorded again after the 1,000 cycles and are shown in Figure 3.6a in red lines. Extracting the ΔT % values from the chronoabsorptiometry plot shows no change in contrast. This result demonstrates the high stability of AcDOT polymer with linear side chains. It is hypothesized that the high oxidation potential required to change P(BAcDOT) from aromatic to quinoidal form contributes to its shorter switching lifetime.

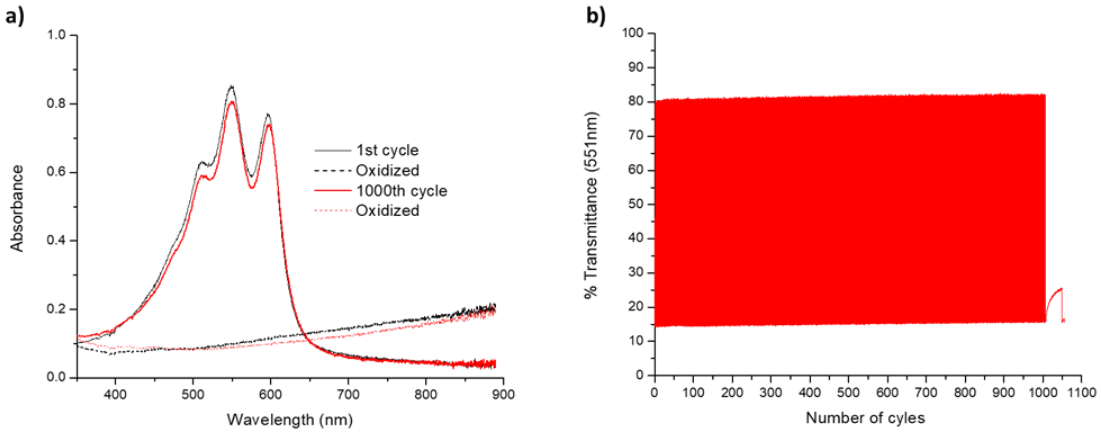

Figure 3.6. a) Absorbance spectra recorded before and after 1,000 cycles in the charge neutral (-0.5 V) and oxidized state (+0.8 V). b) Absorbance spectra of P(LAcDOT) at λ_{max} switched from the charge neutral state (-0.5 V) to the oxidized state (+0.8 V) in 0.5 M $TBAPF_6$/PC for 1,000 cycles (10 s step).

3.4.8 Aggregation effects and molecular parking of polymers

The optical spectra of conjugated polymers are composed of absorbance from the inter-chain aggregation, inter-chain aggregation, and unaggregated species. Evaluating P(LAcDOT-BAcDOT) as an example in Figure 3.7b, the polymer is fully dissolved in dilute solution. There the absorbance arises solely from intra-chain and unaggregated excitations giving rise to a broad single peak. In the solid state, where the P(LAcDOT-BAcDOT) is densely packed, the absorbance arises from intra-chain and inter-chain aggregation polymer. This is evident by the two distinct absorption peaks and a red-shift in absorbance with respect to the solution spectra, Figure 3.11 in the experimental section. On the other hand, the absorption profile of P(LAcDOT), even at a dilute solution, is nearly identical to that observed in a solid film. This indicates highly ordered aggregates as shown in Figure 3.7a. In essence, this result indicates that linear side chains in P(LAcDOT) allows the polymer to form strong π–π stacking in solution at 25 °C, resembling the molecular geometry of the highly ordered polymer chains found in solid films. This result was surprising since most XDOT polymers have featureless absorption profiles in dilute solutions.

To answer the question of what causes the formation of ordered structures in P(LAcDOT) in dilute solution, temperature-dependent UV-Vis measurements in toluene was performed. Even though the polymers dissolve more readily in chloroform than in toluene, toluene was chosen because it has a higher boiling point than chloroform (111 °C *vs.* 61 °C), which allows the study of solutions over a much wider temperature range. The polymer solutions were first heated to 105 °C, which is the maximum temperature for the apparatus as well as the temperature at which each polymer is truly molecularly dissolved. This is evident by the featureless and broad spectral shape, which is attributed to disordered chain

conformation. The polymers were then cooled from 105 °C to room temperature in increments of 10 °C. The solutions were allowed to thermally equilibrate at each temperature for ten minutes before each absorption spectrum was recorded. For P(LAcDOT) at the starting temperature of 105 °C, the spectrum has one broad peak with a λ_{max} = 510 nm. Upon cooling from 105 °C to 75 °C the broad absorption spectrum red-shifted and concurrently gained intensity (dashed lines in Figure 3.7a. The red shifts and increase in intensity have been attributed to the planarization of the disordered chains that leads to an increase in conjugation length.[146] Decreasing the temperature to 55 °C, the absorption in the higher energy region of the spectrum decreases, while three distinct vibronic peaks appear at lower energy. These vibronic peaks have been attributed to ordered chains in an aggregated phase.[146] Below 55 °C, the absorption spectrum undergoes the most significant changes. The three distinct vibronic peaks gain intensity and red-shift; this is indicated by peaks with λ_{max} = 610 nm and λ_{max} = 540 nm with a shoulder peak at 510 nm. This red-shift in the absorption is associated with a further planarization of the aggregated chains.[146] In summary, the order-disorder transition of P(LAcDOT), occurs in three steps as the temperature is decreased: (a) planarization of the disordered phase, (b) aggregate formation, (c) planarization of the aggregated phase. The other polymers also red-shift as the temperature is cooled to room temperature however the polymers do not become aggregates, as shown in Figure 3.7 b-e.

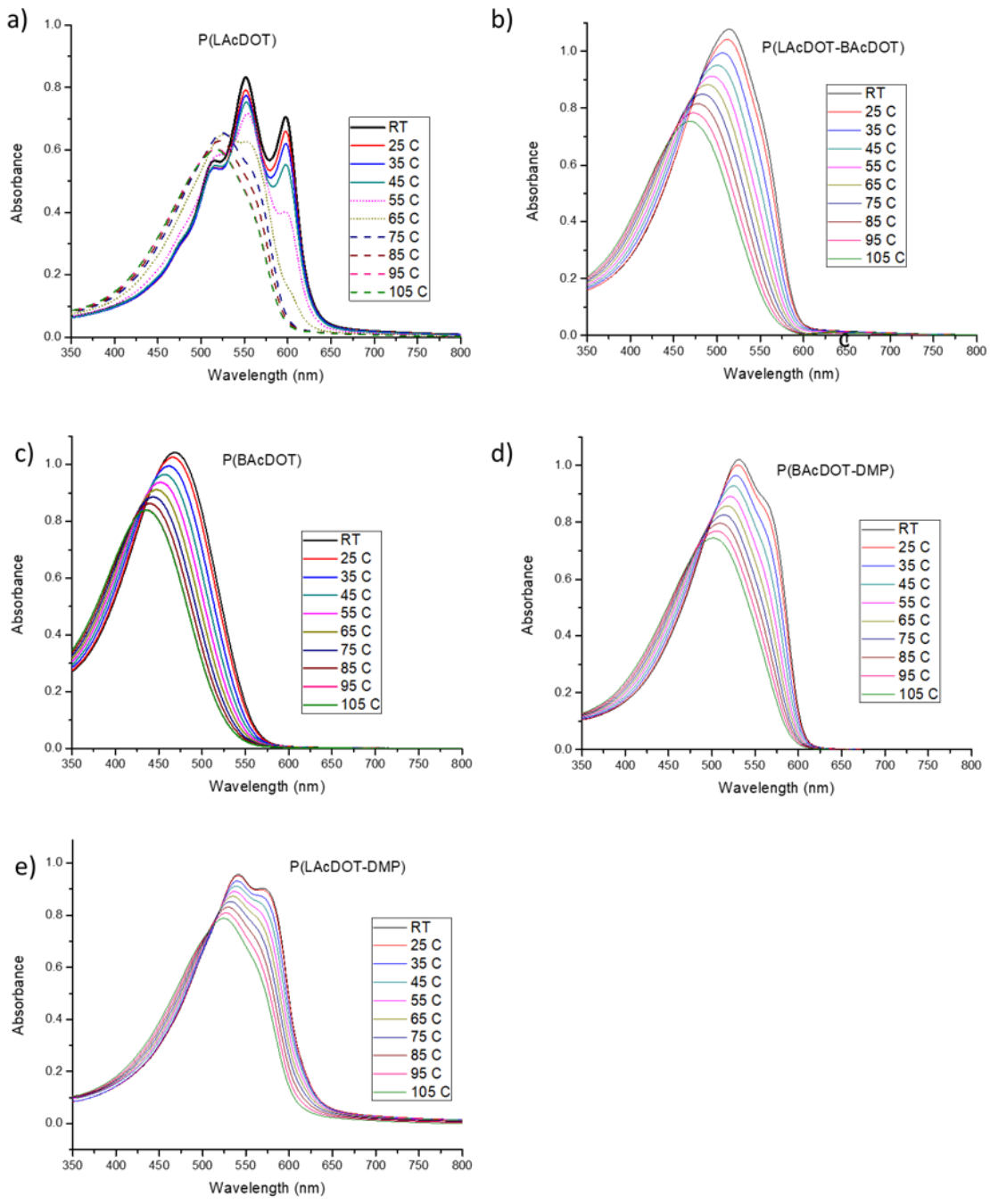

Figure 3.7. (a) Absorbance of P(LAcDOT) in toluene solution (~10 µg/mL). Spectra that correspond to the three different temperature ranges described in the text are indicated by dashed, dotted, and straight lines to show aggregate formation. (b-e) The absorbance of P(BAcDOT-LAcDOT), P(BAcDOT), P(BAcDOT-DMP) and P(LAcDOT-DMP) in toluene solution (~10 µg/mL), showing minimal changes with decreasing temperature.

The surprise from the temperature-depended UV-vis studies prompted the thermal studies on all five polymers. Thermogravimetric analysis (TGA) was performed to determine their decomposition temperatures, and differential scanning calorimetry (DSC) was used to study any thermal transitions. TGA was performed on solid samples with masses ranging from 3-5 mg in platinum pan, using a heating rate of 10 °C/min from 50 °C to 600 °C while maintaining the chamber under nitrogen. All the polymers exhibited good thermal stability with a 5% weight loss temperature in the range of 250 °C to 325 °C, as shown in Figure 3.8a. After the TGA measurements, DSC measurements were conducted by loading samples with masses ranging from 3 to 6 mg into an aluminum pan and hermetically sealing it with an aluminum lid. Thermal transitions of the polymers were scanned for three cycles at a rate of at 10 °C/min from -50 °C to temperatures below their decomposition. The first cycle was used to erase the thermal history of the samples and remove inconsistencies between samples, while the second and third cycles were used to establish reproducibly and stability. In Figure 3.8b, the third cycle thermograms for P(LAcDOT) show a melting peak temperature at 169 °C upon heating and a crystallization peak temperature 149 °C upon cooling. These peaks are a further indication of the strong intermolecular ordering in P(LAcDOT).

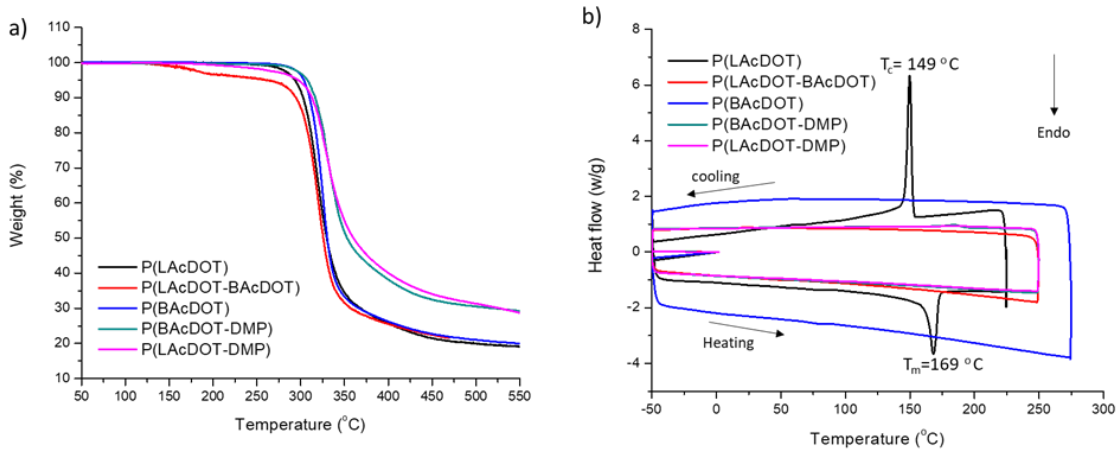

Figure 3.8. TGA studies performed at a rate of 10 °C/min and b) The third cycle DSC thermogram for five polymers reported in this dissertation in Chapter 3 performed at 10 °C/min.

3.5 Conclusion and Discussion

In this chapter, the synthesis, characterization, and structure-property relationships of on acyclic poly(dioxythiophene)s are reported. Until now, this class of materials has been marginally studied as electrochromic polymers, especially compared to its more popular counterpart ProDOT-based polymers. It was shown that varying side chain structure significantly affected solubility, the onset of oxidation, color, switching speed, electrochromic contrast, and long-term switching stability. Furthermore, varying the side chains from linear to branched decreased interchain interactions in the conjugated polymers and modified their aggregation in solution, as shown by the temperature dependent UV-vis. These results illustrate that side chains influence the optoelectronic properties of ECPs and should be considered when designing new conjugated polymer for electrochromic devices.

3.6 Experimental details

3.6.1 Reagents

Dimethoxythiophene (98%), purchased from Oxchem, and Pivalic acid (99%), purchased from Sigma, were used as received. $Pd(OAc)_2$ (98%, Strem Chemicals), K_2CO_3 (anhydrous, Oakwood Products), 18-Crown-6 (99%, Acros), and diethyldithiocarbamic acid diethylammonium salt (97%, TCI America) were all used as received. DMF (anhydrous) was purchased from EMD and used as received. DMAc (HPLC grade, Alfa Aesar) was filtered through a pad of basic alumina (Sigma Aldrich) prior to use. Methanol, acetone, toluene, and chloroform were purchased from Fisher chemicals and used without purification. Hexanes were purchased from VWR chemicals and used as received. ^{1}H-NMR and ^{13}CNMR spectra were collected on either a Varian Mercury Vx 300 MHz or 700 MHz instruments using $CDCl_3$ as a solvent. 3,3-Dimethyl-3,4-dihydro-2H-thieno[3,4-b][1,4] (DMP)[170], 3,4-(2-Ethylhexyloxy)-thiophene[98], 2,5-dibromo-3,4-bis((2-ethylhexyl)oxy)thiophene[78] and P(BAcDOT)[98] were prepared using a published methods and confirmed by ^{1}H-NMR.

3.6.2 Instrumental and measurements details

Structural characterization: ^{1}H and ^{13}C NMR spectra of monomers were collected using 300 MHz spectrometer. ^{1}H NMR spectra for the polymers were collected using the Bruker Corporation DRX 700 MHz spectrometer. The chemical shift was set based on residual $CHCl_3$ (in the $CDCl_3$ solvent) as an internal standard set to 7.26 ppm. The molecular weight and dispersity of the polymer were obtained using either a chloroform GPC at 40 °C or a THF GPC at 35 °C, both calibrated *vs.* polystyrene standards.

Differential pulse voltammograms (DPV) and Cyclic voltammograms (CV) were carried out using an EG&G Princeton Applied Research model 273A potentiostat/galvanostat under CorrWare control using a three-electrode cell with a platinum flag as a counter electrode and a Ag/Ag^+ reference electrode (filled with 10 mM $AgNO_3$, 0.5 M tetra (n-butylammonium) hexafluorophosphate (98 % Acros, recrystallized from ethanol, $TBAPF_6$), acetonitrile (ACN) as the electrolyte). The working electrode consisted of a thin film of polymer drop-casted from a 0.5-1 mg/mL toluene solution onto a platinum disk electrode (0.02 cm^2) or a glassy carbon (0.07 cm^2). The electrolyte solution was 0.5 M $TBABF_6$ in PC. The $TBABF_4$ was ≥99.0% purity and purchased from Sigma-Aldrich. The PC was anhydrous (99.7% purity) purchased from Sigma-Aldrich and used as received. All absorbance spectra were acquired using a Varian Cary 5000 Scan dual-beam UV−vis−near-IR spectrophotometer. For the spectroelectrochemistry measurements, the working electrode was a thin film of polymer sprayed from a 0.5-1 mg/mL toluene solution onto ITO glass slides (7 × 50 × 0.7 mm, sheet resistance, R_s 8–12 Ω/sq, Delta Technologies, Ltd.) using a commercial airbrush sprayer (Iwata Eclipse, Revolution Series). Prior to spraying the films, the ITO glass slides were dipped into a 10mM solution of 1-dodecylphosphonic acid (95%, Alfa Aesar) for 5 to 10 minutes. Colorimetry measurements were obtained by converting the absorbance spectras to CIELAB L*a*b* color space using Star-Tek colorimetry software using a D50 illuminant, 2-degree observer. Photography was performed in a light booth designed to exclude outside light with a D50 lamp located in the back of the booth providing illumination, using a Nikon D90 SLR camera with a Nikon 18-105 mm VR lens. Photos of the films were taken as-sprayed, after break-in at -0.5 V, and at the most transmissive oxidized state (+0.8V). The photographs are presented

without any manipulation apart from cropping. Thermogravimetric analysis (TGA) was carried out on a PerkinElmer Pyrus 1 to determine the decomposition temperature (T_d) at which chemical decomposition of the material occurs (5%). DSC was performed using a TA Instruments Q200 to determine where morphological or phase changes occur.

3.6.3 Monomer synthesis

Synthesis of 3,3-dimethyl-3,4-dihydro-2H-thieno[3,4-b][1,4]dioxepine

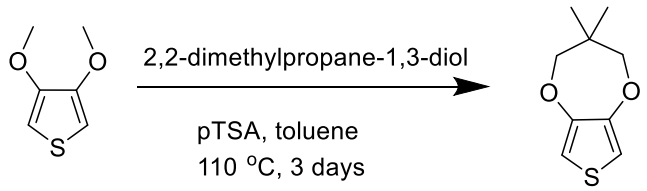

In a dry 1,000 mL round bottom flask with a magnetic stir bar, dimethoxythiophene (20.0 g, 0.138 mol) and 2,2-dimethylpropane (144.0 g, 1.38 mol) were added under argon followed by anhydrous toluene (600 mL). While the solution was stirring, *p*-toluenesulfonic acid (2.6g, 0.015 mol) was added slowly. The reaction was refluxed for three days at 110 °C. After completion, the flask was cooled to ambient temperature and quenched with 200 mL of a saturated $NaHCO_3$ solution. The organic layer was extracted 3 times with diethyl ether and dried using magnesium sulfate ($MgSO_4$). The solvent was concentrated and the crude was purified by silica gel chromatography using pure hexanes to obtain 14.300 g (55.6%) of a white solid. ^{1}H NMR (300 MHz, $CDCl_3$) δ (ppm) 6.47 (s, 2H), 3.73 (s, 4H), 1.03 (s, 6H). ^{13}C NMR (75 MHz, $CDCl_3$) δ (ppm) 149.96, 105.50, 80.07, 38.87, 21.66.

Synthesis of 3,4-bis(octyloxy)thiophene

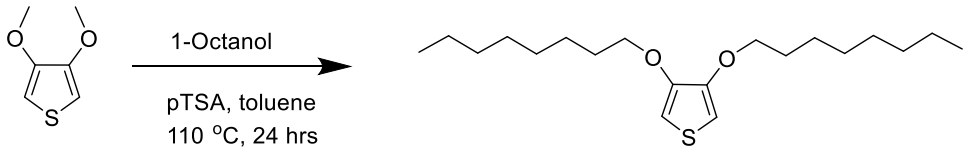

In a dry 500 mL round bottom flask with a magnetic stir bar, dimethoxythiophene (10.0 g, 0.069 mol) and 1-octanol (24.0 g, 0.185 mol) was added under argon followed by anhydrous toluene (300 mL). *p*-toluenesulfonic acid (1.3g, 0.006 mol) was added while the solution was stirring. The reaction was refluxed overnight at 110 °C. After completion, the flask was cooled to ambient temperature and quenched with 100 mL of a saturated $NaHCO_3$ solution. The organic layer was extracted 3 times with DCM and dried using $MgSO_4$. The solvent was concentrated and the crude was purified by silica gel chromatography using pure hexanes to obtain 17.800 g of a clear white solids (75%). ^{1}H NMR (300 MHz, $CDCl_3$) δ (ppm) 6.15 (s, 2H), 3.97 (t, *J* = 6.8 Hz, 4H), 1.81 (p, 4H), 1.49 – 1.37 (m, 4H), 1.31 (b, *J* = 12.7, 9.5 Hz, 16H), 0.96 – 0.81 (m, 6H).^{13}C NMR (75 MHz, $CDCl_3$) δ(ppm) 147.67, 96.93, 70.72, 31.96, 29.51, 29.41, 29.14, 26.12, 22.82, 14.26.

Synthesis of 2,5-dibromo-3,4-bis(octyloxy)thiophene.

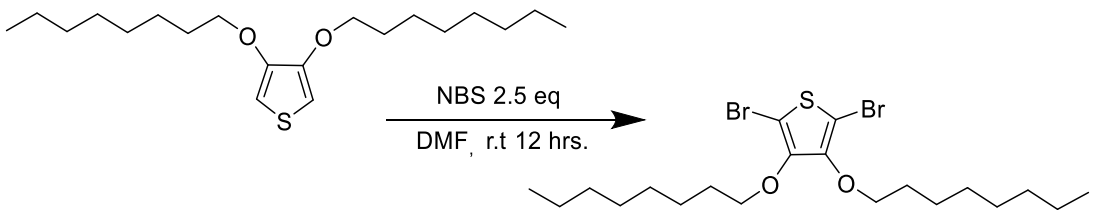

In a dry 250 mL round bottom flask with a magnetic stir bar, 3,4-bis(octyloxy)thiophene (1.000 g, 0.0029 mol) was added. The flask was then degassed before 100 mL of anhydrous DMF was added via syringe. The solution was stirred for ten

minutes at 0 °C under argon. While stirring at 0 °C, a solution of 1.340 g of N-bromosuccinimide (NBS) (0.0075 mol, 2.5 eq) in anhydrous DMF was added dropwise. The vessel was brought to room temperature and then allowed to stir for 12 hrs while covered with aluminum foil. After completion, the product was washed with brine and extracted with 200 mL of 1:1 ethyl ether/ethyl acetate. The organic layer was then washed three times with deionized water and then dried over magnesium sulfate. The solvent was removed under reduced pressure. The resulting crude oil was purified by column chromatography using hexanes on neutral silica resulting in a clear, colorless oil 1.160 g (80.3%). ^{1}H NMR (300 MHz, $CDCl_3$) δ (ppm) 4.05 (t, *J* = 6.6 Hz, 4H), 1.72 (p, 4H), 1.53 – 1.39 (m, 4H), 1.39 – 1.21 (m, 16H), 0.94 – 0.82 (m, 6H).^{13}C NMR (75 MHz, $CDCl_3$) δ (ppm) 147.75, 95.40, 74.10, 31.98, 30.08, 29.49, 29.42, 26.01, 22.81, 14.26.

Synthesis of 2,5-dibromo-3,4-bis((2-ethylhexyl)oxy)thiophene

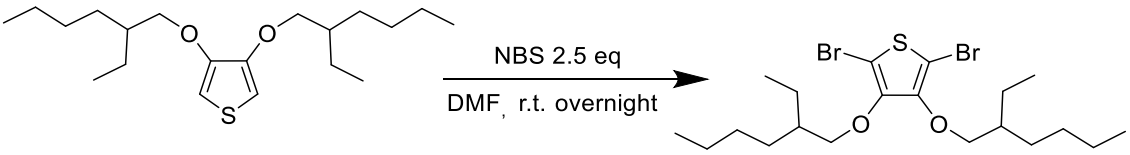

A dry 500 mL with a magnetic stir bar, 3,4-bis(octyloxy)thiophene (5.000 g, 0.014 mol) was added. The flask was then degassed before 100 mL of anhydrous DMF was added. The solution was stirred for ten minutes at 0 °C under argon. While stirring at 0 °C, a solution of 6.53 g of NBS (0.036 mol, 2.5 eq.) in anhydrous DMF was added dropwise. The vessel was brought to room temperature and then allowed to stir overnight while covered with aluminum. After completion, the product was washed with brine and extracted with 200 mL of 1:1 ethyl ether/ethyl acetate. The organic layer was then washed three times with deionized water and then dried over magnesium sulfate ($MgSO_4$). The

solvent was removed under reduced pressure. The resulting crude oil was purified by column chromatography using hexanes on neutral silica resulting in a clear, colorless oil 5.05 g (70.0%). ^{1}H NMR (300 MHz, $CDCl_3$) δ (ppm) 3.96 (d, 2H), 1.65 (dt, *J* = 17.8, 6.0 Hz, 2H), 1.41 (b, 16H), 1.01 – 0.81 (m, 12H).

3.6.4 Polymer Synthesis

Typical oxidative polymerization procedure

In a round-bottomed flask equipped with a stir bar, iron (III) chloride (4.290 g, 3.0 eq.) was dissolved in 20 ml of ethyl acetate for ten minutes in an ice bath. 3,4-Di(2-ethylhexyloxy)thiophene (3.000 g, 1.0 eq) was dissolved in ethyl acetate (40 mL) and added to the stirring solution of iron (III) chloride. The reaction mixture immediately turned dark green and was stirred for an additional 10 minutes in the ice bath. The solution was then removed from the ice bath and allowed to stir overnight at room temperature. Once the reaction was complete, the solution was precipitated into a beaker containing 250 mL of methanol and the mixture was stirred for 5 min. The doped polymer was collected by suction filtration using a Nylon pad (with a pore size of 20 μm) and washed with methanol (2 x 80 mL). The doped polymer was suspended in chloroform (50 mL) and hydrazine monohydrate (2 mL) was added dropwise, effecting a change in color of the mixture to light-orange/brown. The mixture was concentrated to ~10 mL and precipitated into a stirring solution of methanol (100 mL). The mixture was concentrated again to ~10 mL and precipitated into a stirring solution of methanol (100 mL). The precipitate was vacuum filtered, using a Nylon pad (with a pore size of 20 μm) as the filter. The dried polymer was collected into a vial and left to dry under high vacuum for two to three days.

Typical direct arylation polycondensation procedure

To a 50 mL Schlenk tube equipped with stir bar 2,5-dibromo-3,4-bis(octyloxy)thiophene (1.000 g, 1.0 eq.), 3,3-dimethyl-3,4-dihydro-2H-thieno[3,4-b][1,4]dioxepine (0.371g, 1.0 eq.) palladium(II) acetate (0.009 g, 2 mol%), pivalic acid (0.103 g, 0.5 eq.), and potassium carbonate (0.691 g, 2.5 eq.) were added. 20 mL of DMAc was added to dissolve the contents and the tube was sealed under a blanket of argon. The reaction mixture was premixed for 5 minutes before it was lowered into a 140 °C oil bath. The solution was left to stir vigorously overnight (~12 hours). After the flask was removed from the oil bath and allowed to cool to room temperature, the polymer was precipitated into methanol and stirred for one hour. The precipitate was filtered into a Soxhlet extraction thimble and washed with methanol, acetone, hexanes, toluene, and chloroform. The washings were conducted until the color was no longer observed during extraction. ~20 mg of a palladium scavenger (diethylammonium diethyldithiocarbamate) and ~20 mg of 18-crown-6, was added to the chloroform fraction and then stirred for 2 hours at 50 °C. The chloroform was removed under reduced pressure and polymer was precipitated into ~300 mL of methanol. The precipitate was vacuum filtered using a nylon pad (with a pore size of 20 μm) and washed with a large volume of methanol before letting it air dry. The dried material was collected into a vial and dried under vacuum for two days.

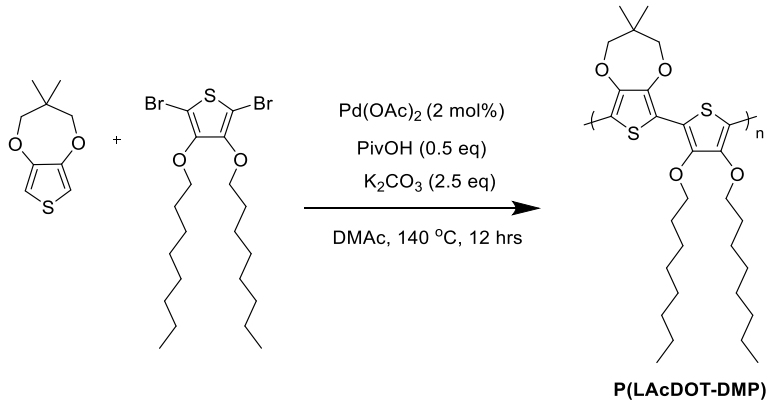

The polymer was obtained as a black solid in 68% yield (0.7048 g). ^{1}H NMR (700 MHz, $CDCl_3$) δ (ppm) 4.08 (s, 4H), 3.79 (s, 4H), 2.04 – 1.79 (m, 4H), 1.57 – 1.18 (m, 30H), 0.87 (s, 6H). Anal. calcd. for $C_{29}H_{44}O_4S_2$ C 66.88, H 8.52, S 12.31, Found C 66.61, H 8.47, S 12.06. M_n: 5 kDa, M_w/M_n: 1.4, vs. PS in $CHCl_3$ at 40 °C.

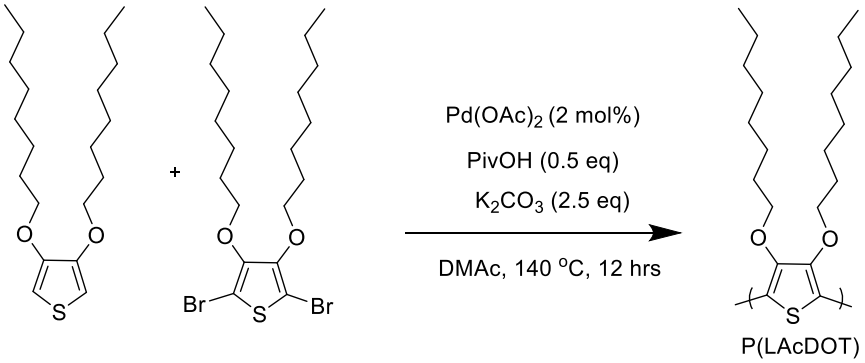

The polymer was obtained as a metallic looking purple solid in 50% yield (0.4938 g). ^{1}H NMR (700 MHz, $CDCl_3$) δ 4.16 (Br, 4H), 1.91 (s, 4H), 1.31 (dd, J = 13.6, 6.3 Hz, 18H), 0.89 (t, J = 6.9 Hz, 6H). Anal. calcd. for $C_{20}H_{34}O_2S$ C 70.96, H 10.12, S 9.47, Found C 70.69, H 10.03, S 9.48. M_n: 15 kDa, M_w/M_n: 2.2, *vs.* PS in $CHCl_3$ at 40 °C.

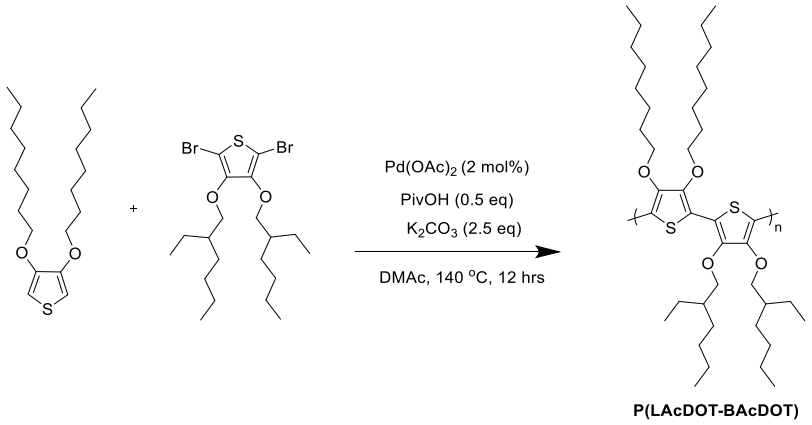

The polymer was obtained as a red sticky polymer 56% yield (0.5531 g). ^{1}H NMR (700 MHz, $CDCl_3$) δ (ppm) 4.07 (br, 4H), 3.95 (br, *J* = 17.0 Hz, 4H), 3.66 (s, 3H), 1.82 (br, 6H), 1.62 – 1.50 (m, 2H), 1.42 (dt, *J* = 32.8, 23.2 Hz, 10H), 1.28 (br, 28H), 0.94 – 0.82 (m, 18H). Anal. calcd. for $C_{34}H_{52}O_6S_2$ C 70.96, H 10.12, S 9.47, Found C 70.09, H 10.31, S 9.16. M_n: 16 kDa, M_w/M_n: 2.6, *vs.* PS in $CHCl_3$ at 40 °C.

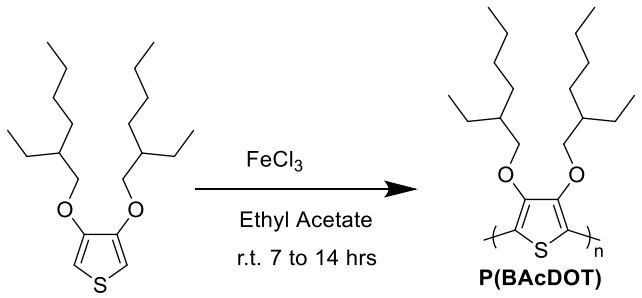

The orange polymer was collected by suction filtration and dried *in vacuo*. Polymer yield was 1.300 g (43%). ^{1}H NMR (700 MHz, $CDCl_3$) δ (ppm) 3.92 (d, *J* = 4.5 Hz, 4H), 1.81 – 1.70 (m, 2H), 1.59 – 1.49 (m, 2H), 1.45 – 1.36 (m, 4H), 1.35 – 1.21 (m, 11H), 0.91 – 0.80 (m, 12H). Anal. calcd. for $C_{20}H_{34}O_2S$ C 70.96, H 10.12, S 9.47, Found C 70.85, H 10.05, S 9.48. M_n: 44 kDa, M_w/M_n: 3.0, *vs.* PS in THF at 35 °C.

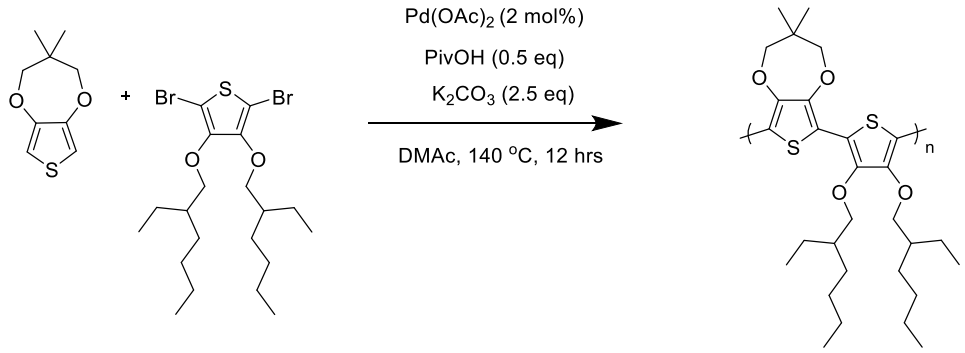

P(BAcDOT-DMP)

The polymer was obtained as a reddish polymer in 55% yield (0.5598 g). ^{1}H NMR (700 MHz, $CDCl_3$) δ (ppm) 3.96 (s, 4H), 3.83 (s, 4H), 1.63 – 1.23 (m, 18H), 1.08 (d, *J* = 30.1 Hz, 6H), 0.99 – 0.82 (m, 10H). Anal. calcd. for $C_{29}H_{44}O_4S_2$ C 66.88, H 8.52, S 12.31, Found C 66.38, H 8.35, S 12.44. M_n: 15 kDa, M_w/M_n: 2.1, *vs.* PS in $CHCl_3$ at 40 °C.

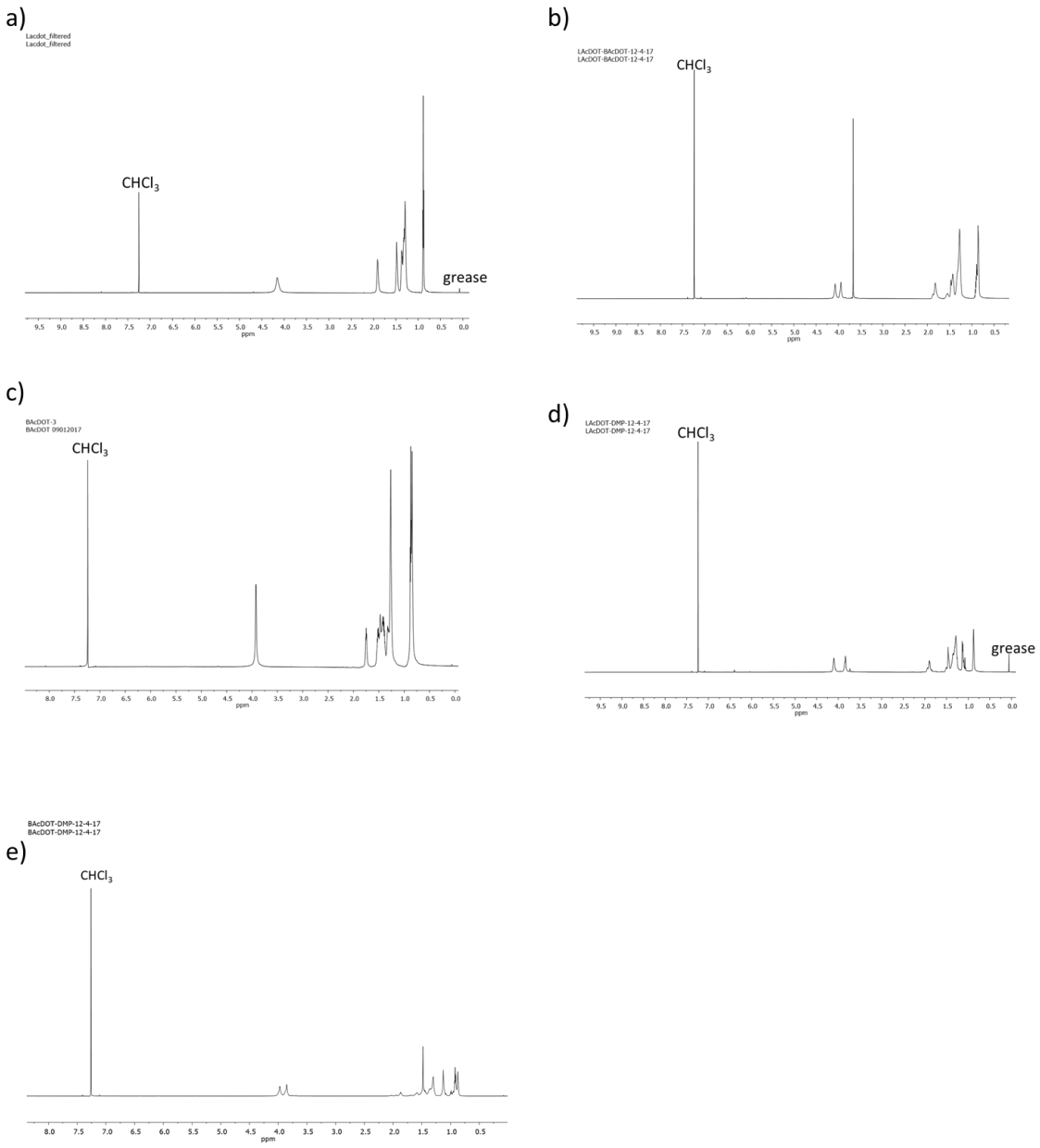

Figure 3.9. ^{1}H-NMR spectra (700 MHz in $CHCl_3$ at 50 °C) of a) P(LAcDOT), b) P(LAcDOT-BAcDOT), c) P(BAcDOT), d) P(LAcDOT-DMP), and e) P(BAcDOT-DMP.

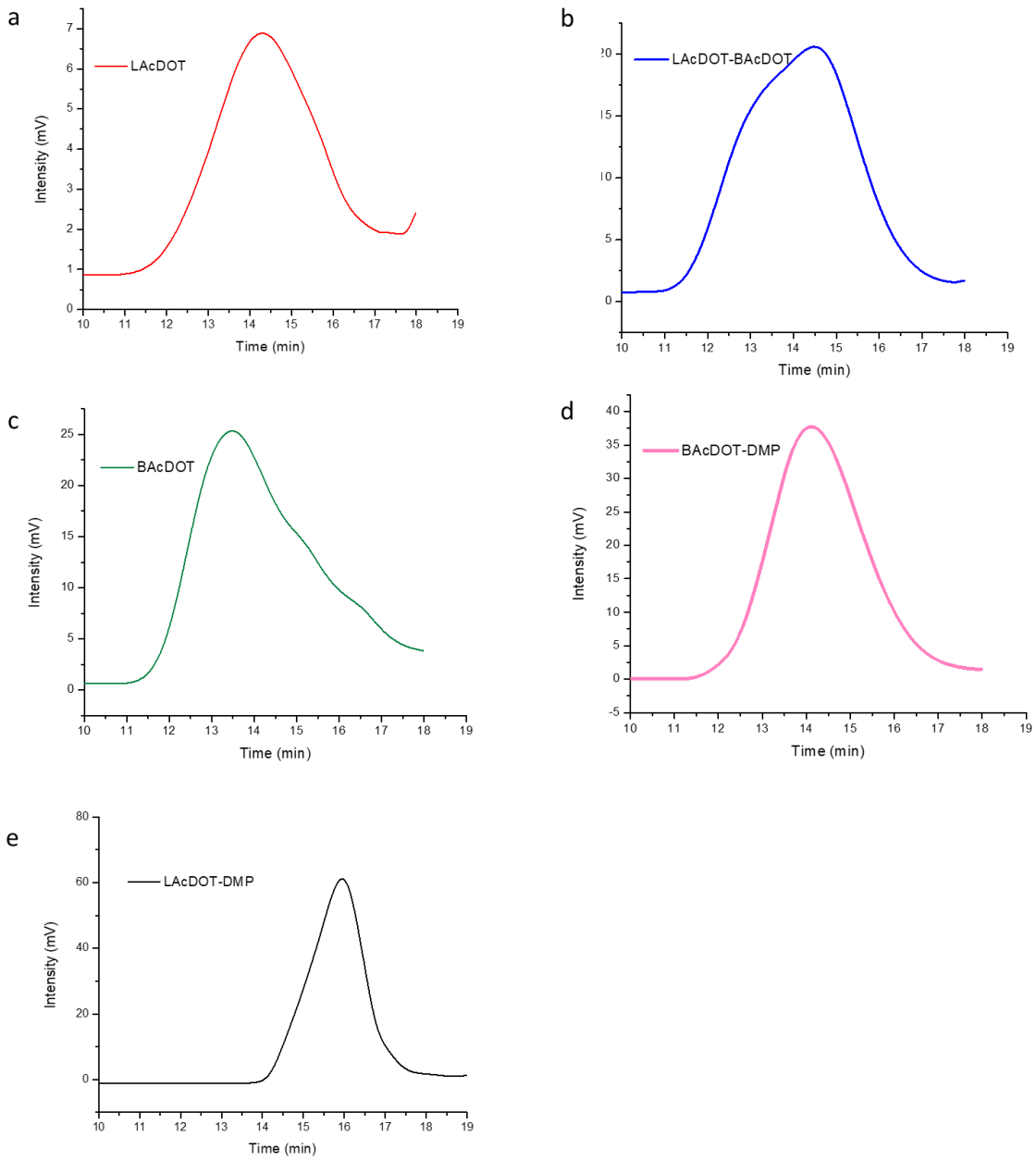

Figure 3.10. GPC traces of a) P(LAcDOT), b) P(LAcDOT-BAcDOT), c) P(BAcDOT), d) P(BAcDOT-DMP), and e) P(LAcDOT-DMP). All polymers measured using $CHCl_3$ at 40 °C (calibrated *vs.* polystyrene standards) except for P(BAcDOT), which was measured using THF at 35 °C (calibrated *vs.* polystyrene standards) due to the higher solubility of this polymer in ethereal solvents.

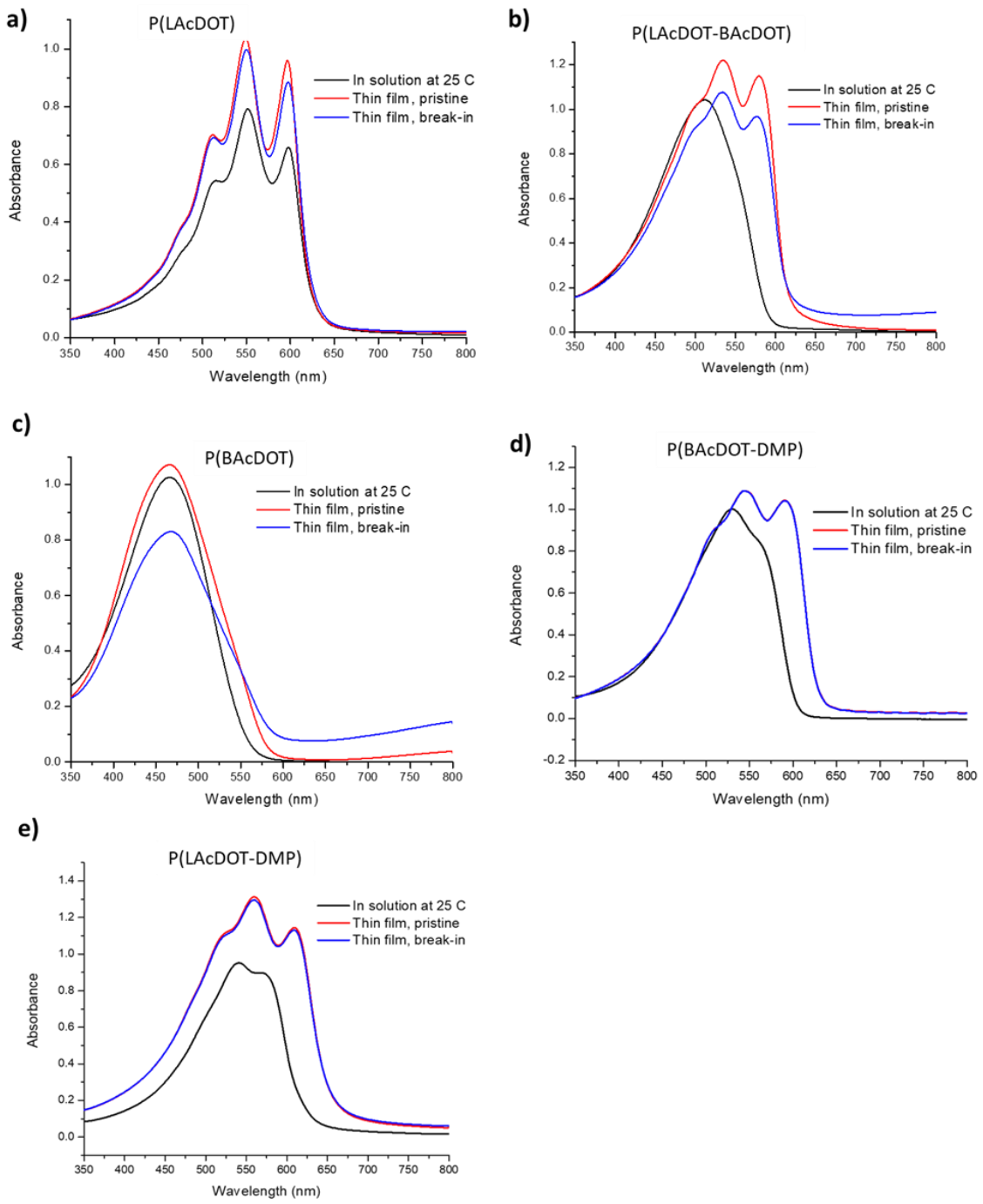

Figure 3.11. UV-Vis absorbance spectra of the polymers in toluene solution (~10mg/mL) and thin films pristine and after break-in on ITO glass slides. solution and thin films.

CHAPTER 4. THE EFFECTS OF SIDE CHAIN BRANCHING POSITION ON THE REDOX AND OPTOELECTRONIC PROPERTIES OF 3,4-DIOXYTHIOPHENES

4.1 Introduction

In Chapter 3, structural design and synthesis of five XDOT-based polymers with linear and branched side chains were reported. Using a range of analysis methods, it was determined that changing from linear to branched side chains affects ionization potential, optical bandgap, perceived color, electrochromic contrast, switching speed, and switching stability. The polymers with branched side chains showed increased solubility, higher onsets of oxidation, greater optical bandgaps, and demonstrate sudden coloration change compared to polymers with linear side chains. In addition to the optoelectronic properties, it was demonstrated that aggregations can be tuned through the choice of the side chain structure.

Apart from side chain type and length, recent studies in OFETs have shown that the branching position could enhance charge carrier mobilities.[171-172] In these studies, the improvement of the charge carrier mobilities were attributed to better intermolecular assembly in solution resulting in more crystalline structures in solid-state. However, systematic studies on side chain branching position on redox and optoelectronic properties on dioxythiophenes haa not been examined. To understand if different branching position can affect the electrochromic properties, two polymers with varying composition were synthesized and analyzed. It was determined that by changing the branching point from the

second carbon to the first carbon away from the conjugated backbone significantly changed the effective conjugation length, thus red-shifting the λ_{max} by 100 nm. This resulted in a polymer with a smaller optical band gap and therefore a purple-colored polymer instead of an orange-colored polymer.

4.1.1 Design Principles

To understand how branching point on branched alkyl side chains affects optoelectronic properties in XDOTs, two AcDOT homopolymers where the branching point was on the first or the second carbon from the conjugated backbone were designed and synthesized. To reduce the number of variables in the results, the polymers were designed to have i) an AcDOT conjugated backbone, ii) the same number of carbon atoms (eight) in the alkoxy side chains, and iii) different branching position. As illustrated in Scheme 4.1, it was hypothesized that moving the branching point closer to the conjugated backbone would induce more torsional strain between the aromatic rings. This strain would lead to a decrease in the effective conjugation length, giving rise to higher energy (lower wavelength) absorption transitions.

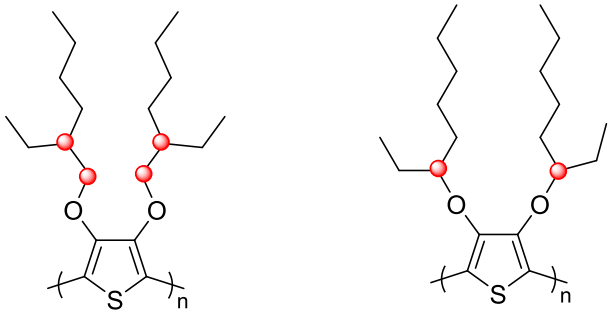

Scheme 4.1. Chemical structures of the XDOT polymers synthesized oxidative polymerization.

4.1.2 Synthesis of polymers

The monomers were synthesized through the same method as reported in Chapter 3. The repeat unit structures of the polymers, shown in Scheme 4.1, were synthesized via oxidative polymerization; detailed synthetic routes are outlined in the experimental section below.[98] The ^{1}H-NMR and elemental analyses correspond to the expected repeat unit structures as shown in the experimental section. The molecular weights of the polymers were estimated by gel permeation chromatography (GPC) in tetrahydrofuran (THF). The results, summarized in Table 5.1, indicated that P(2-BAcDOT) at M_n of 44 kDa, and P(1-BAcDOT) at M_n 22 kDa, have surpassed the effective conjugation length where optical properties are thought to become independent of molecular weight. The polymers exhibit good solubility in common organic solvents.

Table 4.1 Molecular weights of the polymers obtained via GPC.

Polymer	Mn (kDa) [a]	Mw (kDa) [a]	$Đ$ (M_w/M_n) [a]
P(2-BAcDOT)	44[b]	138[b]	3.0[b]
P(1-BAcDOT)	22	69	2.1

[a]Values obtained from GPC in THF at 35 °C calibrated *vs.* polystyrene standards. [b] Values calculated from corresponding GPC results and repeat unit mass.

4.2 Results

4.2.1 Electrochromic properties

To investigate the electrochemical properties of the polymer series, the polymers were dissolved in toluene at 1.0 mg/mL. From these solutions, 4.0 μL of each solution was drop-cast on glassy carbon electrodes and then electrochemically cycled between −0.5 V and 0.8 V (*vs.* Ag/Ag^{+}) twenty-five times to condition the films to the influx of electrolyte

(referred to as electrochemical annealing, or break-in).[159] After repeated electrochemical cycling, the polymers are thought to assume their lowest energy conformation in their charge neutral states. Following the electrochemical break-in, the films were used to determine the onset of oxidation by differential pulse voltammetry (DPV); the results are presented in Table 4.2.

Table 4.2. Optical and electrochemical properties of the studied ECPs.

Polymer	E_{ox}[a] (V *vs.* Ag/Ag^+)	E_{HOMO}[b]	λ_{max}[c] (nm)	$E_{g,opt}$[c]
P(2-BAcDOT)	0.33	-5.43	449	2.12
P(1-BAcDOT)	0.14	-5.24	554	1.96

[a]Values determined by DPV as the onset of the anodic peak. [b]Calculated from equation 2. [c]For films cast onto ITO-coated glass. [c]Bandgap determined by the high-energy onset of light absorption from thin films.

P(1-BAcDOT) compared to P(2-BAcDOT) has a significantly lower onset of oxidation as shown in Table 4.2. This surprisingly at it was hypothesized that moving the branching point closer to the polymer backbone would increase steric hindrance due to the large van der Waals radii. To have a better understanding of the results, the highest occupied molecular orbital (HOMO) levels of these polymers were calculated according to the equation (2) below[173]:

$$E_{HOMO} = -(E_{[onste,ox\ vs.Fc+/Fc]} + 5.1)\ (eV) \quad (2)$$

The higher HOMO and the low oxidation potential indicates that P(1-BAcDOT) has a longer effective conjugation length which is more prone to oxidative doping.

4.2.2 Optical Properties

To allow for direct comparison of the optical properties between several films,

measurements of optical density rather than film thickness was used.[98, 160] Once the polymer was spray cast, the films were electrochemically conditioned for 25 CV cycles. After break-in, the normalized spectra of each thin film and solution film, shown in Figure 4.2a, were analyzed and compared for more insight into the structural difference imparted by the specific side chain structure while distinguishing between differences in effective conjugation length and degree of aggregation. The optical spectra of conjugated polymers are composed of absorbance from interchain interactions in aggregated species as well as intrachain unaggregated species. In dilute toluene solutions (~10 μg/mL) where the polymer is well dissolved, the absorbance arises solely from intrachain and unaggregated excitations. As shown in Figure 4.1a, P(2-BAcDOT) has a λ_{max} at 465 nm while P(2-BAcDOT) has a λ_{max} at 505 nm, indicating that moving the branching point one carbon closer to the backbone results in a polymer with longer effective conjugation length. This is further supported by the photographs in Figure 4.2b, which shows that moving the branching point closer to the backbone results in a color change from orange to magenta. Upon solidification, the absorption spectra broaden, and the onset of absorption is red shifted, a common feature observed for conjugated polymers as they adopt a more planar conformation in the solid-state. The extent of broadening and red shifting of the as-cast spectrum is polymer dependent. As seen in Figure, 4.2a, the red-shift in P(2-BAcDOT) is not significant while P(1-BAcDOT) has a 49 nm bathochromic shift, indicating the presence of inter-chain interactions in the solid state. This is further supported by the presence of vibronic coupling in the absorbance. This phenomenon suggests that stronger intermolecular π-π interaction may be formed in the P(1-BAcDOT) film than in P(2-BAcDOT) film, which indicates that branching point at the second carbon have higher

steric interaction than when the branching point is on the first carbon from the backbone.

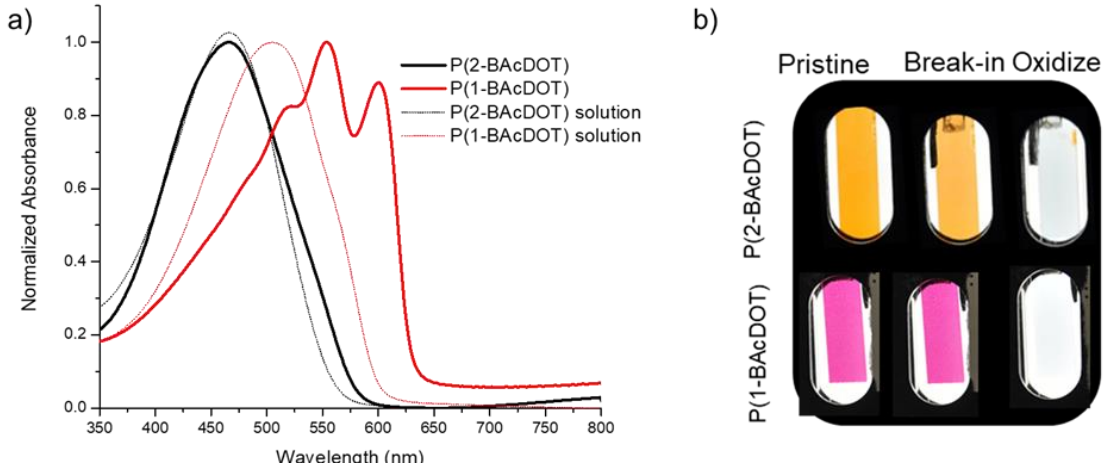

Figure 4.1 a) normalized absorption spectra comparing the two homopolymers on ITO-coated glass in 0.5 M $TBAPF_6$/PC electrolyte solution normalized to an optical density of 1.0. b) Photographs of the films in their pristine, post break-in (-0.5 V), and oxidized states (+0.8V), all on ITO-coated glass in a three-electrode cell setup.

4.2.3 Spectroelectrochemistry

Spectroelectrochemistry was carried out on the two polymers in the same three-electrode set-up used to determine the onset of oxidation. During spectroelectrochemical measurement, the desired potential was applied to the film and held at that potential until the absorbance measurements were taken. The applied potential was increased by 0.1 V increments, starting with -0.5 mV to +1.1 V, the highest stable potential as determined by the CV. A careful comparison of the spectroelectrochemical data for the polymers reveals that branching point from the side chains influences the presence of vibronic fine structures in the solid state. P(1-BAcDOT) has three distinct vibronic peaks at 517 nm, 554 nm, and 600 nm while P(2-BAcDOT) does not show any vibronic features. This result supports the idea that the absence of vibronic fine structure indicates that the film is more amorphous and point of branching can be used to tune order/disorder in conjugated polymers.

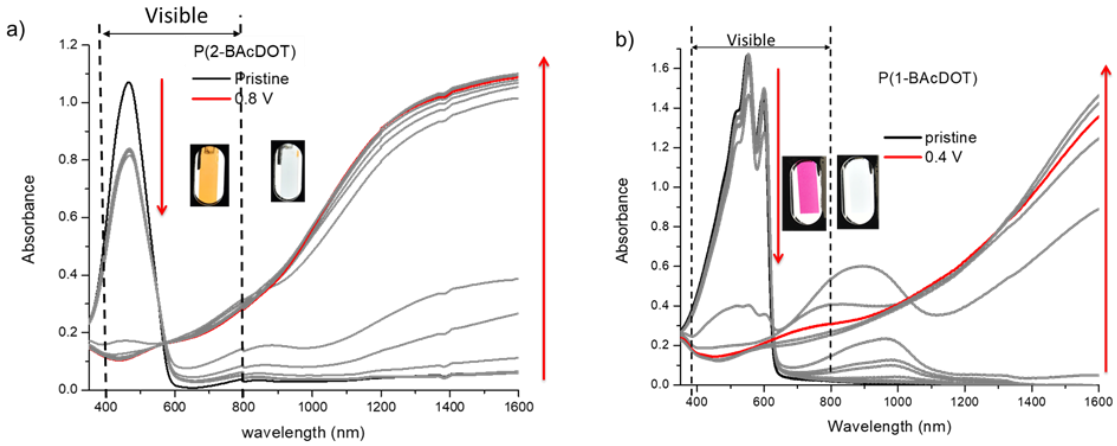

Figure 4.2. Spectroelectrochemistry of a) P(LAcDOT), b) P(LAcDOT-BAcDOT), c) P(BAcDOT), d) P(LAcDOT-DMP), e) P(BAcDOT-DMP). The applied potential was increased by 100 mV steps between the fully colored and bleached states in 0.5 M TBAPF$_6$/PC.

4.2.4 Chronoabsorptiometry

To determine how side chains affect the switching kinetics in spray-cast films, the Δ%T was monitored during the application of a square wave potential as shown in Figure 4.3. The potential square waves were executed between −0.5 V (neutral state) and +0.8 V (fully oxidized state) with a various potential residence time of 60 s, 30 s,10 s, 2 s, 1 s, followed by another 30 s. The switching speeds for the polymers were reported as the time required for the polymer to reach 95% of full contrast upon bleaching and coloring during the 60 s switching period. The P(2-BAcDOT) takes 3.6 s to switch from colored to clear but is significantly slower when switching from clear to colored, 10.6 s. On the other had, P(1-BAcDOT) has the same switching time, 3.3 s, when switching from colored to clear and then *vice versa*. The slower switching speed in P(2-BAcDOT), relative to P(1-BAcDOT) may be due to the branching point at the second carbon sterically hindering the

counterions from diffusion in and out of the film, slowing the charge balancing of the redox sites within the polymer film.

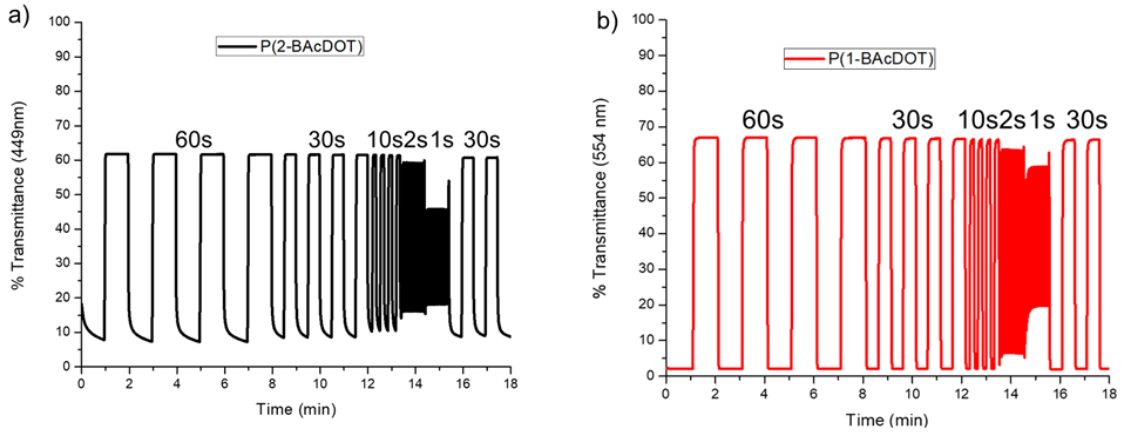

Figure 4.3. Potential square-wave measurement where %T at λ_{max} is monitored as a function of switching time between -0.5 V and 0.8 V from 60 sec down to 1.0 sec in 0.5 M $TBAPF_6$/PC for a) P(2-BAcDOT) and b) P(1-BAcDOT).

4.3 Conclusion

In conclusion, two polymers where the position of the branching point on the alky side chain were synthesized. A combination of analytical tools to evaluate the optoelectronic properties revealed that nature of the branched side chain substituent significantly affects the effective conjugation length. This in turn affect the onset of oxidation, color, and switching speed. These results demonstrate that optoelectronic properties in electrochromic conjugated polymers can be modulated by the branching point in the branched alkyl side chain. These results highlight the important of engineering the branching point of branched alkyl side chains and suggest the guidelines in the design of new electrochromic conjugated polymers.

4.4 Experimental section

4.4.1 Materials

Dimethoxythiophene (98%), purchased from Oxchem, and Pivalic acid (99%), purchased from Sigma, were used as received. $Pd(OAc)_2$ (98%, Strem Chemicals), K_2CO_3 (anhydrous, Oakwood Products), 18-Crown-6 (99%, Acros), and diethyldithiocarbamic acid diethylammonium salt (97%, TCI America) were all used as received. DMF (anhydrous) was purchased from EMD and used as received. DMAc (HPLC grade, Alfa Aesar) was filtered through a pad of basic alumina (Sigma Aldrich) prior to use. Methanol, acetone, toluene, and chloroform were purchased from Fisher chemicals and used without purification. Hexanes were purchased from VWR chemicals and used as received. ^{1}H-NMR and ^{13}CNMR spectra were collected on either a Varian Mercury Vx 300 MHz or 700 MHz instruments using $CDCl_3$ as a solvent. 3,4-(2-Ethylhexyloxy)-thiophene and P(2-BAcDOT)[98] were prepared using a published methods and confirmed by ^{1}H-NMR.

4.4.2 Instrumentation and measurements details

Structural characterization: ^{1}H and ^{13}C NMR spectra of monomers were collected using 300 MHz spectrometer. ^{1}H NMR spectra for the polymers were collected using the Bruker Corporation DRX 700 MHz spectrometer. The chemical shift was set based on residual $CHCl_3$ (in the $CDCl_3$ solvent) as an internal standard set to 7.26 ppm. The molecular weight and dispersity of the polymer were obtained using either a chloroform GPC at 40 °C calibrated *vs.* polystyrene standards. Differential pulse voltammograms (DPV) and Cyclic voltammograms (CV) were carried out using an EG&G Princeton Applied Research model 273A potentiostat/galvanostat under CorrWare control using a

three-electrode cell with a platinum flag as a counter electrode and a Ag/Ag^+ reference electrode (filled with 10 mM $AgNO_3$, 0.5 M tetra (n-butylammonium) hexafluorophosphate (98 % Acros, recrystallized from ethanol, $TBAPF_6$), acetonitrile (ACN) as the electrolyte). The working electrode consisted of a thin film of polymer drop-casted from a 1 mg/mL toluene solution onto a glassy carbon (0.07 cm^2). The electrolyte solution was 0.5 M $TBABF_6$ in PC. The $TBABF_4$ was ≥99.0% purity and purchased from Sigma-Aldrich. The PC was anhydrous (99.7% purity) purchased from Sigma-Aldrich and used as received. All absorbance spectra were acquired using a Varian Cary 5000 Scan dual-beam UV−vis−near-IR spectrophotometer. For the spectroelectrochemistry measurements, the working electrode was a thin film of polymer sprayed from a 1 mg/mL toluene solution onto ITO glass slides (7 × 50 × 0.7 mm, sheet resistance, R_s 8–12 Ω/sq, Delta Technologies, Ltd.) using a commercial airbrush sprayer (Iwata Eclipse, Revolution Series). Prior to spraying the films, the ITO glass slides were dipped into a 10 mM solution of 1-dodecylphosphonic acid (95%, Alfa Aesar) for 5 to 10 minutes. The photographs are presented without any manipulation apart from cropping.

4.4.3 Monomer synthesis

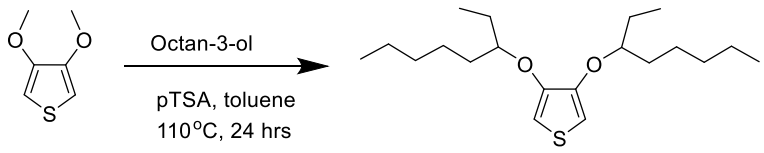

M4.2

Synthesis of 3,4-bis(octan-3-yloxy)thiophene

In a dry 500 mL round bottom flask with a magnetic stir bar, dimethoxythiophene (10.0 g, 0.069 mol), 3-octanol (50.0 g, 0.384 mol), and *p*-toluenesulfonic acid (1.3g, 0.006 mol) were added under argon followed by anhydrous toluene (300 mL). The reaction was

refluxed for 24 hours at 110 °C. After completion, the flask was cooled to ambient temperature and quenched with 100 mL of a saturated $NaHCO_3$ solution. The organic layer was extracted 3 times with DCM and dried using magnesium sulfate ($MgSO_4$) and filtered to remove the $MgSO_4$. The solvent was removed by rotary evaporation under reduced pressure the crude oil was purified by Silica chromatography using hexanes. ^{1}H NMR (300 MHz, $CDCl_3$) δ (ppm) 6.14 (s, 2H), 4.01 (p, *J* = 5.8 Hz, 2H), 1.79 – 1.51 (m, 8H), 1.50 – 1.20 (m, 12H), 0.92 (dt, *J* = 13.7, 7.2 Hz, 12H). ^{13}C NMR (75 MHz, $CDCl_3$) δ (ppm) 148.10, 99.07, 82.47, 33.53, 32.10, 26.68, 25.36, 22.77, 14.20, 9.85.

Polymer synthesis

The polymers were synthesized using the same procedure outlined in chapter 3.6.4.

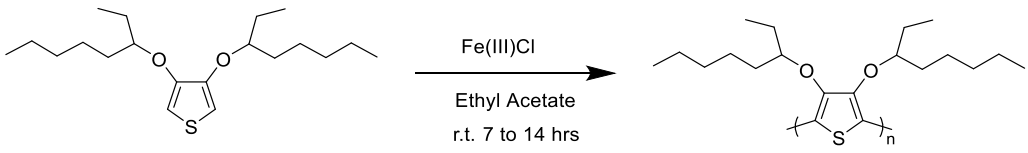

The polymer was obtained as purple solid in 67% yield (0.66 g). ^{1}H NMR (700 MHz, $CDCl_3$) δ (ppm) 3.5 (b, *J* = 4.5 Hz, 2H), 1.69 – 1.57 (m, 8H), 1.33 – 1.22 (m, 12H), 0.89 – 0.83 (m, 12H). Anal. calcd. for $C_{20}H_{34}O_2S$ C 70.96, H 10.12, S 9.47, Found: 70.32, H 10.20, S 9.51 M_n: 22 kDa, Đ: 2.1, vs. PS in $CHCl_3$ at 40 °C.

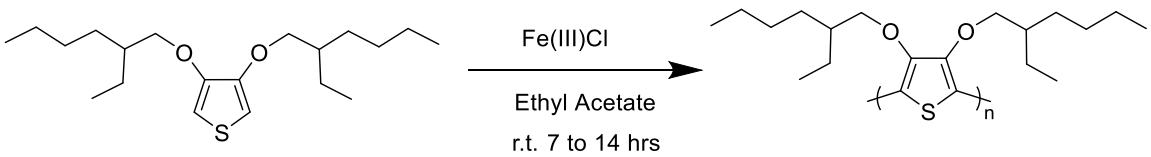

The orange polymer was collected by suction filtration and dried *in vacuo*. Polymer yield was 1.300 g (43%). ^{1}H NMR (700 MHz, $CDCl_3$) δ (ppm) 3.92 (d, *J* = 4.5 Hz, 4H), 1.81 –

1.70 (m, 2H), 1.59 – 1.49 (m, 2H), 1.45 – 1.36 (m, 4H), 1.35 – 1.21 (m, 11H), 0.91 – 0.80 (m, 12H). Anal. calcd. for $C_{20}H_{34}O_2S$ C 70.96, H 10.12, S 9.47, Found C 70.85, H 10.05, S 9.48. M_n: 44 kDa, M_w/M_n: 3.0, *vs.* PS in THF at 35° C.

CHAPTER 5. THE EFFECTS OF OLIGOETHER SIDE CHAINS ON REDOX AND OPTOELECTRONIC PROPERTIES OF DIOXYTHIOPHNE-BASED POLYMERS

5.1 Introduction

In this dissertation, Chapters 3 and 4 focused on understanding how alkyl side chains, specifically side chain type, length and density, altered optoelectronic properties of DOT-based polymers. However, one aspect of the side chains that has remained unaddressed in this dissertation and, to an appreciable extent in the literature, relates to their role in aqueous electrolyte compatibility and ionic conductivity. Hence, this chapter focuses on the synthesis of two water-compatible copolymers with oligo(ether) and alkyl side chains, with the aim of understanding how the hydrophobic/hydrophilic character of a polymer can influence its optoelectronic and redox properties.

5.1.1 The importance of water-compatibility

Traditionally, conjugated polymers have been functionalized with alkyl side chains, resulting in electroactive materials that undergo redox processes in organic electrolytes. Recently, conjugated polymers have made their way into electrochemical applications that require reversible doping and dedoping in aqueous electrolytes, with possible applications in bioelectronics.[174-177] Two areas of bioelectronics that have received the most attention are redox-controlled drug release and biologically-compatible organic electrochemical transistors (OECTs). OECT feature a three-terminal architecture comprising of a source, drain, and gate electrode.[178-174] In a typical OECT, a gate voltage drives ions from an

aqueous electrolyte into the bulk of the conjugated polymers, thus modulating its doping state and conductivity.[179-181] This makes OECTs capable of simultaneously transporting ions and electrons to amplify small biological signals at low electrochemical potentials (< 1 V).[181-182]

In the field of OECTs, most literature uses poly(3,4-ethylenedioxythiophene) polystyrene sulfonate (PEDOT:PSS) as an active channel material because of its high conductivity (up to ~3,000 S/cm), low doping potentials, aqueous electrolyte compatibility, and widespread availability.[183] Some of the disadvantage of PEDOT:PSS include (1) the fact the PSS is acidic, leading to corrosion in printheads and materials surrounding the active layer.[174] (2) PEDOT:PSS requires cross-linkers such as 3-glycidoxypropyl trimethoxysilane (GOPS) to prevent the film from dissolving in water. While GOPS is an effective approach to render the film insoluble, unfortunately, it lowers the ionic mobility.[184] These problems have motivated researchers to find alternative materials with good electronic and ionic properties. However, there is a delicate balance between ionic and electronic properties to achieve an efficient OECT device. Electronic transport within the film favors planar backbone for tight π-stacking while ionic transport favors more amorphous/hydrogel like morphology.[174, 185] In 2016, McCulloch group reported the synthesis and characterization of five homopolymer and copolymers, that contained oligoether-functionalized BDT or bithiophene (T) units: gBDT, gBDT-T, gBDT-2T, gBDT-g2T, and g2T-T.[186] The polymers containing BDT had poor performance as OECTs due to the relatively large π-stacking distance of 3.7 Å. Moreover, the polymers containing BDT did not show any electrochromic response when potential was swept from -0.2 V to 0.6 V vs Ag/Ag^+, partially due to the low-lying HOMO around -4.85 eV.[186] In

contrast, the more electron rich polymerg2T-T, showed complete bleaching of the π–π* absorption band with a concurrent appearance of a broad polaron absorption band around 850 nm. The polymer also had stable cycling between colored and bleached state. This was attributed to the low onset of oxidation potential and high HOMO energy level.[186]

In 2018, a different approach to synthesize conjugated polymers for OECTs was introduced by the Reynolds group.[117] The polymer utilized an oligo-ether functionalized ProDOT monomer copolymerized with DMP. The resulting polymer not only had comparable OECT performance to PEDOT:PSS but it also had excellent electrochromic performance; it was able to switch from a blue-purple in the neutral state to transmissive in the oxidized state in both the organic and aqueous electrolytes. The switching speed in the aqueous electrolytes was less than 2 seconds while maintaining an electrochromic contrast above 70%. The fast switching speed in aqueous electrolytes was attributed to the higher ionic conductivity of 0.5 M NaCl/H_2O when compared to 0.5 M $TBAPF_6$/PC.

The last five years have seen great progress in the design of water-compatible conjugated polymers for bioelectronics and these benefits can be transferred to other branches of organic electronics such as ECDs. ECDs would benefit from the increased ionic mobility and conductance of aqueous electrolytes since ions moving in and out of the film affects how fast the conjugated polymers switch colors. Additionally, the use of aqueous electrolyte would reduce the environmental impact while increasing safety for the personnel. Lastly, when considering device fabrication, water compatible polymers may reduce the cost associated with manufacturing by eliminating the need to keep the polymers from oxygen and moisture. For these reasons, it is essential for researchers to move towards polymers that switch in aqueous electrolytes.

5.1.2 Design strategy

To understand how hydrophilicity/hydrophobic character of polymers affects the optoelectronic properties of DOTs, two polymers that are soluble in organic solvents and can form films that are stable in aqueous electrolytes were synthesized *via* DHAP. For valid comparison, the polar-functionalized monomer was kept constant while the comonomer was changed. The first polymer replaced the methyl groups in the ProDOT(OE)-DMP with ((2-ethylhexyl)oxy)methyl (EOM), a more sterically hindered side chain. The second polymer introduced an acyclic dioxythiophene with linear alkyl side chain containing 12 carbons, *n*-dodecane. It was hypothesized that: OEM and *n*-dodecane would decrease the hydrophilicity of the polymers, which would change the hydration of the polymer. This decrease in hydrophilicity would hinder the counterion diffusion in and out of the film, resulting in slower switching speeds. (2) Compared to the dimethyl side chains, the bulky side chain, OEM would decrease the effective conjugation length, giving rise to higher energy (lower wavelength) absorption transitions. (3) The unbridged AcDOT monomer, which is more sterically hindered, will reduce the effective conjugated length.[98] The specific electrochromic properties measured are (1) onset of oxidation potential, optical band gap, electrochromic contrast, and switching speed.

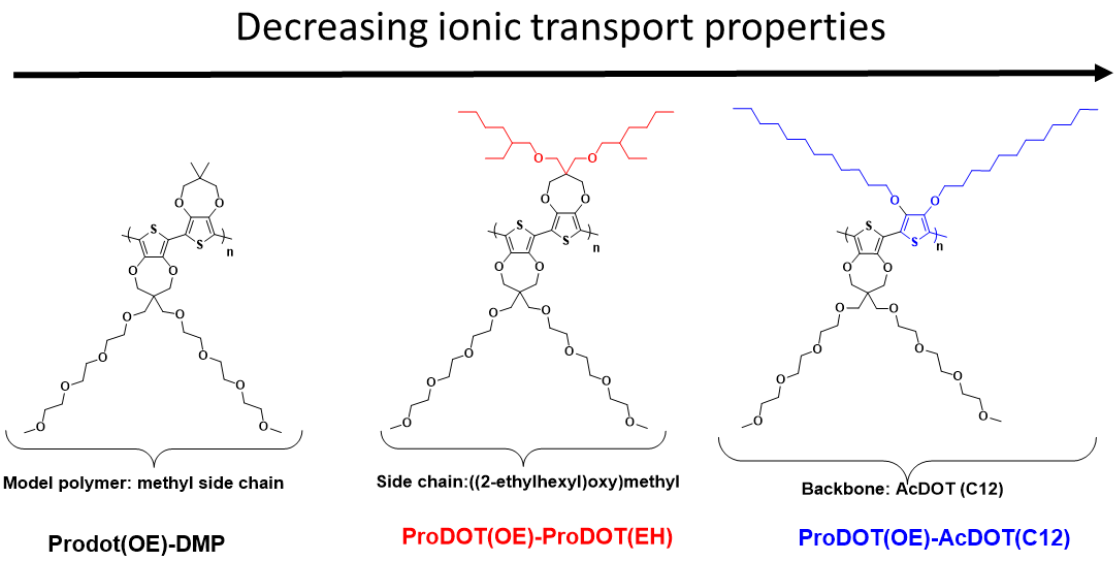

Scheme 5.1 representation of structure variations of the polymers synthesized.

5.1.3 Polymer synthesis and characterization

The polymers were synthesized *via* DHAP, using the same conditions described in Chapter 2. The ^{1}H-NMR and elemental analyses correspond to the expected repeat unit structure, theoretical chemical composition, and high purity, as shown in the experimental section. The molecular weights of the polymers were estimated by GPC relative to PS standards, using chloroform as the eluent at 40 °C. The results, summarized in Table 5.1, indicate that all the polymers are of sufficient molecular weight.

Table 5.1. Polymerization yield and molecular weights of the polymers obtained *via* chloroform GPC.

Polymer	Yield (%)	Mn (kDa)	Mw (kDa)	$Đ$ (M_w/M_n)
ProDOT(OE)-DMP[117]	92	22	46	2.0
ProDOT(OE)-ProDOT(EH)	68	47	85	1.8
ProDOT(OE)-AcDOT(C12)	69	15	24	1.6

Both polymers are soluble in toluene up to 20 mg/mL, allowing for airbrush spray-processing and drop-casting for film formation. The thermal stability of the polymers was determined by TGA. As shown in Figure 5.1, the polymers show excellent thermal stability, with degradation temperatures (threshold of 5 % mass loss) around 300 °C.

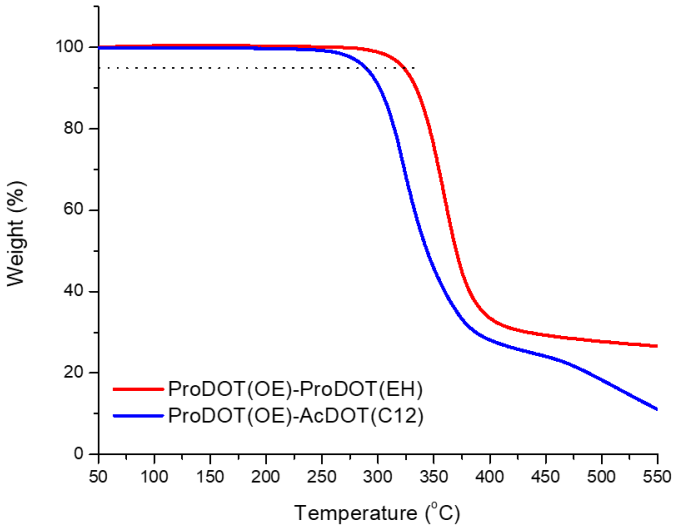

Figure 5.1 TGA trace of ProDOT(OE)-ProDOT(EH) and ProDOT(OE)-AcDOT(C12) at 10 °C/minute.

5.2 Results

5.2.1 Optoelectronic properties

To investigate the optoelectronic properties of the polymer series, the polymers were dissolved in chloroform at 2.0 mg/mL. From these solutions, 2.0 μL was drop-casted on the surface of glassy carbon electrode in a 1.0 μL aliquots and left to dry at ventilated hood at room temperature. The films were then electrochemically cycled between −0.8 V and 0.8 V vs. Ag/AgCl in 0.5 M NaCl/H_2O twenty-five times to condition the films to the influx of electrolyte.[159] After repeated electrochemical cycling, the polymers are thought to assume their lowest energy conformation in their charge neutral states. Following the

electrochemical break-in, the films were used to determine the onset of oxidation by differential pulse voltammetry (DPV); the results are presented in Table 5.2. The onset of oxidations for both polymers are higher than the oxidation onset of ProDOT(OE)-DMP. As shown in Table 5.2, ProDOT(OE)-ProDOT(EH) has an onset of oxidation at +0.07 V, while the onset of oxidation for ProDOT(OE)-AcDOT(C12) is at +0.10 V vs Ag/AgCl. The higher onset of oxidation is due to the increase of the alkyl side chain length from a methyl group to OEM or *n*-dodecane.

Table 5.2. Optical and electrochemical properties of the studied ECPs.

Polymer	E_{ox}[a] (V *vs.* Ag/Ag^+)	λ_{max}[b] (nm)	$E_{g,opt}$[b]
ProDOT(OE)-DMP[117]	-0.29	581	1.83
ProDOT(OE)-ProDOT(EH)	0.07	549,593	1.95
ProDOT(OE)-AcDOT(C12)	0.1	559	1.89

[a]Values determined by DPV as the onset of the anodic peak for films dropcasted on a glassy carbon button electrode (I am assuming?). [b]Value determined for films spray-cast onto ITO-coated glass. [b]Bandgap determined by the high-energy onset of light absorption for thin films.

To examine the optical properties, the polymer films were airbrush sprayed onto ITO glass electrodes to a proximate optical density of 1.0 absorbance before subjecting the films to electrochemical annealing by CV. Prior to coating, the ITO glass electrodes were pre-rinsed and sonicated in an aqueous solution of sodium dodecylsulfate-, deionized water, acetone, and isopropanol, and then dried under a stream of N_2 gas. The absorption spectra of ProDOT(OE)-ProDOT(EH) compared to ProDOT(OE)-DMP, after electrochemical conditioning, is slightly blue-shifted, as shown in Figure 5.2a. This is due to the bulky alkyl side chains introducing steric strain and increasing the band gap to 1.89 eV, shown in Table 5.2. The small blue-shift in absorbance results in a polymer that is more purple in color. The same trend is seen when the ProDOT(OE) monomer is copolymerized

with AcDOT(C12) monomer. The removal of the propylene bridge and the long linear side chain increases steric hindrance in the conjugated backbone resulting in a blue shift in the absorbance. This blue shift in absorbance increases the band gap to 1.95 eV and results in a purple color.

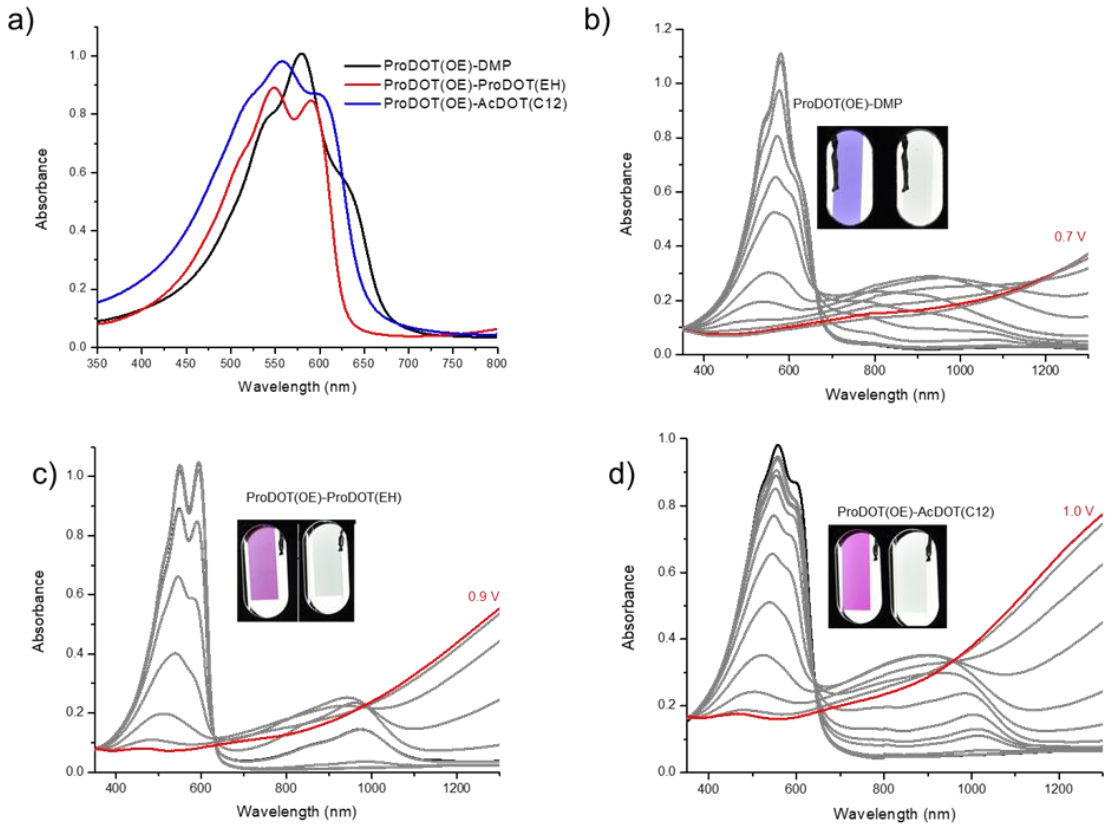

Figure 5.2. Potential-dependent spectra of ProDOT(OE)-DMP[117], ProDOT(OE)-ProDOT(EH) and ProDOT(OE)-AcDOT(C12) films on ITO glass recorded every 0.1 V 0.5 m NaCl/H_2O from −0.5 to +1.0 V vs Ag/AgCl.

Spectroelectrochemical measurements were performed on polymer films sprayed on ITO glass in 0.5 M NaCl in water with a Pt flag as the counter electrode and a Ag/AgCl reference electrode. The spectroectrochemical studies of the two new polymers in comparison to ProDOT(OE)-DMP are shown in Figure 5.2. As a pristine film, ProDOT(OE)-ProDOT(EH) shown in Figure 5.2b, absorbs with two nearly identical λ_{max}

at 549 nm and 595 nm giving rise to a purple colored polymer. While ProDOT(OE)-AcDOT(C12) has one λ_{max} at 554 nm, resulting in a purple colored polymer. As the potential is increased, the $\pi-\pi^*$ absorption bands (380−660 nm) decreases, while absorption bands originating from polaronic and bipolaronic charge carriers increase in the NIR, leaving a minimally absorbing film when fully oxidized. Interestingly, the energy of the polaron band is not particularly affected by the choice of DOT unit, as it has been shown in previous studies that used branched side chains on the AcDOT unit instead of the linear side chain.[78, 98] This may be due to the linear side chains being able to stabilize the polaron charge carriers better than the branched side chain. It could also mean that the oxidized state quinoidalization acts as a greater driving force to planarize the polymer backbone than the side chains have on twisting the polymer backbone out of plane.[23] The voltage necessary to switch the polymer from colored to fully transmissive increases from 0.7 V for the ProDOT(OE)-DMP to 0.9 V for ProDOT(OE)-ProDOT(EH) and 1.0 V for ProDOT(OE)-AcDOT(C12). The increase in oxidation potential is attributed to the steric hindrance from the bulky branched side chains on ProDOT and long linear side chain on AcDOT, which cause the thiophene rings to partly twist out of the plane.[23, 64, 78] Figure 5.2. suggests that the polymers have preferential doping of H-aggregated species when the ratio of the intensity of the 0-0 of 0-1 transition are compared. [168-169] This preferential doping of the H-aggregates has also been shown in ProDOT(OE)-DMP.[117]

5.2.2 Colorimetry

The color change as a function of oxidation potential was quantified by converting the visible absorbance spectra into *L*a*b** color coordinates to shows how the *a*,b** values of the polymers change upon electrochemical oxidation. ProDOT(OE)-ProDOT(EH) and

ProDOT(OE)-AcDOT(C12) both have vibrant purple color as confirmed by their $+a^*$ and $-b^*$ values. By replacing the ProDOT(EH) monomer with AcDOT(C12), the steric hindrance between chains does not change; in fact, the ProDOT(OE)-AcDOT(C12) seems to be more purple than ProDOT(OE)-ProDOT(EH). This is also confirmed by the photographs in Figure 5.2b. These two polymers expand the library of repeat units that can be used to obtain purple-to-colorless ECPs.

Table 5.3. *L*a*b color coordinates for all polymers in the neutral and transmissive states and total change in contrast upon switching from 0.5 V to 0.9 V 0.5M NaCl/H_2O for ProDOT(OE)-ProDOT(EH) or 1.0 V for ProDOT(OE)-AcDOT(C12).**

Polymer	$\Delta\%T^a$ (at λ_{max})	neutral state L*, a*, b* color coordinates	oxidized state L*, a*, b* color coordinates
ProDOT(OE)-ProDOT(EH)	70	54, 49, -34	93, -2, 0
ProDOT(OE)-AcDOT(C12)	60	50, 32, -25	86, -1, 1

[a]Difference between steady-state transmittance at λ_{max} measured at fully oxidized and fully neutral states

5.2.3 Chronoabsorptiometry

Fast switching between doped and de-doped states is a desirable property for sensors, logic circuits, and display applications. Therefore, great effort has been spent on understanding how switching occurs and how to improve redox kinetics. Importantly, the rate determining steps for switching speed include both mobility of the charge carriers within an active material combined with insertion/ejection processes of ions from the electrolyte. In the previous report by Savagian et al., the ProDOT(OE)-DMP films maintained 95% of their maximum contrast for switching times as low as 2 s in 0.5 M $TBAPF_6$/PC and <1 s in NaCl/H_2O.[117] The faster switching time, shown in Figure 5.2a, in the aqueous electrolyte was attributed to the higher ionic conductivity of the electrolyte

solution. To understand how the choice of side chains influenced switching speed, the Δ%T was monitored during the application of a square wave potential as shown in Figure 5.3b and 5.3c. The potential square waves were executed between −0.5 V (neutral state) and +0.9 V or +1.0 V (fully oxidized state) with various potential residence times of 60s, 30 s,10 s, 2 s, 1 s, followed by another 30 s, Figure 5.3 b and Figure 5.3c. As shown in Figure 5.2d, each polymer exhibit ΔT above 60% when the residence time is 60 seconds. As switching speed is decreased to 1 s, ProDOT(OE)-DMP does not show any changes while ProDOT(OE)-ProDOT(EH) show a decrease in Δ%T at a potential residence time of 2 seconds. The change in Δ%T is more significant in ProDOT(OE)-AcDOT(C12) as the switching speed is successively increased to 1 second. It is hypothesized that the decrease in Δ%T, which corresponds to lower switching kinetics, is due to the inability of the long linear alkyl side chains to transport hydrated ions and result in bulk doping. Hence, the redox process is compromised.

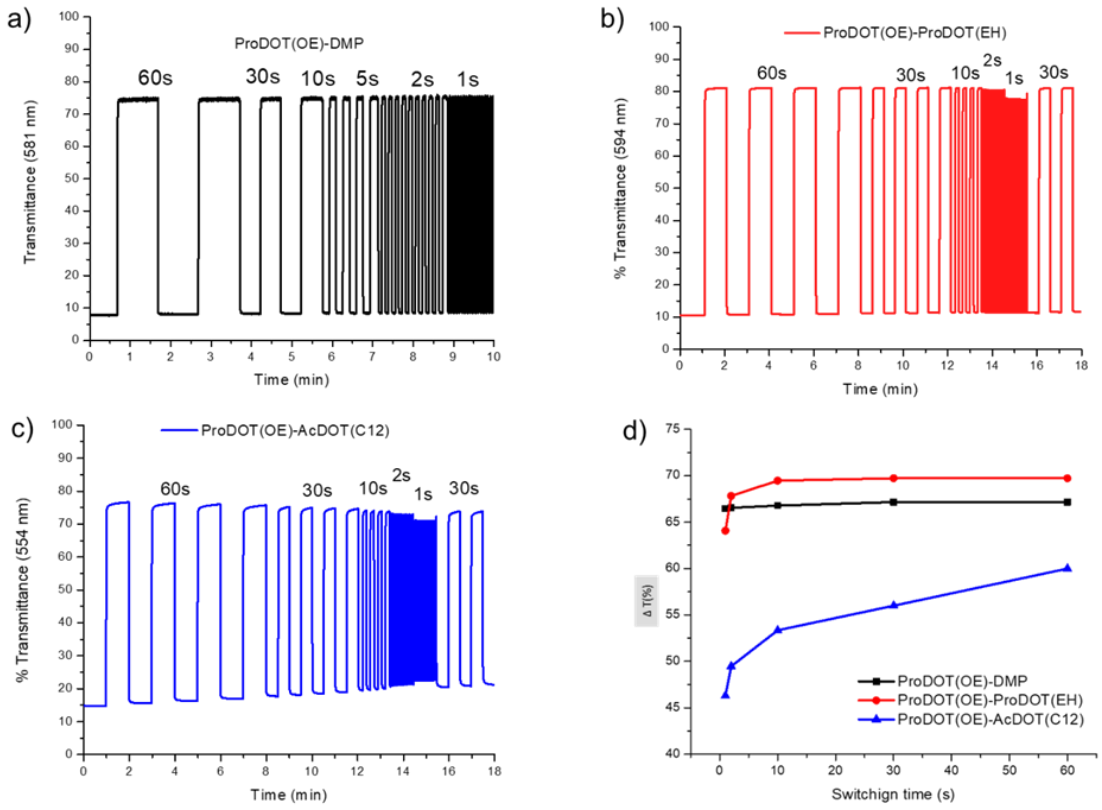

Figure 5.3. Chronoabsorptometry of polymers in 0.5 M NaCl/H_2O measured at λ_{max}. Polymers were switched between -0.5 V to a) +0.7 V, b) +0.9 V, c) +1.0 V for periods ranging from 60 se to 1 s. d) The change in transmittance at λ_{max} as a function of switching time from 60 s to 1 sfor all polymers.

5.3 Conclusion

Few researchers have attempted to understand how different side chains and backbone affect ionic and electronic properties in DOTs. In an effort to expand the range of side chains and backbone selection, two oligo ether and alkyl functionalized DOT-based polymers were prepared through DHAP. The alkyl side chains allowed the polymers to be soluble in common organic solvents while the oligo ether side chains provided water compatibility. When ProDOT(OE)-DMP is compared to ProDOT(OE)-ProDOT(EH), the introduction of 3-(ethoxymethyl)heptane branched side chain in place of the smaller dimethyl group on the ProDOT results in a higher onset of oxidation and slower switching

speed. When the monomer is copolymerized with AcDOT(C12), the *n*-dodecane side chain increases steric hindrance associated with planarization of the conjugated backbone, resulting in a polymer with a higher onset of oxidation and slower switching speeds. These results show that beyond the primary motivation of solubility, side chains can be further exploited to tune electronic and ionic properties of polymers, such as oxidation onset and switching speed.

5.4 Path Forward

As stated earlier, the polarity of the polymer side chain has been shown to regulate ion penetration and doping in conjugated polymers, thereby dictating the mode of transistor operation in OECT. To understand how OEM and *n*-dodecane influence ionic conductivity, Lisa Savagian will fabricate OECT devices and measure transconductance, gate voltages, and volumetric capacitance. Furthermore, she will characterize how the morphology of these materials evolves during electrochemical doping/dedoping processes and as ion/solvent are transported across the polymer/electrolyte interface using electrochemical strain microscopy (ESM). This may allow us to gain insight into how polymer structure influences the formation and electrochemical accessibility of different domains in thin films and how these domains actuate and locally respond to electrochemical biases.

5.5 Experimental section

5.5.1 Materials

Dimethoxythiophene (98%), purchased from Oxchem, and Pivalic acid (99%), purchased from Sigma, were used as received. $Pd(OAc)_2$ (98%, Strem Chemicals), K_2CO_3 (anhydrous, Oakwood Products), 18-Crown-6 (99%, Acros), diethyldithiocarbamic acid diethylammonium salt (97%, TCI America) and NaH (57-63% oil dispersion, Alfa Aesar) were all used as received. DMAc (HPLC grade, Alfa Aesar) was filtered through a pad of basic alumina (Sigma Aldrich) prior to use. Methanol, acetone, hexanes, and chloroform were purchased from Fisher chemicals and used without purification. ^{1}H-NMR and ^{13}CNMR spectra were collected on either a Varian Mercury Vx 300 MHz or 700 MHz instruments using $CDCl_3$ as a solvent. 3,3-bis(bromomethyl)-3,4-dihydro-2H-thieno[3,4-b][1,4]dioxepine[4], and 3,3-di(2,5,8,11-tetraoxadodecyl)-3,4-dihydro-2H-thieno[3,4b] [1,4]dioxepine[117] were prepared using a published methods and confirmed by ^{1}H-NMR.

5.5.2 Instrumentation

Structural characterization: ^{1}H and ^{13}C NMR spectra of monomers were collected using 300 MHz spectrometer. ^{1}H NMR spectra for the polymers were collected using the Bruker Corporation DRX 700 MHz spectrometer. The chemical shift was set based on residual $CHCl_3$ (in the $CDCl_3$ solvent) as an internal standard set to 7.26 ppm. The molecular weight and dispersity of the polymer were obtained using either a chloroform GPC at 40 °C *vs.* polystyrene standards. Differential pulse voltammograms (DPV) and Cyclic voltammograms (CV) were carried out using an EG&G Princeton Applied Research model 273A potentiostat/galvanostat under CorrWare control using a three-electrode cell

with a platinum flag as a counter electrode and a Ag/AgCl reference electrode (3M NaCl). The working electrode consisted of a thin film of polymer drop-casted from a 2 mg/mL chloroform solution onto a glassy carbon (0.07 cm^2). The electrolyte solution was 0.5 M NaCl in H_2O. All absorbance spectra were acquired using a Varian Cary 5000 Scan dual-beam UV−vis−near-IR spectrophotometer. For the spectroelectrochemistry measurements, the working electrode was a thin film of polymer sprayed from a 2 mg/mL chloroform solution onto ITO glass slides (7 × 50 × 0.7 mm, sheet resistance, R_s 8–12 Ω/sq, Delta Technologies, Ltd.) using a commercial airbrush sprayer (Iwata Eclipse, Revolution Series). Colorimetry measurements were obtained by converting the absorbance spectras to CIELAB L*a*b* color space using Star-Tek colorimetry software using a D50 illuminant, 2-degree observer. Photography was performed in a light booth designed to exclude outside light with a D50 lamp located in the back of the booth providing illumination, using a Nikon D90 SLR camera with a Nikon 18-105 mm VR lens. Photos of the films were taken as-sprayed, after break-in at -0.5 V, and at the most transmissive oxidized state (+0.8V). The photographs are presented without any manipulation apart from cropping.

5.5.3 monomer synthesis

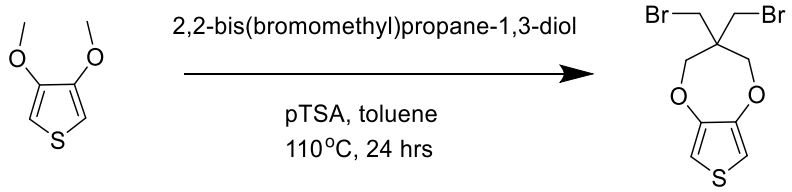

M5.1

Synthesis of 3,3-bis(bromomethyl)-3,4-dihydro-2H-thieno[3,4-b][1,4]dioxepine.[4]

In a 1,000 mL round bottom flask equipped with magnetic stir bar, dimethoxythiophene (21.1 g, 0.15 mol) and 2,2-bis(bromomethyl)propane-1,3-diol (42.1 g, 0.16 mol) were added into anhydrous toluene (600 mL). The solution was premixed for 10 minutes before adding *p*-toluenesulfonic acid (2.78 g, 0.015 mol) slowly. The reaction was refluxed for 24 hours, after which the reaction was quenched with 175 mL of deionized (DI) water. The organic layer was extracted 3 times into diethyl ether then passed over a silica plug using 4:1 hexanes:dichloromethane and evaporated to yield 42 g of white solid (85%) . ^{1}H NMR (300 MHz, $CDCl_3$) δ (ppm) 6.50 (s, 2H), 4.10 (s, 4H), 3.61 (s, 4H). ^{13}C NMR (75 MHz, $CDCl_3$) δ (ppm) 148.62, 105.73, 74.10, 46.20, 34.40.

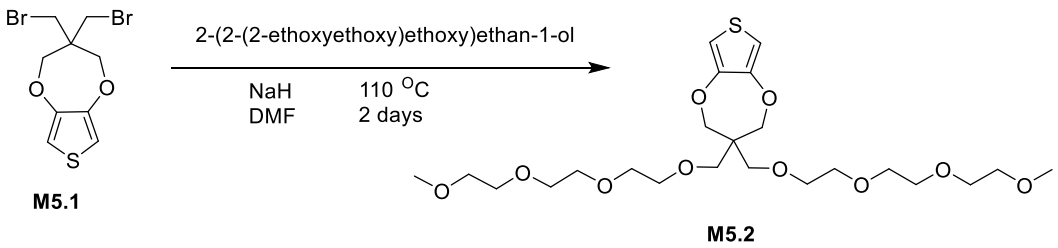

Synthesis of 3,3-di(2,5,8,11-tetraoxadodecyl)-3,4-dihydro-2H-thieno[3,4b][1,4]dioxepine.[117]

In a dry 1,000 mL round bottom flask with a magnetic stir bar, 3-bis(bromomethyl)-3,4-dihydro-2H-thieno[3,4-b][1,4]dioxepine (6.7 g, 60 mmol) and 2-(2-(2-ethoxyethoxy)ethoxy)ethan-1-ol (10.0 g, 0.561 mol) and 400 mL of anhydrous DMF were added under argon. NaH (3.71 g, 57-63%) was added slowly to the reaction mixture while stirring. After the hydride was fully dissolved, the reaction was heated at 100 °C for two days. The reaction was cooled to room temperature. The organic layer was extracted 3 times with DCM and brine before being dried using $MgSO_4$ and filtered to remove the $MgSO_4$. The solvent was concentrated, and the crude product was purified by silica gel

chromatography using DCM to obtain 6.0 g of a clear, slightly yellow oil (60%). ^{1}H NMR (300 MHz, $CDCl_3$) δ (ppm) 6.42 (s, 2H), 3.99 (s, 2H), 3.66 – 3.50 (m, 28H), 3.36 (d, *J* = 1.3 Hz, 6H).

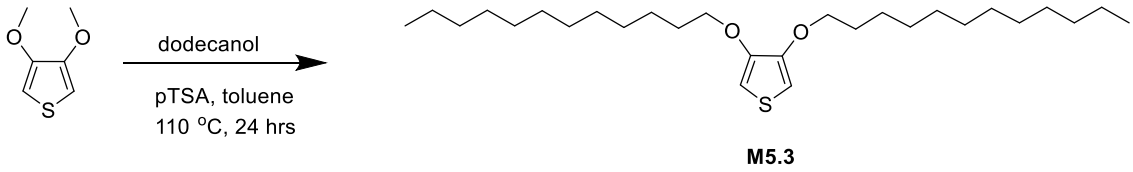

M5.3

Synthesis of 3,4-bis(dodecyloxy)thiophene

In a dry 500 mL round bottom flask with a magnetic stir bar, dimethoxythiophene (5.0 g, 0.034 mol) and dodecanol (16.17 g, 0.086 mol) was added under argon followed by anhydrous toluene (150 mL). *p*-toluenesulfonic acid (0.65g, 0.003 mol) was added while the solution was stirring. The reaction was refluxed overnight at 110 ˚C. After completion, the flask was cooled to ambient temperature and quenched with 50 mL of a saturated $NaHCO_3$ solution. The organic layer was extracted 3 times with DCM and dried using $MgSO_4$ and filtered to remove the $MgSO_4$. The solvent was concentrated, and the crude was purified by silica gel chromatography using hexanes to obtain 17.8 g of a clear white solid (63.4 %).^{1}H NMR (300 MHz, $CDCl_3$) δ (ppm) 4.04 (t, *J* = 6.6 Hz, 4H), 1.78 – 1.65 (m, 4H), 1.51 – 1.38 (m, 4H), 1.26 (s, 32H), 0.93 – 0.83 (m, 6H). ^{13}C NMR (75 MHz, $CDCl_3$) δ (ppm) 156.8, 87.9, 69.10, 31.9, 29.6, 29.3, 25.9, 22.7, 14.1.

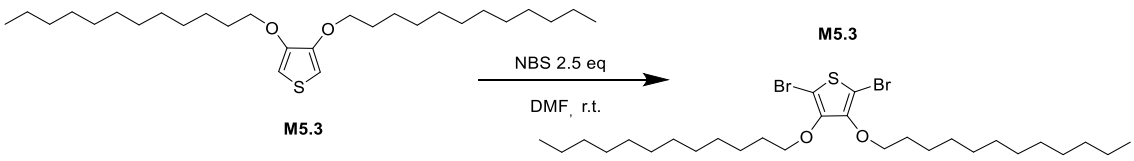

Synthesis of 2,5-dibromo-3,4-bis(octyloxy)thiophene

In a dry 500 mL round bottom flask with a magnetic stir bar, 3,4-bis(dodecyloxy)thiophene (3.0 g, 0.006 mol) was added. The flask was then degassed before adding 200 mL of anhydrous THF. The solution was stirred for ten minutes at 0 °C under argon. While stirring the solution at 0 °C, a solution of 3 g of NBS (0.016mol, 2.5 eq) in anhydrous THF was added drop wise. The vessel was brought to room temperature and then allowed to stir overnight while covered with aluminum foil. After completion, the product was washed with brine and extracted with 200 mL of ethyl acetate. The organic layer was then washed three times with deionized water and then dried over $MgSO_4$ and filtered to remove the $MgSO_4$. ^1H NMR (300 MHz, $CDCl_3$) δ (ppm) 4.04 (quint, J = 6.6 Hz, 4H), 1.72 (quint, 4H), 1.44 (m,4), 1.37 – 1.20 (m, 32H), 0.92 – 0.83 (m, 6H).

5.5.4 Polymers Synthesis

Synthesis of ProDOT(OE)-ProDOT(EH)

To a 50 mL Schlenk tube equipped with a magnetic stir bar ProDOT(OE) (1.12 g, 1.0 eq) and 3,3-bis(((2-ethylhexyl)oxy)methyl)-3,4-dihydro-2H-thieno[3,4-b][1,4]dioxepine (0.78g 1.0 eq) palladium(II) acetate (0.013 g, 2 mol%), pivalic acid (0.06 g, 0.5 eq.), and potassium carbonate (0.60 g, 2.5 eq.) were added. 25 mL of DMAc was added to dissolve the contents and the tube was sealed under a blanket of argon. The reaction mixture was premixed for 5 minutes before it was lowered into a 140 °Coil bath.

The solution was left to stir vigorously overnight. After the flask was removed from the oil bath and allowed to cool to room temperature, the polymer was precipitated into methanol and stirred for one hour. The precipitate was filtered into a Soxhlet extraction thimble and washed with methanol, acetone, hexanes, toluene, and chloroform. The washings were conducted until the color was no longer observed during extraction. ~20 mg of a palladium scavenger (diethylammonium diethyldithiocarbamate) and ~20 mg of 18- crown-6, was added to the chloroform fraction and then stirred for 2 hours at 50 °C. The chloroform was removed under reduced pressure and polymer was precipitated into ~300 mL of methanol. The precipitate was vacuum filtered using a nylon pad (with a pore size of 20 μm) and washed with a large volume of methanol before letting it air dry. The dried material was collected into a vial and dried under vacuum for two days.

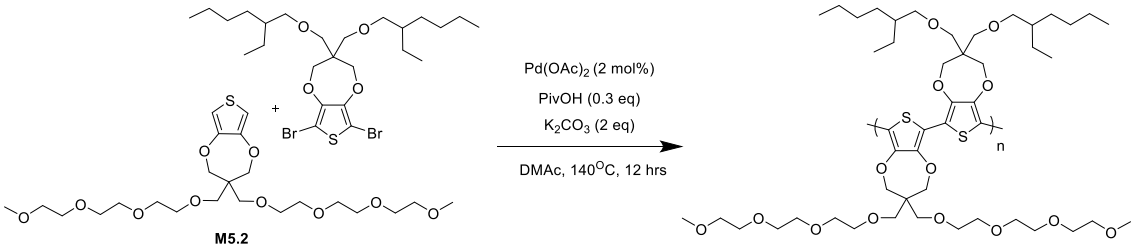

M5.2

The polymer was obtained as a purple polymer in 68% yield (0.61 g). ^{1}H NMR (700 MHz, $CDCl_3$) δ (ppm) 4.16 (b, *J* = 19.4 Hz, 8H), 3.77 – 3.54 (m, 28H), 3.54 – 3.49 (m, 4H), 3.39 – 3.25 (m, 10H), 1.52 (s, 2H), 1.44 – 1.23 (m, 16H), 0.93 – 0.85 (m, 12H). M_n: 47 kDa, Đ: 1.8, *vs*. PS in $CHCl_3$ at 40 °C. Anal. calcd. for $C_{48}H_{82}O_{14}S_2$ C 60.86, H 8.73, S 6.77, Found C 60.99, H 8.50, S 6.84.

Synthesis of ProDOT(OE)-AcDOT(C12)

To a 50 mL Schlenk tube equipped with stir bar ProDOT(OE) (0.83 g, 1.0 eq.), 2,5-dibromo-3,4-bis(octyloxy)thiophene (0.99 g, 1.0 eq.) palladium(II) acetate (cat. Amount) pivalic acid (0.33 g, 0.5 eq.), and potassium carbonate (0.56 g, 2.5 eq.) were added. 16 mL of DMAc was added to dissolve the contents and the tube was sealed under a blanket of argon. The reaction mixture was premixed for 5 minutes before it was lowered into a 140 °C oil bath. The solution was left to stir vigorously overnight. After the flask was removed from the oil bath and allowed to cool to room temperature, the polymer was precipitated into methanol and stirred for one hour. The precipitate was filtered into a Soxhlet extraction thimble and washed with methanol, acetone, hexanes, toluene, and chloroform. The washings were conducted until the color was no longer observed during extraction. ~20 mg of a palladium scavenger (diethylammonium diethyldithiocarbamate) and ~20 mg of 18-crown-6, was added to the chloroform fraction and then stirred for 2 hours at 50 °C. The chloroform was removed under reduced pressure and polymer was precipitated into ~300 mL of methanol. The precipitate was vacuum filtered using a nylon pad (with a pore size of 20 μm) and washed with a large volume of methanol before letting it air dry. The dried material was collected into a vial and dried under vacuum for two days.

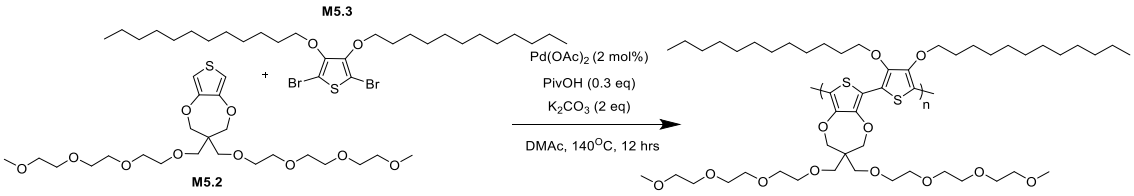

The polymer was obtained as a black/purple polymer in 64.8 % yield (1.2 g). ^{1}H NMR (700 MHz, $CDCl_3$) δ (ppm) 4.14 (d, *J* = 60.8 Hz, 8H), 3.67 (dt, *J* = 31.4, 18.8 Hz, 24H), 3.56 –

3.46 (m, 4H), 3.39 – 3.29 (m, 6H), 1.92 (s, 4H), 1.46 (t, *J* = 31.7 Hz, 4H), 1.32 (d, *J* = 75.5 Hz, 32H), 0.88 (t, *J* = 6.1 Hz, 6H). Anal. calcd. for $C_{51}H_{88}O_{12}S_2$ C 63.98, H 9.27, S 6.70, Found C 63.19, H 9.50, S 6.40. M_n: 15 kDa, Đ: 1.6, *vs.* PS in $CHCl_3$ at 40 °C.

CHAPTER 6. PERSPECTIVE AND RECOMMENDATIONS FOR FUTURE RESEARCH

In the past three decades, solution-processable cathodically coloring π-conjugated polymers, specifically those based on dioxythiophene (PXDOT), have received significant attention as an active layer in electrochromic devices (ECDs). The interest in these materials is due to their ability to undergo facile chemical modification (which allows for a wide range of colors and optical band gaps), low oxidation potentials (enabling low-power devices with high stability), high optical contrast between their colored neutral state and their transmissive oxidized states, and solution processability (which facilitates the facile printing and patterning of active materials).

In general, the π-conjugated backbone dictates the optoelectronic properties of the resulting polymer. Consequently, most research efforts have focused on tailoring optoelectronic properties through chemical modifications of the conjugated backbone. While these studies have led to significant advances in polymer design, solubilizing side chains generally have only been used to expand polymerization methods, increase the molecular weight of polymers, and improve their processability. The research presented in this dissertation has shown that side chain structure not only affects the properties like solubility and processability, but they also can drastically influence the optical and electrochemical properties of PXDOTs. Systematic investigations into the effects of side chains on the optoelectronic properties XDOTs has led to new design rules for manipulating the electrochromic properties of these materials.

6.1 Alkyl side chains

In Chapter 3, the structural design and synthesis of five XDOT-based polymers with linear and branched side chains were reported. Using a range of analysis methods, it was determined that changing from linear to branched side chains affects ionization potential, optical bandgap, perceived color, electrochromic contrast, switching speed, and switching stability. The polymers with branched side chains showed higher onsets of oxidation, greater optical bandgaps, and demonstrate sudden coloration change compared to polymers with linear side chains. In addition to the optoelectronic properties, it was demonstrated that aggregations can be tuned through the choice of side chain structure. Branched side chains reduced interchain interactions and increase solubility in organic solvents. In Chapter 4, six polymers with varying branching position, length, and density were synthesized and analyzed. It was determined that by changing the branching point from the second carbon to the to the first carbon away from the backbone significantly changed the effective conjugation length, red-shifting the λ_{max} by 100 nm. This resulted in a polymer with a smaller optical bandgap and therefore a purple color, instead of an orange color.

6.1.1 Limitations and path forward

The families of polymers with alkyl side chains were designed and synthesized with the goal of examining the effects of the side chain structure and chemistry on optoelectronic properties by introducing torsional strain, which increases the energy associated with planarization of two neighboring rings. Further research on alkyl side chains should focus on:

1. The influence of side chain on the interring bond lengths and the torsional angle between rings of adjacent units. This can be accomplished through density functional theory (DFT) calculation on the polymers in the neutral state and the oxidized state.

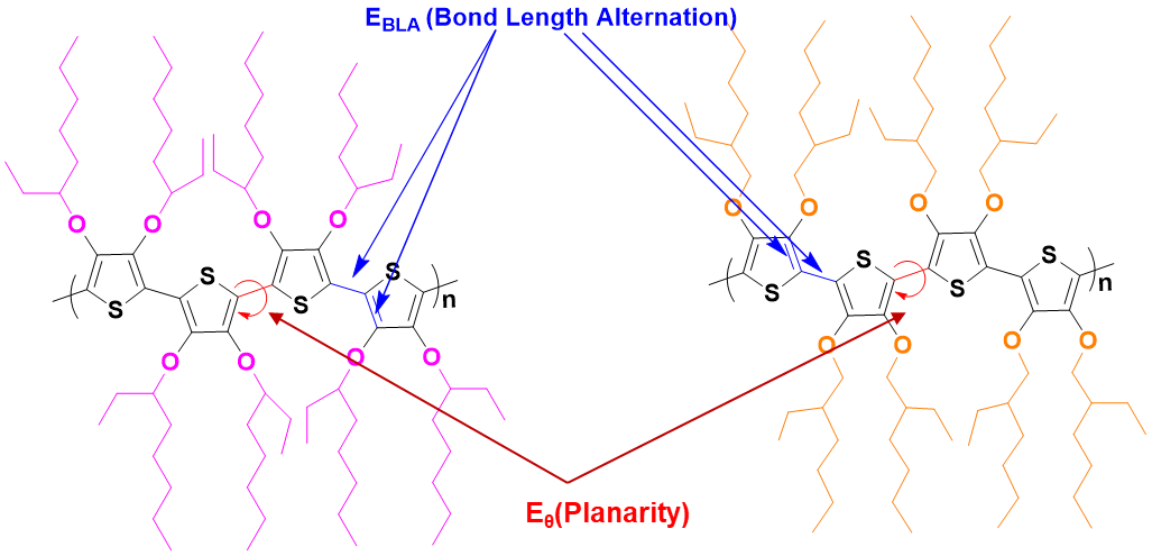

Figure 6.1. Determine the interring bond lengths and the torsional angle between rings of adjacent units through density functional theory (DFT) calculation on the polymers in the neutral state and the oxidized state

2. The synthesis of new DOTs polymers where the side chain length is systematically increased.
3. The effects of aggregation and π-π stacking on optoelectronic properties. The linear homopolymer, P(LAcDOT) synthesized in Chapter 3 was able to switch for 1,000 full redox cycles and did not show any changes in optical contrast, while the branched homopolymer, P(BAcDOT), showed a significant change in absorbance after 50 switches. It is unclear if the P(LAcDOT) is stable to electrochemical cycling due to the low oxidation potential or due to its aggregated morphological features.

6.2 Oligoether side chains

In an effort to expand the number of water-compatible polymers based on XDOTs, in Chapter 5, two oligoether and alkyl functionalized DOT-based polymers were prepared through DHAP. The alkyl side chains allowed the polymers to be soluble in common organic solvents, while the oligoether side chains provided aqueous electrochemical compatibility. Hence the polymers were able to dope and dedoped in aqueous electrolytes without dispersing or dissolving. The optoelectronic properties of the two new polymers, ProDOT(OE)-ProDOT(EOM) and ProDOT(OE)-AcDOT(C12), were compared to ProDOT (OE)-DMP. The introduction of ((2-ethylhexyl)oxy)methyl (EOM) branched side chain in ProDOT(OE)-ProDOT(OEM) in place of the smaller dimethyl group on the ProDOT(OE)-DMP resulted in a higher onset of oxidation and slower switching speed. When the ProDOT(OE) monomer was copolymerized with AcDOT(C12), the *n*-dodecane side chain increased the steric hindrance associated with planarization of the conjugated backbone, resulting in a polymer with a higher onset of oxidation and slower switching speeds. The higher onset of oxidation of the two polymers relative to ProDOT(OE)-DMP can be explained by the bulky side chains, which introduced steric effects on the backbone. The slow switching speed is due to the alkyl side chains increasing the overall polymer hydrophobicity. Beyond the primary motivation of improving solubility, oligoether side chains can be further exploited to tune optoelectronic and ionic properties of polymers, such as oxidation onset and switching speed.

6.2.1 Recommendation: synthesis of new water-compatible polymers

The ProDOT(OE) monomer was copolymerized with ProDOT(OEM) and AcDOT(C12), resulting in materials that absorb in the middle of the visible spectrum hence appearing magenta or purple. Synthesis of new water-compatible polymers should focus on expanding the oligoether functionalized DOTs family. The ProDOT(OE) monomer should be copolymerized with different arylene groups with varied redox and spectral properties using DHAP, as shown in Figure 6.1. The key synthon should be the same ProDOT monomer bearing long oligoether side chains. To synthesized higher gap materials (red, orange, and yellow), the ProDOT(OE) monomers should be copolymerized with high highly twisted monomers, such as triphenylamine (TPA), to increase torsional interactions between aromatic rings along the polymer backbone. This minimizes sulfur-oxygen (S-O) interactions that cause planarization on the backbone, subsequently blue-shifting the absorption to the high energy portion of the visible range. To provide a material with a cyan or green color, the ECP must have a dual-band absorption profile where it absorbs both in the long and short wavelength range of the visible spectrum and transmits light between 450 – 600 nm. With these considerations, the ProDOT(OE) monomer should be copolymerized with acceptor molecules, such as isoindigo and thienoisoindigo. These will result in donor-acceptor polymers with dual absorbance profiles. Copolymerizing ProDOT(OE) with different electron rich and electron poor monomers will yield water-compatible polymers that span the whole visible spectrum and are easily purified and fully characterized using standard methods (NMR, GPC, etc.).

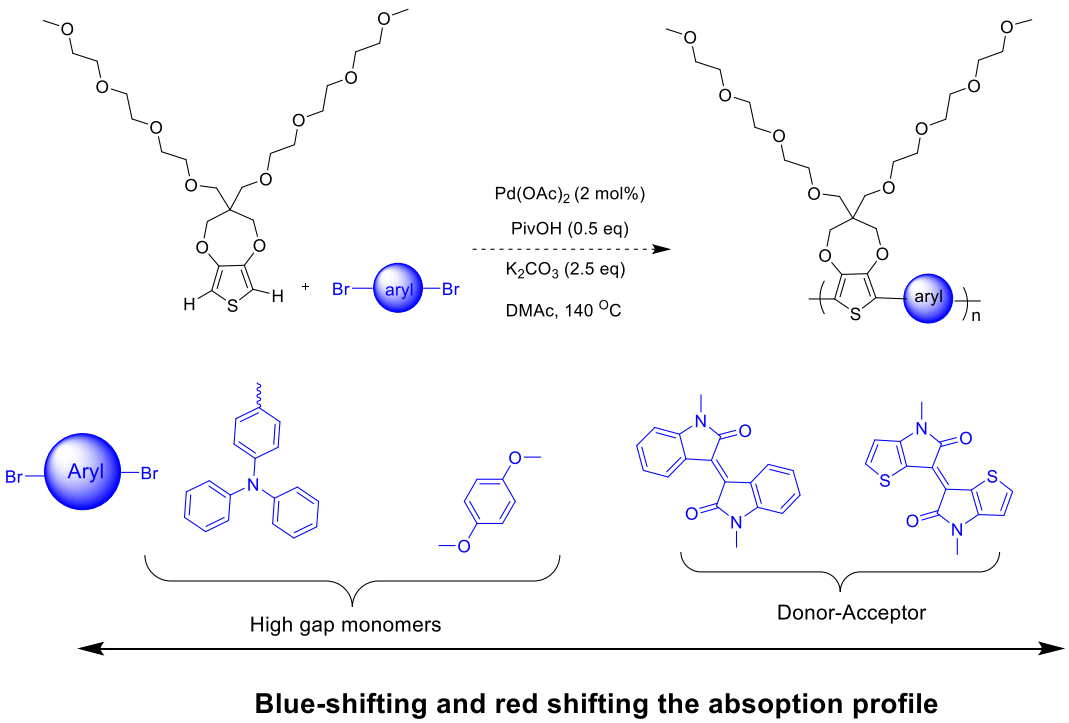

Figure 6.2. Proposed water-compatible polymers

6.3 Broader impact

Traditionally, tuning optoelectronic properties have been accomplished through careful selection of 1) heteroatom, 2) comonomer, and 3) the presence or absence of oxygen atoms in the β positions. Side chains, on the other hand, have been used primarily as a means of improving processability. However, studies including those presented in this dissertation have shown that the solubilizing group can also affect the optoelectronic properties of the resulting ECP. Optoelectronic properties can be tuned by changing the steric interactions through the use or linear and branched side chains in the β positions. The branching position, length, and density can also affect the optoelectronic properties. Shorter and linear alkyl side chains increase backbone planarity, resulting in lower band gaps while longer and branched side chain increases the torsional angle along the conjugated backbone, hence increases the optical gaps. This also results in a decreased

effective conjugation length and increases the onset of oxidation. While researchers have often chosen different side chains to achieve solubility in desired solvents, this dissertation has shown that side chains can also be used to tune ionic conductivity and optoelectronic properties. Therefore, chemist should the effects of side chains when designing new conjugated polymers for electrochromic devices.

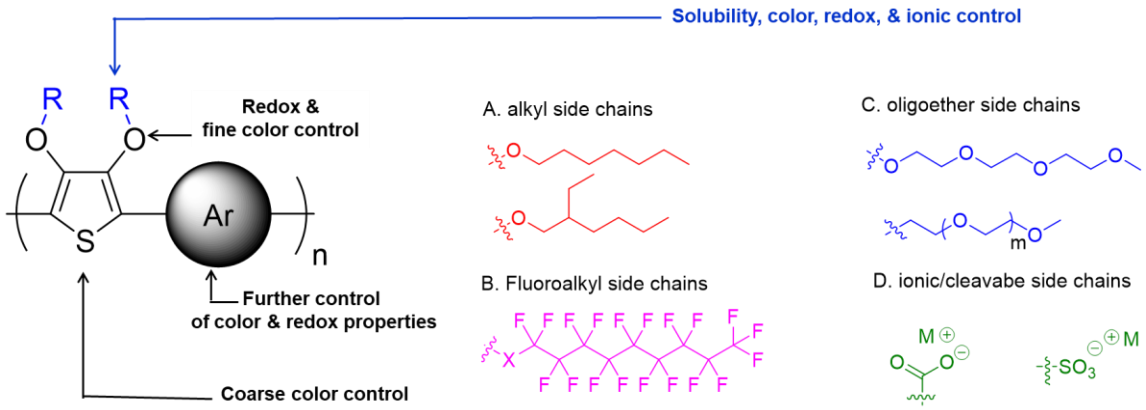

Figure 6.3. A new model for tuning optoelectronic properties.

REFERENCES

1. Roncali, J.; Shi, L. H.; Garreau, R.; Garnier, F.; Lemaire, M., Tuning of the aqueous electroactivity of substituted poly(thiophene)s by ether groups. *Synthetic Metals* **1990,** *36* (2), 267-273.

2. Kumar, A.; Reynolds, J. R., Soluble Alkyl-Substituted Poly(ethylenedioxythiophenes) as Electrochromic Materials. *Macromolecules* **1996,** *29* (23), 7629-7630.

3. Li, L.; Counts K. E.; Kurosawa, S.; Teja. A. S.; David D. M., Tuning the Electronic Structure and Solubility of Conjugated Polymers with Perfluoroalkyl Substituents: Poly(3-perfluorooctylthiophene), the First Supercritical CO2-soluble Conjugated Polymer. *Advanced Materials* **2004,** *16* (2), 180-183.

4. Reeves, B. D.; Grenier, C. R. G.; Argun, A. A.; Cirpan, A.; McCarley, T. D.; Reynolds, J. R., Spray Coatable Electrochromic Dioxythiophene Polymers with High Coloration Efficiencies. *Macromolecules* **2004,** *37* (20), 7559-7569.

5. Li, L.; Collard, D. M., Tuning the Electronic Structure of Conjugated Polymers with Fluoroalkyl Substitution: Alternating Alkyl/Perfluoroalkyl-Substituted Polythiophene. *Macromolecules* **2005,** *38* (2), 372-378.

6. Sonmez, G.; Sonmez, H. B.; Shen, C. K. F.; Jost, R. W.; Rubin, Y.; Wudl, F., A Processable Green Polymeric Electrochromic. *Macromolecules* **2005,** *38* (3), 669-675.

7. Zhao, X.; Pinto, M. R.; Hardison, L. M.; Mwaura, J.; Müller, J.; Jiang, H.; Witker, D.; Kleiman, V. D.; Reynolds, J. R.; Schanze, K. S., Variable Band Gap Poly(arylene ethynylene) Conjugated Polyelectrolytes. *Macromolecules* **2006,** *39* (19), 6355-6366.

8. Grenier, C. R. G.; George, S. J.; Joncheray, T. J.; Meijer, E. W.; Reynolds, J. R., Chiral Ethylhexyl Substituents for Optically Active Aggregates of π-Conjugated Polymers. *Journal of the American Chemical Society* **2007,** *129* (35), 10694-10699.

9. Kline, R. J.; DeLongchamp, D. M.; Fischer, D. A.; Lin, E. K.; Richter, L. J.; Chabinyc, M. L.; Toney, M. F.; Heeney, M.; McCulloch, I., Critical Role of Side-Chain Attachment Density on the Order and Device Performance of Polythiophenes. *Macromolecules* **2007,** *40* (22), 7960-7965.

10. Beaujuge, P. M.; Ellinger, S.; Reynolds, J. R., Spray Processable Green to Highly Transmissive Electrochromics via Chemically Polymerizable Donor–Acceptor Heterocyclic Pentamers. *Advanced Materials* **2008,** *20* (14), 2772-2776.

11. Amb, C. M.; Beaujuge, P. M.; Reynolds, J. R., Spray-Processable Blue-to-Highly Transmissive Switching Polymer Electrochromes via the Donor–Acceptor Approach. *Advanced Materials* **2010,** *22* (6), 724-728.

12. Shi, P.; Amb, C. M.; Dyer, A. L.; Reynolds, J. R., Fast Switching Water Processable Electrochromic Polymers. *ACS Applied Materials & Interfaces* **2012,** *4* (12), 6512-6521.

13. Oguzhan, E.; Bilgili, H.; Baycan Koyuncu, F.; Ozdemir, E.; Koyuncu, S., A new processable donor–acceptor polymer displaying neutral state yellow electrochromism. *Polymer* **2013,** *54* (23), 6283-6292.

14. Mei, J.; Bao, Z., Side Chain Engineering in Solution-Processable Conjugated Polymers. *Chemistry of Materials* **2014,** *26* (1), 604-615.

15. Meng, B.; Song, H.; Chen, X.; Xie, Z.; Liu, J.; Wang, L., Replacing Alkyl with Oligo(ethylene glycol) as Side Chains of Conjugated Polymers for Close π–π Stacking. *Macromolecules* **2015,** *48* (13), 4357-4363.

16. Xu, Z.; Chen, X.; Mi, S.; Zheng, J.; Xu, C., Solution-processable electrochromic red-to-transmissive polymers with tunable neutral state colors, high contrast and enhanced stability. *Organic Electronics* **2015,** *26*, 129-136.

17. Beaujuge, P. M.; Reynolds, J. R., Color Control in π-Conjugated Organic Polymers for Use in Electrochromic Devices. *Chemical Reviews* **2010,** *110* (1), 268-320.

18. Bredas, J. L.; Street, G. B., Polarons, bipolarons, and solitons in conducting polymers. *Accounts of Chemical Research* **1985,** *18* (10), 309-315.

19. Reynolds, J. R.; Kumar, A.; Reddinger, J. L.; Sankaran, B.; Sapp, S. A.; Sotzing, G. A., Unique variable-gap polyheterocycles for high-contrast dual polymer electrochromic devices. *Synthetic Metals* **1997,** *85* (1), 1295-1298.

20. Kumar, A.; Welsh, D. M.; Morvant, M. C.; Piroux, F.; Abboud, K. A.; Reynolds, J. R., Conducting Poly(3,4-alkylenedioxythiophene) Derivatives as Fast Electrochromics with High-Contrast Ratios. *Chemistry of Materials* **1998,** *10* (3), 896-902.

21. Krishnamoorthy, K.; Ambade, A. V.; Kanungo, M.; Contractor, A. Q.; Kumar, A., Rational design of an electrochromic polymer with high contrast in the visible region: dibenzyl substituted poly(3,4-propylenedioxythiophene). *Journal of Materials Chemistry* **2001,** *11* (12), 2909-2911.

22. Österholm, A. M.; Shen, D. E.; Kerszulis, J. A.; Bulloch, R. H.; Kuepfert, M.; Dyer, A. L.; Reynolds, J. R., Four Shades of Brown: Tuning of Electrochromic Polymer Blends Toward High-Contrast Eyewear. *ACS Applied Materials & Interfaces* **2015,** *7* (3), 1413-1421.

23. Cao, K.; Shen, D. E.; Österholm, A. M.; Kerszulis, J. A.; Reynolds, J. R., Tuning Color, Contrast, and Redox Stability in High Gap Cathodically Coloring Electrochromic Polymers. *Macromolecules* **2016,** *49* (22), 8498-8507.

24. Savagian, L. R.; Österholm, A. M.; Shen, D. E.; Christiansen, D. T.; Kuepfert, M.; Reynolds, J. R., Conjugated Polymer Blends for High Contrast Black-to-Transmissive Electrochromism. *Advanced Optical Materials* **2018,** *6* (19), 1800594.

25. Gaupp, C. L.; Welsh, D. M.; Reynolds, J. R., Poly(ProDOT-Et2): A High-Contrast, High-Coloration Efficiency Electrochromic Polymer. *Macromolecular Rapid Communications* **2002,** *23* (15), 885-889.

26. Ponder, J. F.; Österholm, A. M.; Reynolds, J. R., Conjugated Polyelectrolytes as Water Processable Precursors to Aqueous Compatible Redox Active Polymers for Diverse Applications: Electrochromism, Charge Storage, and Biocompatible Organic Electronics. *Chemistry of Materials* **2017,** *29* (10), 4385-4392.

27. Bulloch, R. H.; Reynolds, J. R., Photostability in dioxyheterocycle electrochromic polymers. *Journal of Materials Chemistry C* **2016,** *4* (3), 603-610.

28. Andersson Ersman, P.; Kawahara, J.; Berggren, M., Printed passive matrix addressed electrochromic displays. *Organic Electronics* **2013,** *14* (12), 3371-3378.

29. Sonmez, G.; Sonmez, H. B., Polymeric electrochromics for data storage. *Journal of Materials Chemistry* **2006,** *16* (25), 2473-2477.

30. Yu, H.; Shao, S.; Yan, L.; Meng, H.; He, Y.; Yao, C.; Xu, P.; Zhang, X.; Hu, W.; Huang, W., Side-chain engineering of green color electrochromic polymer materials: toward adaptive camouflage application. *Journal of Materials Chemistry C* **2016,** *4* (12), 2269-2273.

31. Beaupré, S.; Breton, A.-C.; Dumas, J.; Leclerc, M., Multicolored Electrochromic Cells Based On Poly(2,7-Carbazole) Derivatives For Adaptive Camouflage. *Chemistry of Materials* **2009,** *21* (8), 1504-1513.

32. Kim, Y.; Shin, H.; Han, M.; Seo, S.; Lee, W.; Na, J.; Park, C.; Kim, E., Energy Saving Electrochromic Polymer Windows with a Highly Transparent Charge-Balancing Layer. *Advanced Functional Materials* **2017,** *27* (31), 1701192.

33. Salzner, U.; Lagowski, J. B.; Pickup, P. G.; Poirier, R. A., Comparison of geometries and electronic structures of polyacetylene, polyborole, polycyclopentadiene, polypyrrole, polyfuran, polysilole, polyphosphole, polythiophene, polyselenophene and polytellurophene. *Synthetic Metals* **1998,** *96* (3), 177-189.

34. Roncali, J., Molecular Engineering of the Band Gap of π-Conjugated Systems: Facing Technological Applications. *Macromolecular Rapid Communications* **2007,** *28* (17), 1761-1775.

35. Winkler, S.; Amsalem, P.; Frisch, J.; Oehzelt, M.; Heimel, G.; Koch, N., Probing the energy levels in hole-doped molecular semiconductors. *Materials Horizons* **2015,** *2* (4), 427-433.

36. Oehzelt, M.; Koch, N.; Heimel, G., Organic semiconductor density of states controls the energy level alignment at electrode interfaces. *Nature Communications* **2014,** *5*, 4174.

37. Haynes, D.; McCullough, R., CHAPTER 9 Polythiophenes. In *Conjugated Polymers: A Practical Guide to Synthesis*, The Royal Society of Chemistry: 2014; pp 180-200.

38. Lin, J. W.-P.; Dudek, L. P., Synthesis and properties of poly(2,5-thienylene). *Journal of Polymer Science: Polymer Chemistry Edition* **1980,** *18* (9), 2869-2873.

39. Yamamoto, T.; Sanechika, K.; Yamamoto, A., Preparation of thermostable and electric-conducting poly(2,5-thienylene). *Journal of Polymer Science: Polymer Letters Edition* **1980,** *18* (1), 9-12.

40. Daoust, G.; Leclerc, M., Structure-property relationships in alkoxy-substituted polythiophenes. *Macromolecules* **1991,** *24* (2), 455-459.

41. Roncali, J., Conjugated poly(thiophenes): synthesis, functionalization, and applications. *Chemical Reviews* **1992,** *92* (4), 711-738.

42. Groenendaal, L.; Jonas, F.; Freitag, D.; Pielartzik, H.; Reynolds, J. R., Poly(3,4-ethylenedioxythiophene) and Its Derivatives: Past, Present, and Future. *Advanced Materials* **2000,** *12* (7), 481-494.

43. Groenendaal, L.; Zotti, G.; Aubert, P.-H.; Waybright, S. M.; Reynolds, J. R., Electrochemistry of Poly(3,4-alkylenedioxythiophene) Derivatives. *Advanced Materials* **2003,** *15* (11), 855-879.

44. Wang, Y.; Runnerstrom, E. L.; Milliron, D. J., Switchable Materials for Smart Windows. *Annual Review of Chemical and Biomolecular Engineering* **2016,** *7* (1), 283-304.

45. Eh, A. L.-S.; Tan, A. W. M.; Cheng, X.; Magdassi, S.; Lee, P. S., Recent Advances in Flexible Electrochromic Devices: Prerequisites, Challenges, and Prospects. *Energy Technology* **2018,** *6* (1), 33-45.

46. Percec, S.; Tilford, S., A single-layer approach to electrochromic materials. *Journal of Polymer Science Part A: Polymer Chemistry* **2011,** *49* (2), 361-368.

47. Jensen, J.; Hösel, M.; Dyer, A. L.; Krebs, F. C., Development and Manufacture of Polymer-Based Electrochromic Devices. *Advanced Functional Materials* **2015,** *25* (14), 2073-2090.

48. Rosseinsky, R. D.; Mortimer R. J., Electrochromic Systems and the Prospects for Devices. *Advanced Materials* **2001,** *13* (11), 783-793.

49. Jacob, J.; Markus, H.; L., D. A.; C., K. F., Development and Manufacture of Polymer-Based Electrochromic Devices. *Advanced Functional Materials* **2015,** *25* (14), 2073-2090.

50. Knott, E. P.; Craig, M. R.; Liu, D. Y.; Babiarz, J. E.; Dyer, A. L.; Reynolds, J. R., A minimally coloured dioxypyrrole polymer as a counter electrode material in polymeric electrochromic window devices. *Journal of Materials Chemistry* **2012,** *22* (11), 4953-4962.

51. Eric Shen, D.; Österholm, A. M.; Reynolds, J. R., Out of sight but not out of mind: the role of counter electrodes in polymer-based solid-state electrochromic devices. *Journal of Materials Chemistry C* **2015,** *3* (37), 9715-9725.

52. Dyer, A. L.; Bulloch, R. H.; Zhou, Y.; Kippelen, B.; Reynolds, J. R.; Zhang, F., A Vertically Integrated Solar-Powered Electrochromic Window for Energy Efficient Buildings. *Advanced Materials* **2014,** *26* (28), 4895-4900.

53. Vasilyeva, S. V.; Beaujuge, P. M.; Wang, S.; Babiarz, J. E.; Ballarotto, V. W.; Reynolds, J. R., Material Strategies for Black-to-Transmissive Window-Type Polymer Electrochromic Devices. *ACS Applied Materials & Interfaces* **2011,** *3* (4), 1022-1032.

54. Argun, A. A.; Aubert, P.-H.; Thompson, B. C.; Schwendeman, I.; Gaupp, C. L.; Hwang, J.; Pinto, N. J.; Tanner, D. B.; MacDiarmid, A. G.; Reynolds, J. R., Multicolored Electrochromism in Polymers: Structures and Devices. *Chemistry of Materials* **2004,** *16* (23), 4401-4412.

55. Lee-Sie, E. A.; Ming, T. A. W.; Xing, C.; Shlomo, M.; See, L. P., Recent Advances in Flexible Electrochromic Devices: Prerequisites, Challenges, and Prospects. *Energy Technology* **2018,** *6* (1), 33-45.

56. Gaupp, C. L.; Welsh, D. M.; Rauh, R. D.; Reynolds, J. R., Composite Coloration Efficiency Measurements of Electrochromic Polymers Based on 3,4-Alkylenedioxythiophenes. *Chemistry of Materials* **2002,** *14* (9), 3964-3970.

57. Garino, N.; Zanarini, S.; Bodoardo, S.; Nair, J. R.; Pereira, S.; Pereira, L.; Martins, R.; Fortunato, E.; Penazzi, N., Fast Switching Electrochromic Devices Containing Optimized BEMA/PEGMA Gel Polymer Electrolytes. *International Journal of Electrochemistry* **2013,** *2013*, 10.

58. Cummins, D.; Boschloo, G.; Ryan, M.; Corr, D.; Rao, S. N.; Fitzmaurice, D., Ultrafast Electrochromic Windows Based on Redox-Chromophore Modified Nanostructured Semiconducting and Conducting Films. *The Journal of Physical Chemistry B* **2000,** *104* (48), 11449-11459.

59. Shin, H.; Kim, Y.; Bhuvana, T.; Lee, J.; Yang, X.; Park, C.; Kim, E., Color Combination of Conductive Polymers for Black Electrochromism. *ACS Applied Materials & Interfaces* **2012,** *4* (1), 185-191.

60. Ah, C. S.; Song, J.; Cho, S. M.; Kim, T.-Y.; Kim, H. N.; Oh, J. Y.; Chu, H. Y.; Ryu, H., Double-layered Black Electrochromic Device with a Single Electrode and Long-Term Bistability. *Bulletin of the Korean Chemical Society* **2015,** *36* (2), 548-552.

61. Hassab, S.; Shen, D. E.; Österholm, A. M.; Da Rocha, M.; Song, G.; Alesanco, Y.; Viñuales, A.; Rougier, A.; Reynolds, J. R.; Padilla, J., A new standard method to calculate electrochromic switching time. *Solar Energy Materials and Solar Cells* **2018,** *185*, 54-60.

62. Day, M.; Wiles, D. M., Photochemical degradation of poly(ethylene terephthalate). III. Determination of decomposition products and reaction mechanism. *Journal of Applied Polymer Science* **1972,** *16* (1), 203-215.

63. Abdou, M. S. A.; Holdcroft, S., Mechanisms of photodegradation of poly(3-alkylthiophenes) in solution. *Macromolecules* **1993,** *26* (11), 2954-2962.

64. Kerszulis, J. A.; Amb, C. M.; Dyer, A. L.; Reynolds, J. R., Follow the Yellow Brick Road: Structural Optimization of Vibrant Yellow-to-Transmissive Electrochromic Conjugated Polymers. *Macromolecules* **2014,** *47* (16), 5462-5469.

65. İçli-Özkut, M.; Öztaş, Z.; Algi, F.; Cihaner, A., A neutral state yellow to navy polymer electrochrome with pyrene scaffold. *Organic Electronics* **2011,** *12* (9), 1505-1511.

66. Amb, C. M.; Kerszulis, J. A.; Thompson, E. J.; Dyer, A. L.; Reynolds, J. R., Propylenedioxythiophene (ProDOT)-phenylene copolymers allow a yellow-to-transmissive electrochrome. *Polymer Chemistry* **2011,** *2* (4), 812-814.

67. Meerholz, K.; Heinze, J., Solid state electrochemical experiments on defined oligomers of the poly-p-phenylene-series as models of conducting polymers. *Synthetic Metals* **1991,** *43* (1), 2871-2876.

68. Meerholz, K.; Heinze, J., Electrochemical solution and solid-state investigations on conjugated oligomers and polymers of the α-thiophene and the p-phenylene series. *Electrochimica Acta* **1996,** *41* (11), 1839-1854.

69. Goldenberg, L. M.; Lacaze, P. C., Anodic synthesis of poly(p-phenylene). *Synthetic Metals* **1993,** *58* (3), 271-293.

70. Guan, S.; Elmezayyen, A. S.; Zhang, F.; Zheng, J.; Xu, C., Deterioration mechanism of electrochromic poly(3,4-(2,2-dimethylpropylenedioxy)thiophene) thin films. *Journal of Materials Chemistry C* **2016,** *4* (20), 4584-4591.

71. Jensen, J.; Madsen, M. V.; Krebs, F. C., Photochemical stability of electrochromic polymers and devices. *Journal of Materials Chemistry C* **2013,** *1* (32), 4826-4835.

72. Roncali, J., Synthetic Principles for Bandgap Control in Linear π-Conjugated Systems. *Chemical Reviews* **1997,** *97* (1), 173-206.

73. Arulmozhiraja, S.; Fujii, T., Torsional barrier, ionization potential, and electron affinity of biphenyl—A theoretical study. *The Journal of Chemical Physics* **2001,** *115* (23), 10589-10594.

74. Raos, G.; Famulari, A.; Marcon, V., Computational reinvestigation of the bithiophene torsion potential. *Chemical Physics Letters* **2003,** *379* (3), 364-372.

75. Beaujuge, P. M.; Vasilyeva, S. V.; Liu, D. Y.; Ellinger, S.; McCarley, T. D.; Reynolds, J. R., Structure-Performance Correlations in Spray-Processable Green Dioxythiophene-Benzothiadiazole Donor–Acceptor Polymer Electrochromes. *Chemistry of Materials* **2012,** *24* (2), 255-268.

76. Beaujuge, P. M.; Amb, C. M.; Reynolds, J. R., Spectral Engineering in π-Conjugated Polymers with Intramolecular Donor−Acceptor Interactions. *Accounts of Chemical Research* **2010,** *43* (11), 1396-1407.

77. Ponder, J. F.; Österholm, A. M.; Reynolds, J. R., Designing a Soluble PEDOT Analogue without Surfactants or Dispersants. *Macromolecules* **2016,** *49* (6), 2106-2111.

78. Kerszulis, J. A.; Johnson, K. E.; Kuepfert, M.; Khoshabo, D.; Dyer, A. L.; Reynolds, J. R., Tuning the painter's palette: subtle steric effects on spectra and colour in conjugated electrochromic polymers. *Journal of Materials Chemistry C* **2015,** *3* (13), 3211-3218.

79. DuBois, C. J.; Reynolds, J. R., 3,4-Ethylenedioxythiophene–Pyridine-Based Polymers: Redox or n-Type Electronic Conductivity? *Advanced Materials* **2002,** *14* (24), 1844-1846.

80. Beaujuge, P. M.; Vasilyeva, S. V.; Ellinger, S.; McCarley, T. D.; Reynolds, J. R., Unsaturated Linkages in Dioxythiophene−Benzothiadiazole Donor−Acceptor Electrochromic Polymers: The Key Role of Conformational Freedom. *Macromolecules* **2009,** *42* (11), 3694-3706.

81. İçli, M.; Pamuk, M.; Algi, F.; Önal, A. M.; Cihaner, A., Donor−Acceptor Polymer Electrochromes with Tunable Colors and Performance. *Chemistry of Materials* **2010,** *22* (13), 4034-4044.

82. Wu, C.-G.; Lu, M.-I.; Tsai, P.-F., Full-Color Processible Electrochromic Polymers Based on 4,4-Dioctyl-Cyclopentadithiophene. *Macromolecular Chemistry and Physics* **2009,** *210* (21), 1851-1855.

83. Gunbas, G. E.; Durmus, A.; Toppare, L., A Unique Processable Green Polymer with a Transmissive Oxidized State for Realization of Potential RGB-Based Electrochromic Device Applications. *Advanced Functional Materials* **2008,** *18* (14), 2026-2030.

84. Pei, Q.; Zuccarello, G.; Ahlskog, M.; Inganäs, O., Electrochromic and highly stable poly(3,4-ethylenedioxythiophene) switches between opaque blue-black and transparent sky blue. *Polymer* **1994,** *35* (7), 1347-1351.

85. Balan, A.; Baran, D.; Sariciftci, N. S.; Toppare, L., Electrochromic device and bulk heterojunction solar cell applications of poly 4,7-bis(2,3-dihydrothieno[3,4-b][1,4]dioxin-5-yl)-2-dodecyl-2H-benzo[1,2,3]triazole (PBEBT). *Solar Energy Materials and Solar Cells* **2010,** *94* (10), 1797-1802.

86. Welsh, D. M.; Kloeppner, L. J.; Madrigal, L.; Pinto, M. R.; Thompson, B. C.; Schanze, K. S.; Abboud, K. A.; Powell, D.; Reynolds, J. R., Regiosymmetric Dibutyl-Substituted Poly(3,4-propylenedioxythiophene)s as Highly Electron-Rich Electroactive and Luminescent Polymers. *Macromolecules* **2002,** *35* (17), 6517-6525.

87. Cirpan, A.; Argun, A. A.; Grenier, C. R. G.; Reeves, B. D.; Reynolds, J. R., Electrochromic devices based on soluble and processable dioxythiophene polymers. *Journal of Materials Chemistry* **2003,** *13* (10), 2422-2428.

88. Beaujuge, P. M.; Ellinger, S.; Reynolds, J. R., The donor–acceptor approach allows a black-to-transmissive switching polymeric electrochrome. *Nature Materials* **2008,** *7*, 795.

89. Shi, P.; Amb, C. M.; Knott, E. P.; Thompson, E. J.; Liu, D. Y.; Mei, J.; Dyer, A. L.; Reynolds, J. R., Broadly Absorbing Black to Transmissive Switching Electrochromic Polymers. *Advanced Materials* **2010,** *22* (44), 4949-4953.

90. Neo, W. T.; Cho, C. M.; Shi, Z.; Chua, S.-J.; Xu, J., Modulating high-energy visible light absorption to attain neutral-state black electrochromic polymers. *Journal of Materials Chemistry C* **2016,** *4* (1), 28-32.

91. İçli, M.; Pamuk, M.; Algı, F.; Önal, A. M.; Cihaner, A., A new soluble neutral state black electrochromic copolymer via a donor–acceptor approach. *Organic Electronics* **2010,** *11* (7), 1255-1260.

92. Öktem, G.; Balan, A.; Baran, D.; Toppare, L., Donor–acceptor type random copolymers for full visible light absorption. *Chemical Communications* **2011,** *47* (13), 3933-3935.

93. Lombeck, F.; Komber, H.; Gorelsky, S. I.; Sommer, M., Identifying Homocouplings as Critical Side Reactions in Direct Arylation Polycondensation. *ACS Macro Letters* **2014,** *3* (8), 819-823.

94. Matsidik, R.; Komber, H.; Sommer, M., Rational Use of Aromatic Solvents for Direct Arylation Polycondensation: C–H Reactivity versus Solvent Quality. *ACS Macro Letters* **2015,** *4* (12), 1346-1350.

95. Rudenko, A. E.; Thompson, B. C., Optimization of direct arylation polymerization (DArP) through the identification and control of defects in polymer structure. *Journal of Polymer Science Part A: Polymer Chemistry* **2015,** *53* (2), 135-147.

96. Lombeck, F.; Marx, F.; Strassel, K.; Kunz, S.; Lienert, C.; Komber, H.; Friend, R.; Sommer, M., To branch or not to branch: C–H selectivity of thiophene-based donor–acceptor–donor monomers in direct arylation polycondensation exemplified by PCDTBT. *Polymer Chemistry* **2017,** *8* (32), 4738-4745.

97. Hayashi, S.; Yamamoto, S.-i.; Koizumi, T., Effects of molecular weight on the optical and electrochemical properties of EDOT-based π-conjugated polymers. *Scientific Reports* **2017,** *7* (1), 1078.

98. Dyer, A. L.; Craig, M. R.; Babiarz, J. E.; Kiyak, K.; Reynolds, J. R., Orange and Red to Transmissive Electrochromic Polymers Based on Electron-Rich Dioxythiophenes. *Macromolecules* **2010,** *43* (10), 4460-4467.

99. Chen, X.; Xu, Z.; Mi, S.; Zheng, J.; Xu, C., Spray-processable red-to-transmissive electrochromic polymers towards fast switching time for display applications. *New Journal of Chemistry* **2015,** *39* (7), 5389-5394.

100. Hızalan, G.; Balan, A.; Baran, D.; Toppare, L., Spray processable ambipolar benzotriazole bearing electrochromic polymers with multi-colored and transmissive states. *Journal of Materials Chemistry* **2011,** *21* (6), 1804-1809.

101. Atakan, G.; Gunbas, G., A novel red to transmissive electrochromic polymer based on phenanthrocarbazole. *RSC Advances* **2016,** *6* (30), 25620-25623.

102. Yin, Y.; Li, W.; Zeng, X.; Xu, P.; Murtaza, I.; Guo, Y.; Liu, Y.; Li, T.; Cao, J.; He, Y.; Meng, H., Design Strategy for Efficient Solution-Processable Red Electrochromic Polymers Based on Unconventional 3,6-Bis(dodecyloxy)thieno[3,2-b]thiophene Building Blocks. *Macromolecules* **2018,** *51* (19), 7853-7862.

103. Christiansen, D. T.; Reynolds, J. R., A Fruitful Usage of a Dialkylthiophene Comonomer for Redox Stable Wide-Gap Cathodically Coloring Electrochromic Polymers. *Macromolecules* **2018**.

104. Dey, T.; Invernale, M. A.; Ding, Y.; Buyukmumcu, Z.; Sotzing, G. A., Poly(3,4-propylenedioxythiophene)s as a Single Platform for Full Color Realization. *Macromolecules* **2011,** *44* (8), 2415-2417.

105. Lee, J.-K.; Fong, H. H.; Zakhidov, A. A.; McCluskey, G. E.; Taylor, P. G.; Santiago-Berrios, M. e.; Abruña, H. D.; Holmes, A. B.; Malliaras, G. G.; Ober, C. K., Semiperfluoroalkyl Polyfluorenes for Orthogonal Processing in Fluorous Solvents. *Macromolecules* **2010,** *43* (3), 1195-1198.

106. Wu, J.-G.; Lee, C.-Y.; Wu, S.-S.; Luo, S.-C., Ionic Liquid-Assisted Electropolymerization for Lithographical Perfluorocarbon Deposition and Hydrophobic Patterning. *ACS Applied Materials & Interfaces* **2016,** *8* (34), 22688-22695.

107. Schwendeman, I.; Gaupp, C. L.; Hancock, J. M.; Groenendaal, L.; Reynolds, J.R., Perfluoroalkanoate-Substituted PEDOT for Electrochromic Device Applications. *Advanced Functional Materials* **2003,** *13* (7), 541-547.

108. Neo, W. T.; Ong, K. H.; Lin, T. T.; Chua, S.-J.; Xu, J., Effects of fluorination on the electrochromic performance of benzothiadiazole-based donor–acceptor copolymers. *Journal of Materials Chemistry C* **2015,** *3* (21), 5589-5597.

109. Chen, X.; Zhang, Z.; Ding, Z.; Liu, J.; Wang, L., Diketopyrrolopyrrole-based Conjugated Polymers Bearing Branched Oligo(Ethylene Glycol) Side Chains for Photovoltaic Devices. *Angewandte Chemie International Edition* **2016,** *55* (35), 10376-10380.

110. Li, W.-S.; Yamamoto, Y.; Fukushima, T.; Saeki, A.; Seki, S.; Tagawa, S.; Masunaga, H.; Sasaki, S.; Takata, M.; Aida, T., Amphiphilic Molecular Design as a Rational Strategy for Tailoring Bicontinuous Electron Donor and Acceptor Arrays: Photoconductive Liquid Crystalline Oligothiophene−C60 Dyads. *Journal of the American Chemical Society* **2008,** *130* (28), 8886-8887.

111. Giovannitti, A.; Maria, I. P.; Hanifi, D.; Donahue, M. J.; Bryant, D.; Barth, K. J.; Makdah, B. E.; Savva, A.; Moia, D.; Zetek, M.; Barnes, P. R. F.; Reid, O. G.; Inal, S.; Rumbles, G.; Malliaras, G. G.; Nelson, J.; Rivnay, J.; McCulloch, I., The Role of the Side Chain on the Performance of N-type Conjugated Polymers in Aqueous Electrolytes. *Chemistry of Materials* **2018,** *30* (9), 2945-2953.

112. Giovannitti, A.; Sbircea, D.-T.; Inal, S.; Nielsen, C. B.; Bandiello, E.; Hanifi, D. A.; Sessolo, M.; Malliaras, G. G.; McCulloch, I.; Rivnay, J., Controlling the mode of operation of organic transistors through side-chain engineering. *Proceedings of the National Academy of Sciences* **2016,** *113* (43), 12017.

113. Roncali, J.; Garreau, R.; Delabouglise, D.; Garnier, F.; Lemaire, M., Modification of the structure and electrochemical properties of poly(thiophene) by ether groups. *Journal of the Chemical Society, Chemical Communications* **1989,** (11), 679-681.

114. Perepichka, I. F.; Besbes, M.; Levillain, E.; Sallé, M.; Roncali, J., Hydrophilic Oligo(oxyethylene)-Derivatized Poly(3,4-ethylenedioxythiophenes): Cation-Responsive Optoelectroelectrochemical Properties and Solid-State Chromism. *Chemistry of Materials* **2002,** *14* (1), 449-457.

115. Akoudad, S.; Roncali, J., Modification of the electrochemical and electronic properties of electrogenerated poly(3,4-ethylenedioxythiophene) by hydroxymethyl and oligo(oxyethylene) substituents. *Electrochemistry Communications* **2000,** *2* (1), 72-76.

116. Hu, Y.; Liu, X.; Jiang, F.; Zhou, W.; Liu, C.; Duan, X.; Xu, J., Functionalized Poly(3,4-ethylenedioxy bithiophene) Films for Tuning Electrochromic and Thermoelectric Properties. *The Journal of Physical Chemistry B* **2017,** *121* (39), 9281-9290.

117. Savagian, L. R.; Österholm, A. M.; Ponder Jr., J. F.; Barth, K. J.; Rivnay, J.; Reynolds, J. R., Balancing Charge Storage and Mobility in an Oligo(Ether) Functionalized Dioxythiophene Copolymer for Organic- and Aqueous- Based Electrochemical Devices and Transistors. *Advanced Materials* **2018,** *30* (50), 1804647.

118. Beaujuge, P. M.; Amb, C. M.; Reynolds, J. R., A Side-Chain Defunctionalization Approach Yields a Polymer Electrochrome Spray-Processable from Water. *Advanced Materials* **2010,** *22* (47), 5383-5387.

119. Reeves, B. D.; Unur, E.; Ananthakrishnan, N.; Reynolds, J. R., Defunctionalization of Ester-Substituted Electrochromic Dioxythiophene Polymers. *Macromolecules* **2007,** *40* (15), 5344-5352.

120. Kimbrough, R. D., Toxicity and health effects of selected organotin compounds: a review. *Environmental Health Perspectives* **1976,** *14*, 51-56.

121. Hansen, M. M.; Jolly, R. A.; Linder, R. J., Boronic Acids and Derivatives—Probing the Structure–Activity Relationships for Mutagenicity. *Organic Process Research & Development* **2015,** *19* (11), 1507-1516.

122. McCarley, T. D.; Noble; DuBois, C. J.; McCarley, R. L., MALDI-MS Evaluation of Poly(3-hexylthiophene) Synthesized by Chemical Oxidation with FeCl3. *Macromolecules* **2001,** *34* (23), 7999-8004.

123. Torres, B. B.; Balogh, D. T., Regioregular improvement on the oxidative polymerization of poly-3-octylthiophenes by slow addition of oxidant at low temperature. *Journal of Applied Polymer Science* **2012,** *124* (4), 3222-3228.

124. Niemi, V. M.; Knuuttila, P.; Österholm, J. E.; Korvola, J., Polymerization of 3-alkylthiophenes with FeCl3. *Polymer* **1992,** *33* (7), 1559-1562.

125. Barbarella, G.; Zambianchi, M.; Di Toro, R.; Colonna, M.; Iarossi, D.; Goldoni, F.; Bongini, A., Regioselective Oligomerization of 3-(Alkylsulfanyl)thiophenes with Ferric Chloride. *The Journal of Organic Chemistry* **1996,** *61* (23), 8285-8292.

126. Ando, S.; Ueda, M., Density functional theory calculations of the local spin densities of 3-substituted thiophenes and the oligomerization mechanism of 3-methylsulfanyl thiophene. *Synthetic Metals* **2002,** *129* (2), 207-213.

127. Mercier, L. G.; Leclerc, M., Direct (Hetero)Arylation: A New Tool for Polymer Chemists. *Accounts of Chemical Research* **2013,** *46* (7), 1597-1605.

128. Estrada, L. A.; Deininger, J. J.; Kamenov, G. D.; Reynolds, J. R., Direct (Hetero)arylation Polymerization: An Effective Route to 3,4-Propylenedioxythiophene-

Based Polymers with Low Residual Metal Content. *ACS Macro Letters* **2013,** *2* (10), 869-873.

129. Bura, T.; Blaskovits, J. T.; Leclerc, M., Direct (Hetero)arylation Polymerization: Trends and Perspectives. *Journal of the American Chemical Society* **2016,** *138* (32), 10056-10071.

130. Pouliot, J.-R.; Grenier, F.; Blaskovits, J. T.; Beaupré, S.; Leclerc, M., Direct (Hetero)arylation Polymerization: Simplicity for Conjugated Polymer Synthesis. *Chemical Reviews* **2016,** *116* (22), 14225-14274.

131. Suraru, S.-L.; Lee, J. A.; Luscombe, C. K., C–H Arylation in the Synthesis of π-Conjugated Polymers. *ACS Macro Letters* **2016,** *5* (6), 724-729.

132. Bohra, H.; Wang, M., Direct C–H arylation: a "Greener" approach towards facile synthesis of organic semiconducting molecules and polymers. *Journal of Materials Chemistry A* **2017,** *5* (23), 11550-11571.

133. Bura, T.; Beaupre, S.; Legare, M.-A.; Quinn, J.; Rochette, E.; Blaskovits, J. T.; Fontaine, F.-G.; Pron, A.; Li, Y.; Leclerc, M., Direct heteroarylation polymerization: guidelines for defect-free conjugated polymers. *Chemical Science* **2017,** *8* (5), 3913-3925.

134. Yu, S.; Liu, F.; Yu, J.; Zhang, S.; Cabanetos, C.; Gao, Y.; Huang, W., Eco-friendly direct (hetero)-arylation polymerization: scope and limitation. *Journal of Materials Chemistry C* **2017,** *5* (1), 29-40.

135. Blaskovits, J. T.; Johnson, P. A.; Leclerc, M., Mechanistic Origin of β-Defect Formation in Thiophene-Based Polymers Prepared by Direct (Hetero)arylation. *Macromolecules* **2018,** *51* (20), 8100-8113.

136. Lafrance, M.; Fagnou, K., Palladium-Catalyzed Benzene Arylation: Incorporation of Catalytic Pivalic Acid as a Proton Shuttle and a Key Element in Catalyst Design. *Journal of the American Chemical Society* **2006,** *128* (51), 16496-16497.

137. Wang, Q.; Takita, R.; Kikuzaki, Y.; Ozawa, F., Palladium-Catalyzed Dehydrohalogenative Polycondensation of 2-Bromo-3-hexylthiophene: An Efficient Approach to Head-to-Tail Poly(3-hexylthiophene). *Journal of the American Chemical Society* **2010,** *132* (33), 11420-11421.

138. Lafrance, M.; Lapointe, D.; Fagnou, K., Mild and efficient palladium-catalyzed intramolecular direct arylation reactions. *Tetrahedron* **2008,** *64* (26), 6015-6020.

139. Ponder, J. F.; Schmatz, B.; Hernandez, J. L.; Reynolds, J. R., Soluble phenylenedioxythiophene copolymers via direct (hetero)arylation polymerization: a revived monomer for organic electronics. *Journal of Materials Chemistry C* **2018,** *6* (5), 1064-1070.

140. Hendsbee, A.; Li, Y., Performance Comparisons of Polymer Semiconductors Synthesized by Direct (Hetero)Arylation Polymerization (DHAP) and Conventional Methods for Organic Thin Film Transistors and Organic Photovoltaics. *Molecules* **2018,** *23* (6), 1255.

141. Marzano, G.; Kotowski, D.; Babudri, F.; Musio, R.; Pellegrino, A.; Luzzati, S.; Po, R.; Farinola, G. M., Tin-Free Synthesis of a Ternary Random Copolymer for BHJ Solar Cells: Direct (Hetero)arylation versus Stille Polymerization. *Macromolecules* **2015,** *48* (19), 7039-7048.

142. Andrey, E. R.; Alia, A. L.; Barry, C. T., Influence of β-linkages on the morphology and performance of DArP P3HT–PC 61 BM solar cells. *Nanotechnology* **2014,** *25* (1), 014005.

143. Nielsen, K. T.; Bechgaard, K.; Krebs, F. C., Removal of Palladium Nanoparticles from Polymer Materials. *Macromolecules* **2005,** *38* (3), 658-659.

144. Sakamoto, J.; Rehahn, M.; Wegner, G.; Schlüter, A. D., Suzuki Polycondensation: Polyarylenes à la Carte. *Macromolecular Rapid Communications* **2009,** *30* (9-10), 653-687.

145. Neo, W. T.; Ye, Q.; Chua, S.-J.; Xu, J., Conjugated polymer-based electrochromics: materials, device fabrication and application prospects. *Journal of Materials Chemistry C* **2016,** *4* (31), 7364-7376.

146. Panzer, F.; Bässler, H.; Köhler, A., Temperature Induced Order–Disorder Transition in Solutions of Conjugated Polymers Probed by Optical Spectroscopy. *The Journal of Physical Chemistry Letters* **2017,** *8* (1), 114-125.

147. Tsumura, A.; Koezuka, H.; Ando, T., Macromolecular electronic device: Field-effect transistor with a polythiophene thin film. *Applied Physics Letters* **1986,** *49* (18), 1210-1212.

148. Sirringhaus, H., 25th Anniversary Article: Organic Field-Effect Transistors: The Path Beyond Amorphous Silicon. *Advanced Materials* **2014,** *26* (9), 1319-1335.

149. Tang, C. W.; VanSlyke, S. A., Organic electroluminescent diodes. *Applied Physics Letters* **1987,** *51* (12), 913-915.

150. Kordt, P.; van der Holst, J. J. M.; Al Helwi, M.; Kowalsky, W.; May, F.; Badinski, A.; Lennartz, C.; Andrienko, D., Modeling of Organic Light Emitting Diodes: From Molecular to Device Properties. *Advanced Functional Materials* **2015,** *25* (13), 1955-1971.

151. Kang, H.; Lee, W.; Oh, J.; Kim, T.; Lee, C.; Kim, B. J., From Fullerene–Polymer to All-Polymer Solar Cells: The Importance of Molecular Packing, Orientation, and Morphology Control. *Accounts of Chemical Research* **2016,** *49* (11), 2424-2434.

152. Zhang, G.; Zhao, J.; Chow, P. C. Y.; Jiang, K.; Zhang, J.; Zhu, Z.; Zhang, J.; Huang, F.; Yan, H., Nonfullerene Acceptor Molecules for Bulk Heterojunction Organic Solar Cells. *Chemical Reviews* **2018,** *118* (7), 3447-3507.

153. You, J.; Dou, L.; Yoshimura, K.; Kato, T.; Ohya, K.; Moriarty, T.; Emery, K.; Chen, C.-C.; Gao, J.; Li, G.; Yang, Y., A polymer tandem solar cell with 10.6% power conversion efficiency. *Nature Communications* **2013,** *4*, 1446.

154. Amb, C. M.; Dyer, A. L.; Reynolds, J. R., Navigating the Color Palette of Solution-Processable Electrochromic Polymers. *Chemistry of Materials* **2011,** *23* (3), 397-415.

155. Dyer, A. L.; Thompson, E. J.; Reynolds, J. R., Completing the Color Palette with Spray-Processable Polymer Electrochromics. *ACS Applied Materials & Interfaces* **2011,** *3* (6), 1787-1795.

156. Österholm, A. M.; Shen, D. E.; Gottfried, D. S.; Reynolds, J. R., Full Color Control and High-Resolution Patterning from Inkjet Printable Cyan/Magenta/Yellow Colored-to-Colorless Electrochromic Polymer Inks. *Advanced Materials Technologies* **2016,** *1* (4), 1600063.

157. Beaujuge, P. M.; Amb, C. M.; Reynolds, J. R., A Side-Chain Defunctionalization Approach Yields a Polymer Electrochrome Spray-Processable from Water. *Advanced Materials* **2010,** *22* (47), 5383-5387.

158. Meier, H.; Stalmach, U.; Kolshorn, H., Effective conjugation length and UV/vis spectra of oligomers. *Acta Polymerica* **1997,** *48* (9), 379-384.

159. Heinze, J.; Frontana-Uribe, B. A.; Ludwigs, S., Electrochemistry of Conducting Polymers—Persistent Models and New Concepts. *Chemical Reviews* **2010,** *110* (8), 4724-4771.

160. Kumar, A.; Otley, M. T.; Alamar, F. A.; Zhu, Y.; Arden, B. G.; Sotzing, G. A., Solid-state electrochromic devices: relationship of contrast as a function of device preparation parameters. *Journal of Materials Chemistry C* **2014,** *2* (14), 2510-2516.

161. Conboy, G.; Spencer, H. J.; Angioni, E.; Kanibolotsky, A. L.; Findlay, N. J.; Coles, S. J.; Wilson, C.; Pitak, M. B.; Risko, C.; Coropceanu, V.; Brédas, J.-L.; Skabara, P. J., To bend or not to bend – are heteroatom interactions within conjugated molecules effective in dictating conformation and planarity? *Materials Horizons* **2016,** *3* (4), 333-339.

162. Padilla, J.; Seshadri, V.; Sotzing, G. A.; Otero, T. F., Maximum contrast from an electrochromic material. *Electrochemistry Communications* **2007,** *9* (8), 1931-1935.

163. Lim, J. Y.; Ko, H. C.; Lee, H., Systematic prediction of maximum electrochromic contrast of an electrochromic material. *Synthetic Metals* **2005,** *155* (3), 595-598.

164. Turbiez, M.; Frère, P.; Allain, M.; Videlot, C.; Ackermann, J.; Roncali, J., Design of Organic Semiconductors: Tuning the Electronic Properties of π-Conjugated

Oligothiophenes with the 3,4-Ethylenedioxythiophene (EDOT) Building Block. *Chemistry – A European Journal* **2005,** *11* (12), 3742-3752.

165. Leclerc, M., Optical and Electrochemical Transducers Based on Functionalized Conjugated Polymers. *Advanced Materials* **1999,** *11* (18), 1491-1498.

166. Yang, C.; Orfino, F. P.; Holdcroft, S., A Phenomenological Model for Predicting Thermochromism of Regioregular and Nonregioregular Poly(3-alkylthiophenes). *Macromolecules* **1996,** *29* (20), 6510-6517.

167. Mario, L., Optical and Electrochemical Transducers Based on Functionalized Conjugated Polymers. *Sensors Update* **2000,** *8* (1), 21-38.

168. Eder, T.; Stangl, T.; Gmelch, M.; Remmerssen, K.; Laux, D.; Höger, S.; Lupton, J. M.; Vogelsang, J., Switching between H- and J-type electronic coupling in single conjugated polymer aggregates. *Nature communications* **2017,** *8* (1), 1641-1641.

169. Hestand, N. J.; Spano, F. C., Expanded Theory of H- and J-Molecular Aggregates: The Effects of Vibronic Coupling and Intermolecular Charge Transfer. *Chemical Reviews* **2018,** *118* (15), 7069-7163.

170. Welsh, D. M.; Kumar, A.; Meijer, E. W.; Reynolds, J. R., Enhanced Contrast Ratios and Rapid Switching in Electrochromics Based on Poly(3,4-propylenedioxythiophene) Derivatives. *Advanced Materials* **1999,** *11* (16), 1379-1382.

171. You, H.; Kim, D.; Cho, H.-H.; Lee, C.; Chong, S.; Ahn, N. Y.; Seo, M.; Kim, J.; Kim, F. S.; Kim, B. J., Shift of the Branching Point of the Side-Chain in Naphthalenediimide (NDI)-Based Polymer for Enhanced Electron Mobility and All-Polymer Solar Cell Performance. *Advanced Functional Materials* **2018,** *28* (39), 1803613.

172. Lee, M.-H.; Kim, J.; Kang, M.; Kim, J.; Kang, B.; Hwang, H.; Cho, K.; Kim, D.-Y., Precise Side-Chain Engineering of Thienylenevinylene–Benzotriazole-Based Conjugated Polymers with Coplanar Backbone for Organic Field Effect Transistors and CMOS-like Inverters. *ACS Applied Materials & Interfaces* **2017,** *9* (3), 2758-2766.

173. Cardona, C. M.; Li, W.; Kaifer, A. E.; Stockdale, D.; Bazan, G. C., Electrochemical Considerations for Determining Absolute Frontier Orbital Energy Levels of Conjugated Polymers for Solar Cell Applications. *Advanced Materials* **2011,** *23* (20), 2367-2371.

174. Moser, M.; Ponder Jr, J. F.; Wadsworth, A.; Giovannitti, A.; McCulloch, I., Materials in Organic Electrochemical Transistors for Bioelectronic Applications: Past, Present, and Future. *Advanced Functional Materials* **2018,** *0* (0), 1807033.

175. Berggren, M.; Richter-Dahlfors, A., Organic Bioelectronics. *Advanced Materials* **2007,** *19* (20), 3201-3213.

176. Feron, K.; Lim, R.; Sherwood, C.; Keynes, A.; Brichta, A.; Dastoor, P. C., Organic Bioelectronics: Materials and Biocompatibility. *International journal of molecular sciences* **2018,** *19* (8), 2382.

177. Someya, T.; Bao, Z.; Malliaras, G. G., The rise of plastic bioelectronics. *Nature* **2016,** *540*, 379.

178. White, H. S.; Kittlesen, G. P.; Wrighton, M. S., Chemical derivatization of an array of three gold microelectrodes with polypyrrole: fabrication of a molecule-based transistor. *Journal of the American Chemical Society* **1984,** *106* (18), 5375-5377.

179. Rivnay, J.; Leleux, P.; Ferro, M.; Sessolo, M.; Williamson, A.; Koutsouras, D. A.; Khodagholy, D.; Ramuz, M.; Strakosas, X.; Owens, R. M.; Benar, C.; Badier, J.-M.; Bernard, C.; Malliaras, G. G., High-performance transistors for bioelectronics through tuning of channel thickness. *Science Advances* **2015,** *1* (4), e1400251.

180. Khodagholy, D.; Rivnay, J.; Sessolo, M.; Gurfinkel, M.; Leleux, P.; Jimison, L. H.; Stavrinidou, E.; Herve, T.; Sanaur, S.; Owens, R. M.; Malliaras, G. G., High transconductance organic electrochemical transistors. *Nature communications* **2013,** *4*, 2133-2133.

181. Musumeci, C.; Vagin, M.; Zeglio, E.; Ouyang, L.; Gabrielsson, R.; Inganäs, O., Organic electrochemical transistors from supramolecular complexes of conjugated polyelectrolyte PEDOTS. *Journal of Materials Chemistry C* **2019**.

182. Braendlein, M.; Lonjaret, T.; Leleux, P.; Badier, J.-M.; Malliaras, G. G., Voltage Amplifier Based on Organic Electrochemical Transistor. *Advanced Science* **2017,** *4* (1), 1600247.

183. Shi, H.; Liu, C.; Jiang, Q.; Xu, J., Effective Approaches to Improve the Electrical Conductivity of PEDOT:PSS: A Review. *Advanced Electronic Materials* **2015,** *1* (4), 1500017.

184. Håkansson, A.; Han, S.; Wang, S.; Lu, J.; Braun, S.; Fahlman, M.; Berggren, M.; Crispin, X.; Fabiano, S., Effect of (3-glycidyloxypropyl)trimethoxysilane (GOPS) on the electrical properties of PEDOT:PSS films. *Journal of Polymer Science Part B: Polymer Physics* **2017,** *55* (10), 814-820.

185. Rivnay, J.; Inal, S.; Collins, B. A.; Sessolo, M.; Stavrinidou, E.; Strakosas, X.; Tassone, C.; Delongchamp, D. M.; Malliaras, G. G., Structural control of mixed ionic and electronic transport in conducting polymers. *Nature Communications* **2016,** *7*, 11287.

186. Nielsen, C. B.; Giovannitti, A.; Sbircea, D.-T.; Bandiello, E.; Niazi, M. R.; Hanifi, D. A.; Sessolo, M.; Amassian, A.; Malliaras, G. G.; Rivnay, J.; McCulloch, I., Molecular Design of Semiconducting Polymers for High-Performance Organic Electrochemical Transistors. *Journal of the American Chemical Society* **2016,** *138* (32), 10252-10259.

VITAE

Melony Achieng Ochieng was born on June 23, 1990 to the goal-oriented Mariam Ochieng and best-of-the-bunch Anthony Omburoh in Kisumu Kenya at a time of great bountiful harvest, when the granaries brimmed with crops, the livestock reproduced in droves, and the fire was kept lit all day and night in the kitchen. Her above-average family won the green card lottery in 2000 and migrated to the jungles of Durham, North Carolina in the dead of winter in 2001, so that they may take a portion of the milk and honey advertised on TV and live life more abundantly. After showing little aptitude in the arts, she graduated from North Carolina Central University in 2012 with a B.S. in Chemistry and Pharmaceutical Sciences.

She took a calculated risk and started her graduate career at Duke University, but not having finished her math minor, she ended up making a few wrong turns before transferring to Georgia Institute of Technology (GT). At GT, she took another loss before persuading Dr. John Reynolds to let her join his lab in fall of 2015. In his lab, she worked on understanding how side chains affect optoelectronic properties of dioxythiophenes, a sophisticated way of saying she made a few orange and magenta colored plastics. She plans to graduate in March 2019 and join Intel as a PTD module engineer with the hopes of one day becoming a CEO or marrying a well-to-do-man and becoming the Grand Diva of All Things Domestic. Outside of school, Melony loves to cook, bake bread, and read books.